



Universiteit  
Leiden  
The Netherlands

## **Studies on the pathogenesis of chronic kidney disease**

He, J.

### **Citation**

He, J. (2021, September 15). *Studies on the pathogenesis of chronic kidney disease*. Retrieved from <https://hdl.handle.net/1887/3210130>

Version: Publisher's Version

License: [Licence agreement concerning inclusion of doctoral thesis in the Institutional Repository of the University of Leiden](#)

Downloaded from: <https://hdl.handle.net/1887/3210130>

**Note:** To cite this publication please use the final published version (if applicable).

Cover Page



Universiteit Leiden



The handle <https://hdl.handle.net/1887/3210130> holds various files of this Leiden University dissertation.

**Author:** He, J.

**Title:** Studies on the pathogenesis of chronic kidney disease

**Issue Date:** 2021-09-15



# **Studies on the Pathogenesis of Chronic Kidney Disease**

**Junling He**

## **Colophon**

Title: Studies on the Pathogenesis of Chronic Kidney Disease

Author: Junling He

Ph.D. thesis, University of Leiden, Leiden, The Netherlands

ISBN: 978-94-6416-715-3

Cover design: Daoping Xiong and Shaogui Xiong

Printing: Ridderprint | [www.ridderprint.nl](http://www.ridderprint.nl)

The studies described in this thesis were performed at the Department of Pathology of the Leiden University Medical Center and the Department of Animal Sciences, Institute of Biology Leiden, Leiden University.

The work was supported by the China Scholarship Council (CSC no. 201508500109).

The publication of this thesis was financially supported by ChipSoft and Leiden University.

Copyright © Junling He, 2021

No part of this thesis may be reproduced, stored, or transmitted in any form or by any means, without prior written permission of the authors and corresponding journal.

# **Studies on the Pathogenesis of Chronic Kidney Disease**

Proefschrift

ter verkrijging van

de graad van doctor aan de Universiteit Leiden,

op gezag van rector magnificus prof.dr.ir. H. Bijl,

volgens besluit van het college voor promoties

te verdedigen op woensdag 15 september 2021

klokke 10.00 uur

door

**Junling He**

geboren te Wanzhou, Chongqing, China

in 1988

**Promotores:** Prof. Dr. H. P. Spaink

Prof. Dr. J. A. Bruijn

**Co-promotor:** Dr. J. J. Baelde

**Promotiecommissie:** Prof. Dr. G. P. van Wezel

Prof. Dr. A. H. Meijer

Prof. Dr. J. Bakkers (UMC Utrecht)

Dr. D. H. T. Ijpelaar (GHZ Gouda)

Dr. J. Kers (Amsterdam UMC)

## Contents

|                   |  |     |
|-------------------|--|-----|
| <b>Chapter 1</b>  | General introduction   | 7   |
| <b>Chapter 2</b>  | Glomerular clusterin expression is increased in diabetic nephropathy and protects against oxidative stress–induced apoptosis in podocytes<br><i>Sci Rep. 2020; 10(1):14888.</i>                                    | 35  |
| <b>Chapter 3</b>  | Carnosinase-1 overexpression, but not aerobic exercise training, affects the development of advanced diabetic nephropathy in BTBR <i>ob/ob</i> mice<br><i>Am J Physiol Renal Physiol. 2020;318(4):F1030-F1040.</i> | 59  |
| <b>Chapter 4</b>  | Leptin deficiency affects glucose homeostasis and results in adiposity in zebrafish<br><i>J Endocrinol. 2021 May;249(2):125-134.</i>   | 83  |
| <b>Chapter 5</b>  | <i>Ctns</i> mutant adult zebrafish develop nephropathic cystinosis   | 105 |
| <b>Chapter 6</b>  | Summary and General Discussion   | 121 |
| <b>Chapter 7</b>  | Nederlandse Samenvatting   | 139 |
| <b>Appendices</b> | Curriculum vitae   | 144 |
|                   | List of publications   | 145 |
|                   | Acknowledgements   | 147 |



# Chapter 1

## General introduction



## **Scope of this thesis**

### **Chronic kidney disease**

The scope of this thesis is to study the pathogenesis of chronic kidney disease. Chronic kidney disease is a general term for kidney diseases with a gradual loss of renal function over a long period <sup>1</sup>. The definition of chronic kidney disease is: the occurrence of kidney damage with gradually decreased kidney function ( $\text{GFR} < 60 \text{ mL/min/1.73 m}^2$ ) for three months or more <sup>2</sup>. Kidney damage is characterized by abnormalities in urine or blood tests, and/or defects observed in kidney morphology. In 2017, chronic kidney disease affected almost 700 million people globally, and it is recognized as a worldwide public health problem <sup>3</sup>. Understanding the underlying mechanisms of the development of chronic kidney disease will pave the way for the development of preventative and therapeutic strategies. Based on the location in the kidney where the primary injury is present, chronic kidney disease can be divided into two categories: glomerular diseases (such as diabetic nephropathy, glomerulonephritis, and focal segmental glomerulosclerosis) and tubular diseases (such as nephropathic cystinosis, polycystic kidney disease and pyelonephritis). This thesis focuses on the pathogenesis of diabetic nephropathy and nephropathic cystinosis.



## The kidney

Kidneys are paired bean-shaped organs located on the left and right of the posterior abdominal wall (**Figure. 1A**). The main functions of the kidney are: 1) excretion of excess fluids and waste products out of the blood into the urine; 2) controlling homeostasis by regulating fluid osmolality, acid-base and electrolyte balance; 3) synthesizing hormones, such as erythropoietin and renin.

The basic functional unit of the kidney is called the nephron, consisting of a glomerulus and a renal tubule (**Figure. 1B**). Each human adult kidney contains around 1 million nephrons <sup>4</sup>.

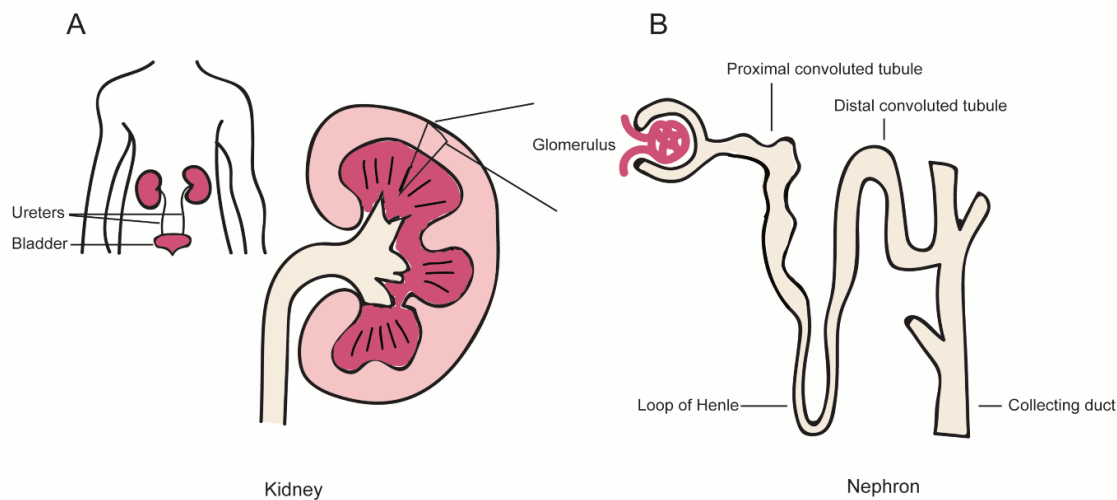


**Figure 1. The gross anatomy of the kidney and the structure of the nephron**

### *Glomerulus*

The glomerulus is a specialized filter unit with a tangle of capillaries (**Figure. 2A**). Afferent arterioles give rise to glomerular capillaries which merge to exit the glomerulus as efferent arterioles. Bowman's capsule is a spherical structure surrounding the glomerulus. Bowman's capsule encloses the capillary tufts creating Bowman's space. Bowman's capsule is covered by parietal epithelial cells. The visceral epithelial cells, also called podocytes, coat the outer surface of the glomerular capillaries. Podocytes together with glomerular basement membrane (GBM) and the fenestrated endothelial cells constitute the glomerular filtration barrier (GFB) that the ultrafiltrate passes through (**Figure. 2B**). The GFB separates the vascular from the urinary space, and it is crucial for ultrafiltration. Under healthy conditions, only water, small solutes, and small proteins can pass through the intact GFB because of its size-selective and

charge-selective properties. However, defects in at least one of the layers of GFB can cause leakage of larger plasma proteins into the urine, resulting in proteinuria.

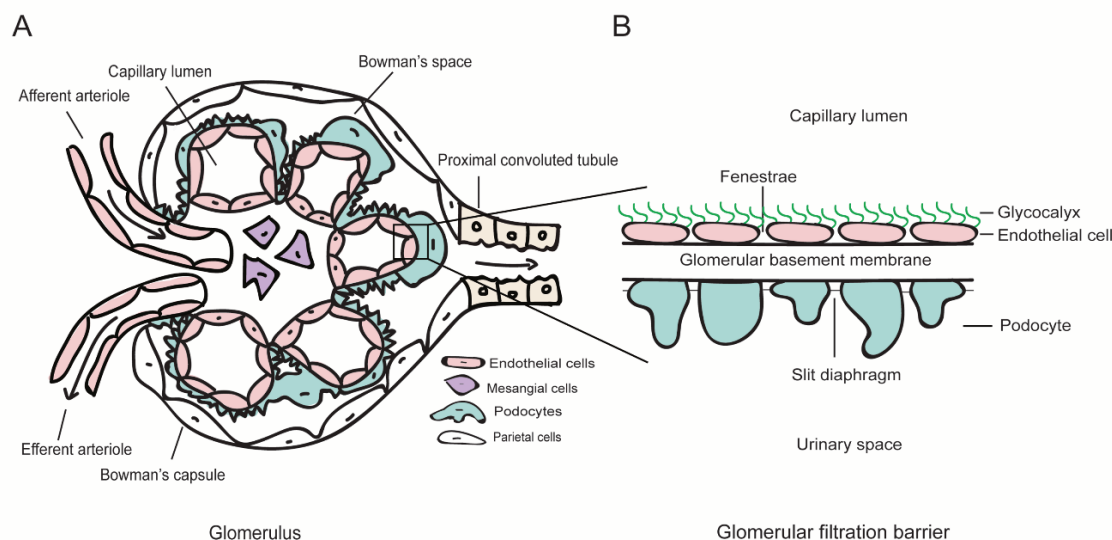


**Figure 2. The structure of the glomerulus and the glomerular filtration barrier**

Glomerular endothelial cells are highly specialized cells lining inside of the glomerular capillaries. The transcellular windows of glomerular endothelium are referred to as fenestrae. It has been demonstrated that a glycocalyx, a network composed of glycoproteins, coats the luminal surface of the glomerular capillaries and bridges the fenestrations of glomerular endothelial cells <sup>5</sup>. It has been reported that the glycocalyx is vital to the permselectivity (selective permeability to certain proteins and molecules) of the glomerular capillary <sup>6,7</sup>. Alterations in endothelial glycocalyx components increase microvascular permeability and cause albuminuria in glomerular diseases <sup>8-10</sup>.

The GBM is a sheet-like structure that consists of extracellular matrix molecules, and it is the only uninterrupted layer in the GFB. It comprises collagens and no collagenous glycoproteins, such as type IV collagen, laminin, nidogen, fibronectin, and heparan sulfate proteoglycan <sup>11</sup>. The network of collagen IV is regarded as a crucial scaffold integrating other components in the GBM. Mutations in collagen IV  $\alpha 3$  result in Alport syndrome, which leads to deafness and kidney failure in children <sup>12</sup>. Ernst Pöschl et al. demonstrated that collagen IV is dispensable for the initiation of GBM assembly. It is essential to maintain the integrity and stability of GBM at later stages of development <sup>13</sup>. Laminin gene mutations can also cause GBM defects. Mutation of laminin  $\beta 2$  in humans results in a congenital manifestation called Pierson syndrome, a disorder characterized by congenital ocular and neurologic abnormalities and nephrotic

syndrome <sup>14</sup>. An experimental study demonstrated that insufficient levels of laminin  $\alpha 5$  to maintain GBM integrity leads to the development of polycystic kidney disease <sup>15</sup>. These studies collectively suggest that collagen networks and laminin components are crucial to support the standard structure and function of GBM. The GBM is negatively charged <sup>16</sup>. Heparan sulfate proteoglycans are assumed to contribute significantly to the net negative charge of GBM <sup>17</sup>. It is generally accepted that the net negative charge of GBM can repel the plasma albumin, which is also negatively charged, therefore prevents the passage of albumin through the GFB. Recent studies have aroused debate on the concept of charge selectivity. Researchers found that the disruption of the GBM charge by mutating the heparan sulfate proteoglycans, such as agrin or perlecan-heparan, does not alter glomerular permselectivity and does not cause proteinuria <sup>18-20</sup>.

Podocytes are terminally differentiated epithelial cells. Podocytes consist of a large cell body, thick primary processes, and intricate interdigitating foot processes. Podocytes can counteract the distensions of GBM and stabilize the architecture of the glomerulus due to their contractile foot processes <sup>21</sup>. The specialized cell-cell junction connecting the foot processes from adjacent podocytes called “slit diaphragm” or “slit pore” <sup>22</sup>, which is crucial for the maintenance of healthy podocytes. Several proteins are essential for keeping the intact function of this slit diaphragm, such as nephrin, podocin, transient receptor potential canonical (TRPC) proteins, Kin of IRRE-like protein 1 (NEPH1), CD2-associated protein (CD2AP) and Tight junction protein-1 (ZO-1). Dysfunction of slit diaphragm results in disconnecting the foot process of adjacent podocytes and flattening of foot processes, termed “foot process effacement”, which is the most common pathological change in podocyte diseases. Recently, it was demonstrated that the slit diaphragm comprises a complex dynamic signaling hub as well as a filter due to their anatomical features to prevent proteinuria <sup>23</sup>. Disruption in any of the slit diaphragm signaling pathways is tightly related to podocyte loss and the filtration defect, directly or indirectly contributing to the development of proteinuria in several glomerular diseases, including focal segmental glomerulosclerosis, diabetic nephropathy and immune-mediated glomerulonephritis.

Mesangial cells are specialized pericytes located on the lumen side of the GBM. They structurally support the glomerular capillaries. Besides, the mesangial cells' contractile potency enables them to alter ultrafiltration surface area and capillary flow in the glomeruli and subsequently regulate the single-nephron glomerular filtration rate (SNGFR) <sup>24</sup>. The mesangial cells synthesize the mesangial matrix consisting of different types of collagen (mainly of type IV and V collagen), laminin, and fibronectin. Mesangial cells and matrix are called mesangium

<sup>25</sup>. The mesangial cells also produce cytokines, chemokines, growth factors and vasoactive factors, which participate in the cross-talk with the adjacent endothelial cells and GBM. Abnormal proliferation of mesangial cells can be found in diabetic nephropathy, IgA nephropathy and lupus nephritis <sup>26</sup>. The mesangial matrix expansion is an early hallmark of diabetic nephropathy, which inversely correlates with glomerular filtration rate <sup>27</sup>.

### ***Renal tubule***

The renal tubules transport and process the ultrafiltrate on its way to the renal pelvis. The renal tubule can be divided into several segments based on morphology and function, including proximal convoluted tubule, loop of Henle, distal convoluted tubule, and collecting duct. The glomeruli, together with the proximal tubules, form the renal cortex. The renal medulla consists mainly of distal tubules and the collecting ducts. The glomerular ultrafiltrate first enters the proximal convoluted tubule, where it reabsorbs the majority of substances in the ultrafiltrates, such as electrolytes, proteins, glucose, phosphates, amino acids, uric acid, and bicarbonate. After passing through the proximal convoluted tubule, the filtrate continues to the loop of Henle, the distal convoluted tubule, and the collecting duct. Finally, the remaining filtrate moves as urine via the pelvis and the ureter to the bladder (**Figure. 1B**).

### **Progression of chronic kidney disease**

Once the kidney has been damaged, it may continue to get worse over time. The progression of chronic kidney disease involves both glomerular and tubular injury and interstitial fibrosis development, which parallels the decline in renal function <sup>28</sup>.

Glomerular injury increases the filtration load by increasing SNGFR of the remaining functioning glomeruli, which leads to glomerular hyperfiltration. Meanwhile, increased filtration pressure in the capillary tufts results in glomerular hypertension. Glomerular hyperfiltration and glomerular hypertension together cause the remaining nephron hypertrophy by increasing the size of the Bowman's capsule, the glomerular tuft, and Bowman's space. The hypertrophy of the remaining nephrons is an adaptive response to the elevated intraglomerular pressure that increases the filtration rate in the remaining intact glomeruli. However, persistent glomerular hyperfiltration and glomerular hypertension accelerate the loss of remnant nephrons. In turn, abnormal function and structure in nephrons further exacerbate the glomerular injury. The GFB is maintained as long as podocytes cover the enlarged filtration surface area. However, podocyte hypertrophy may fail to do so when it is beyond a certain threshold. In that situation, the slit-diaphragm are disrupted, which will cause dysfunction of GFB and protein leakage into the tubular fluid resulting in proteinuria. Endothelial dysfunction, leading to a proinflammatory and prothrombotic state, is also thought to play a pivotal pathophysiological role in glomerular injury <sup>29</sup>. Endothelial cells synthesize a variety of proinflammatory molecules, including vascular cell adhesion molecule and intercellular adhesion molecule, which contribute to inflammatory processes <sup>30</sup>. During endothelial dysfunction, endothelial cells also trigger platelet adhesion, platelet aggregation, and fibrin formation <sup>31</sup>. Recent years have witnessed a growing appreciation that endothelial-podocyte bidirectional cross-talk may play a pivotal role in the pathogenesis of glomerular injury <sup>32</sup>. Endothelial dysfunction likely elicits podocyte dysfunction <sup>33</sup>. It is well known that the vascular endothelial growth factor (VEGF) signaling axis is critical for maintaining the endothelium's normal function. VEGF is produced by various types of cells, and it acts predominantly on endothelial cells. The differentiation, function and survival of glomerular endothelial cells are highly dependent on VEGF, which is typically produced by podocytes <sup>34,35</sup>. In preeclampsia, soluble fms-like tyrosine kinase-1 (sFlt-1), a splice variant of VEGF receptor Flt-1 and a natural inhibitor of VEGF-A, is overexpressed and causes glomerular endotheliosis and proteinuria <sup>36</sup>. The hypertrophy of mesangial cells, increased mesangial cellularity, and increased mesangial matrix expansion jointly lead to mesangial expansion during the development of glomerular injury. With time, the accumulation

of the mesangial matrix, along with mesangial cells, are increasing. This lesion can progress to segmental glomerulosclerosis and eventually leads to global glomerulosclerosis <sup>37</sup>.

The interaction of dysfunctional tubular cells with interstitial tissue results in tubulointerstitial injury, which is the primary causal event associated with the progressive kidney function loss in chronic kidney disease <sup>38</sup>. It has been suggested in the literature that the passage of plasma proteins in the ultrafiltrate plays an essential role in chronic tubulointerstitial injury. The increased filtration of plasma proteins can induce inflammation by upregulation of chemoattractant and adhesive molecules via activation of NF-κB-independent and NF-κB-independent pathways <sup>39</sup>. The interstitial infiltrates of mononuclear cells, such as monocytes and macrophages, contribute to the fibrogenic process via the production of several profibrotic molecules <sup>40</sup>. The abnormal interstitial accumulation of inflammatory cells, fibronectin, and extracellular matrix collagens (I, III, V, VII, and XV) result in interstitial fibrosis <sup>41,42</sup>. Furthermore, the ultrafiltered protein load can promote complement activation, which aggravates tubular and interstitial injury progression <sup>39</sup>.

An excess accumulation of extracellular matrix and a disproportional renal parenchyma loss contribute to renal fibrosis <sup>43</sup>. Renal fibrosis is an inevitable outcome of progressive chronic kidney disease <sup>44</sup>, which leads to a progressive loss of renal function and ultimately results in end-stage renal failure.

## **Diabetic nephropathy**

### ***Diabetes Mellitus***

Diabetes Mellitus is a metabolic disorder characterized by prolonged hyperglycemia. Type 1 Diabetes Mellitus (T1DM) and Type 2 Diabetes Mellitus (T2DM) are the most common types of diabetes. T1DM is referred to as “insulin-dependent diabetes mellitus”. The loss of beta-cells, mainly attributed to autoimmune destruction, fails to produce sufficient insulin to maintain normal blood glucose levels in the pancreas. It is mainly attributed to autoimmune destruction. T2DM is referred to as “non-insulin-dependent diabetes mellitus”. The cells of the patients with T2DM fail to respond appropriately to insulin. T2DM is the most prevalent type in all populations. Maturity onset diabetes of the young (MODY) is caused by a genetic defect that disrupts insulin production. Gestational diabetes occurs in pregnant women who have hyperglycemia without a previous history of diabetes mellitus. It is caused by reduced insulin production or insulin resistance, which may improve or disappear after delivery.

### ***Diabetic vascular complications***

Hyperglycemia-induced diabetic vascular damage may involve the following five underlying mechanisms: 1) increased polyol pathway flux, 2) increased formation of advanced glycation end-products, 3) activated the ligands of advanced glycation end products and increased expression of its receptor, 4) increased protein kinase C activation, 5) and increased the hexosamine pathway flux <sup>45</sup>. One hypothesis is that all five mechanisms are activated by one upstream event: the overproduction of reactive oxygen species. The condition that the overproduction of reactive oxygen species exceeds the cell's antioxidant response is known as oxidative stress <sup>46</sup>, which can cause cellular damage <sup>47,48</sup> and lead to diabetic complications <sup>45</sup>. Most patients with long-lasting diabetes develop both macrovascular and microvascular complications. Macrovascular diseases include coronary heart disease, cerebrovascular disease, and peripheral vascular disease. Microvascular diseases include retinopathy, neuropathy, and nephropathy. However, it is still unknown why a majority of patients with diabetes do not develop these complications.

### ***Diabetic nephropathy: clinical features***

Diabetic nephropathy is a major complication of diabetes and the leading cause of end-stage renal disease. As diabetes itself is a prerequisite of diabetic nephropathy, the diagnosis of diabetic nephropathy mainly bases on diabetes history combining with physical examinations, laboratory evaluation, and imaging of the kidneys <sup>49</sup>. Clinical diabetic nephropathy is diagnosed by increased urinary albumin excretion and reduced glomerular filtration rate, often accompanied by hypertension and dyslipidemia. According to the natural history of diabetic nephropathy, five stages of progression are recognized <sup>50</sup>. Stage 1 is characterized by hyperfiltration and hypertrophy of the glomeruli and increased kidney size. The morphological changes of the kidney are still reversible at this stage. Stage 2 is characterized by glomerular structural alterations like GBM thickening and mesangial matrix expansion without clinical signs. Stage 3 is characterized by the incipient rise in microalbuminuria (urine albumin excretion rate, UAER: 30~ 300 mg/24h) in diabetic patients. Stage 4 is characterized by persistent macroalbuminuria (UAER> 300 mg/24h), which finally progresses to end-stage renal disease (stage 5) due to advanced diabetic nephropathy.

### ***Diabetic nephropathy: histopathology***

Identifying the renal histological abnormalities through a renal biopsy is also crucial to the diagnosis of diabetic nephropathy (**Figure. 3A-3B**). A uniform international accepted

pathological classification has been developed, which improves communication among clinical nephrologists and renal pathologists, and is also useful for the research activities on diabetic nephropathy. The widely used histopathological classification of diabetic nephropathy is as follows: Class I: GBM thickening alone (GBM thickness  $>430\text{nm}$  in men and  $>395\text{nm}$  in women); Class II: mesangial expansion (mesangial expansion present in  $> 25\%$  of the mesangium; mild-IIa; moderate-IIb); Class III: Nodular sclerosis (the presence of Kimmelstiel-Wilson lesion, but  $< 50\%$  diffuse global glomerulosclerosis); Class IV: Advanced diabetic glomerulosclerosis ( $>50\%$  diffuse global glomerulosclerosis with or without nodules) <sup>51</sup>.

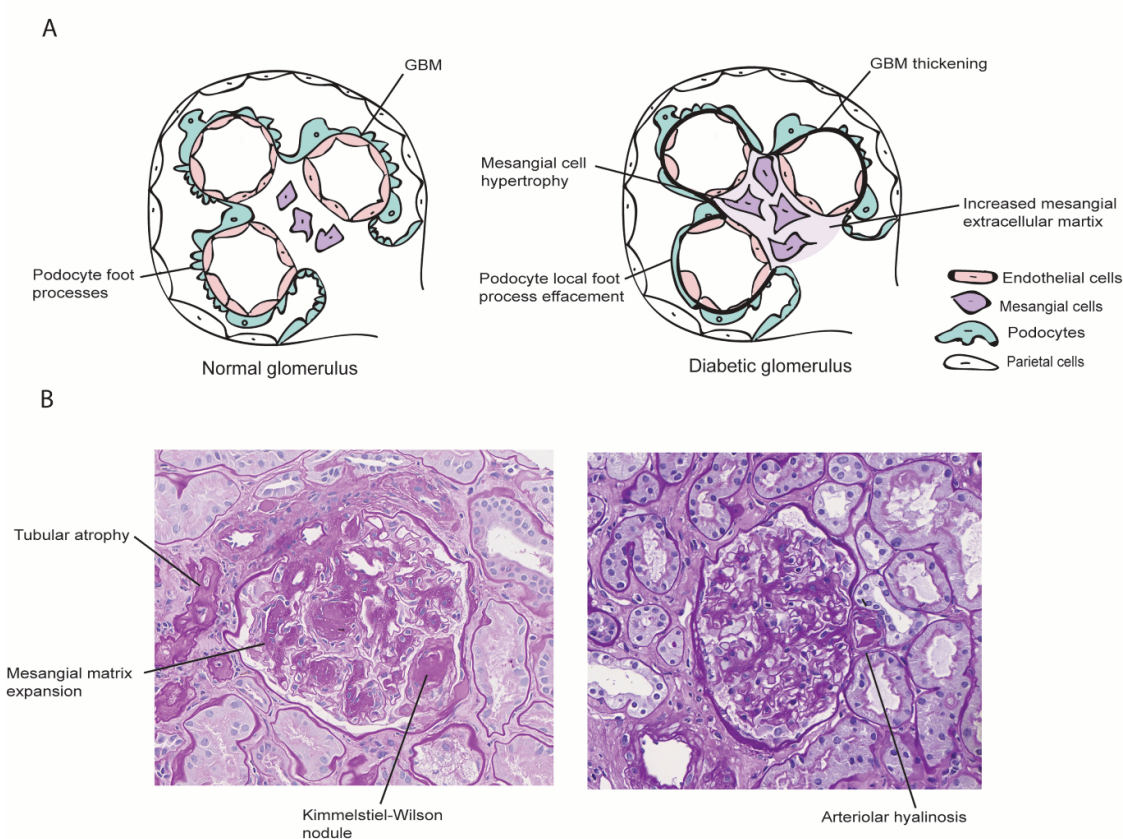


**Figure 3. The renal histological abnormalities in diabetic nephropathy**

A renal biopsy is not routinely taken in patients with diabetic nephropathy because the diagnosis is assumed to exist when proteinuria is present in a patient with diabetic retinopathy. Klessens et al. demonstrated in a large autopsy cohort that diabetic nephropathy is underdiagnosed. They found that 20 of 106 subjects, who had renal histopathological changes characteristic for diabetic nephropathy, did not present any diabetic nephropathy associated clinical features during their lifetime <sup>52</sup>.



### ***Diabetic nephropathy: genetic predisposition***

A genetic predisposition, also called genetic susceptibility, is an increased likelihood of developing a particular disease based on the genetic background under the influence of environmental conditions. Despite the increasing prevalence of diabetes, only a minority of individuals with diabetes develop diabetic nephropathy (30%~50%), suggesting that genetic determinants could influence the development and progression of diabetic nephropathy. Krolewski et al. found that the incidence rate of diabetic nephropathy rises within the first fifteen years and then declines in patients with type 1 diabetes<sup>53</sup>. Familial clustering of the development of diabetic nephropathy has also been observed<sup>54-56</sup>. These studies jointly provide evidence for a genetic predisposition in diabetic nephropathy. Additionally, a meta-analysis reported that the variants of genes, such as *ACE* (the gene coding for the angiotensin-converting enzyme), *APOC1* (the gene coding for apolipoprotein C1), *APOE* (the gene coding for apolipoprotein E), *EPO* (the gene coding for erythropoietin), *VEGFA* (the gene coding for vascular endothelial growth factor-A), associated with diabetic nephropathy<sup>57</sup>. Therefore, understanding the role of the genetic factors in diabetic nephropathy is crucial since it could provide a new sight on early diagnosis or potential therapeutic strategies.

### ***Genes in diabetic nephropathy***

#### **Clusterin (*CLU*) has protective properties in diabetic nephropathy**

Clusterin is a disulfide-linked heterodimeric protein encoded by *CLU*. Clusterin is widely expressed in various tissues, and it participates in several physiological processes, including cell differentiation<sup>58</sup>, lipid transport<sup>59,60</sup>, complement inhibition<sup>61</sup>, and regulation of apoptosis<sup>62,63</sup>. The *CLU* gene produces three different protein isoforms through alternative splicing and post-transcriptional modifications. These three isoforms of clusterin play different roles in the regulation of apoptosis. For instance, the nuclear isoform localizing to the nucleus is proapoptotic, while the cytosolic isoform, localizing to the cytoplasm, and the secretory isoform being secreted out of cells are anti-apoptotic<sup>62,64</sup>.

Clusterin is involved in many processes, including ageing<sup>65</sup>, inflammatory diseases<sup>66</sup>, neurodegenerative diseases<sup>67</sup>, and cancer<sup>64</sup>. A Japanese study reported that polymorphisms of the *CLU* gene were associated with T2DM<sup>68</sup>. Using microarray analysis, our group found that glomerular *CLU* mRNA expression is significantly higher in diabetic nephropathy patients than in healthy individuals<sup>69</sup>. Moreover, Nakatani et al. found that glomerular clusterin protein levels are 2.42-fold higher in diabetic nephropathy patients than non-diabetic controls in an

autopsy cohort <sup>70</sup>. These studies suggested that glomerular clusterin is increased and might play a role in the development of diabetic nephropathy.

In diabetic patients, increased intracellular reactive oxygen species levels lead to oxidative stress, damaging all cell components, including DNA, proteins and lipids <sup>71</sup>. As mentioned previously, the overproduction of the reactive oxygen species can induce diabetic vascular damage <sup>45</sup>. Numerous studies have shown that clusterin could protect cells against oxidative stress-induced damage. For instance, it has been reported that clusterin protects porcine proximal tubular cells against H<sub>2</sub>O<sub>2</sub>-induced damage <sup>72</sup>. Kim et al. demonstrated that exogenous clusterin protects retinal endothelial cells and astrocytes against H<sub>2</sub>O<sub>2</sub>-induced apoptotic cell death <sup>73</sup>. They also reported that clusterin protects retinal pigment epithelial cells against oxidative stress via the PI3K/Akt signalling pathway <sup>74</sup>. Besides, Jun et al. found that clusterin could protect cardiomyocytes from oxidative stress-induced apoptosis by inhibiting the Akt/GSK-3 $\beta$  signalling pathway <sup>75</sup>.

Podocytes are terminally differentiated and highly specialized epithelial cells in the glomerulus, which serve as a critical component of the GFB. It has been reported that the reduced numbers of podocytes are associated with the development of diabetic nephropathy in patients with type 2 diabetes <sup>76</sup>, and changes in the structure and density of podocytes occurred in the early stages of DN <sup>77</sup>. Moreover, Weil et al. reported that podocyte detachment is correlated with albuminuria in these patients <sup>78</sup>. Zheng et al. found that the specific overexpression of metallothionein (an antioxidant protein) in podocytes reduces the podocyte damage/loss and attenuates the pathogenesis of diabetic nephropathy, which provides evidence that oxidative stress in podocytes contributes to the development of diabetic nephropathy <sup>79</sup>. Rastaldi et al. demonstrated that biotinylated clusterin can bind to podocytes via the LDL receptor and prevent PKC activation in membranous glomerulonephritis <sup>80</sup>.

#### The role of carnosinase-1 (*CNDP1*) overexpression in the progression of diabetic nephropathy

Carnosinase-1 is a dipeptidase that belongs to the M20 metalloprotease family. It is an enzyme that hydrolyses carnosine ( $\beta$ -alanyl-L-histidine). Carnosine has been suggested to have a renal protective effect with anti-oxidative <sup>81</sup>, anti-glycation <sup>82</sup>, and carbonyl scavenging <sup>83</sup> properties. Two forms of carnosinase, serum carnosinase (CN-1) and non-specific carnosine dipeptidase (CN-2), are encoded by the *CNDP1* (*CN1*) and *CNDP2* (*CN2*) genes, respectively <sup>84</sup>. *CNDP1* and *CNDP2* genes are both located on chromosome 18q22.3. Vardarli et al. demonstrated the susceptibility to type 2 diabetic nephropathy to be located at chromosome 18q22.3-q23 in a Turkish family-based linkage study <sup>85</sup>. Further research revealed an association between the

variants (five, six, or seven leucine repeats) in the leader peptide of the *CNDP1* gene and the susceptibility for diabetic nephropathy. The homozygous five-leucine allele is associated with a lower carnosinase activity, and six and seven leucine alleles are associated with a higher carnosinase activity<sup>86,87</sup>. The serum carnosinase form is present in the serum in humans but not in rodents<sup>84,88</sup>. In an experimental study, Sauerhöfer et al. generated a hCN1 transgenic *db/db* mice model by overexpression of human *CNDP1* in *db/db* mice, an animal model for T2DM. They found higher human carnosinase-1 levels and lower L-carnosine levels in the serum and significant renal hypertrophy in hCN1 transgenic *db/db* mice compared to non-transgenic *db/db* mice, which confirmed an association of the *CNDP1* variants with diabetic nephropathy<sup>89</sup>.

It has been suggested in the literature that aerobic exercise training could ameliorate renal function and attenuate renal lesions in the diverse diabetic rodent models<sup>90-93</sup>. Physical activities are also suggested to be beneficial to lower microalbuminuria excretion in type 2 diabetic patients<sup>94,95</sup>. A review from Culbertson et al. elucidated that human athletes involved in anaerobic sports have higher concentrations of carnosine in muscle, and exercise performance also increases resting muscle carnosine levels<sup>96</sup>. A higher carnosine content in the circulation was also found in the animals when physically active<sup>97,98</sup>. Carnosine is mainly present in skeletal muscle and has lower amounts in the renal tissue. The supplementation of carnosine has been shown to protect against the progression of diabetic nephropathy in different diabetic animal models<sup>83,99-101</sup>.

#### The role of leptin in the development of diabetes and diabetic nephropathy

The leptin gene was discovered in 1994<sup>102</sup>. Human leptin is a 16-kDa protein hormone encoded by the *LEP* (*ob*) gene. It is predominantly synthesized and secreted by white adipose tissue. Other organs, including placenta, stomach and skeletal muscle can also be leptin synthesis sources<sup>103</sup>. Except as a regulator of the energy homeostasis via suppressing appetite, leptin also participates in diverse physiological processes, including immune regulation<sup>104,105</sup>, endocrine regulation of the energy metabolism<sup>106</sup>, reproduction<sup>107,108</sup>, and lipid metabolism<sup>109,110</sup>.

In humans, patients lacking leptin have evident obesity and glucose tolerance impairments<sup>111,112</sup>. Leptin deficient (*ob/ob* mice)<sup>113,114</sup> and leptin receptor-deficient (*db/db* mice and Zucker diabetic fatty rats) rodents<sup>115,116</sup> are characterized by hyperphagia, obesity, hyperglycemia and insulin resistance. Growing evidence suggests that leptin therapy has a beneficial effect on glucose metabolism and insulin resistance, and it could be a promising therapy for diabetes. The initial thought of a glucose-lowering function of leptin is attributed to the secondary effects of attenuating obesity. Recent research has shown that leptin treatment could improve glucose

metabolism aberrations independent of altering body weight. For instance, Pelleymounter et al. found that a low dose of leptin (0.1mg/kg/day) can normalize the serum glucose levels without lowering body weight in *ob/ob* mice <sup>114</sup>. Furthermore, researchers demonstrated that the acute disruption of leptin signaling using the polyethylene glycosylated mouse leptin antagonist could elevate hepatic glucose production and decrease whole-body insulin sensitivity without significantly altering the body composition in C57BL/6 mice <sup>117</sup>. Yu et al. reported that leptin could reverse hyperglycemia and ketosis by suppressing the action of glucagon on the liver and improving the utilization of glucose in the skeletal muscle in insulin-deficient diabetic rodents <sup>118</sup>. Leptin also can improve insulin sensitivity through both central and peripheral systems <sup>119-121</sup>. Morton et al. found that leptin-receptor gene therapy directed at the area of the hypothalamic arcuate nucleus improves glucose intolerance and insulin sensitivity via the phosphatidylinositol-3-OH kinase signaling pathway <sup>122</sup>. These studies collectively indicated that perturbances in the leptin signaling pathway might be crucial for the development of type 2 diabetes.

Leptin is highly homologous among different species. For instance, human leptin is 83% ~84% identical to rodents' leptin. Meanwhile, the basic structural features and intracellular signaling mechanisms of leptin and its receptor also appear to be conserved throughout vertebrates <sup>123</sup>. Several studies reported that administering exogenous leptin in fish reduces food intake <sup>124-126</sup>, which has also been shown in *ob/ob* and diet-induced obese mice <sup>127</sup>, indicating the conservation of the leptin signaling system's function throughout vertebrates.

Olsen et al. demonstrated that intraperitoneal streptozotocin injection could induce hyperglycemia in adult zebrafish; these streptozotocin-induced diabetic zebrafish exhibited thickening of GBM in the kidney <sup>128</sup>. Anti-diabetic drugs effective for diabetic patients could ameliorate the hyperglycemia in the overfed zebrafish, suggesting that the glucose homeostasis pathways are conserved between zebrafish and human <sup>129</sup>. In zebrafish, there are two paralogous genes encoding leptin, called *lepa* and *lepb* <sup>130</sup>. In a previous study, our group found that the *lepb* gene, but not the *lepa* gene, is significantly downregulated in zebrafish larvae under an insulin-resistance state caused by acute hyperinsulinemia, suggesting the *lepb* might play a crucial role in insulin homeostasis in zebrafish <sup>131</sup>.

### **Nephropathic Cystinosis**

Cystinosis is a genetic disorder that follows an autosomal recessive inheritance pattern, and it belongs to the group of lysosomal storage disease disorders <sup>132</sup>. The incidence of cystinosis is 1/100,000 to 1/200,000 in live births. It is caused by deleterious mutations in the *CTNS* gene

encoding for cystinosin protein, which has an indispensable role in transporting cystine out of the lysosomes<sup>133</sup>. Defective cystine function results in the intralysosomal accumulation of cystine, which causes cell damage and organ dysfunction. The kidney, eye, muscle, liver, endocrine tissues, reproductive system and central nervous system all can be affected by cystinosis. Nephropathic cystinosis is the foremost clinical characteristic of cystinosis, known as renal Fanconi syndrome<sup>134</sup>. The inadequate reabsorption in the renal proximal tubule leads to leaking abnormal amounts of glucose, uric acid, amino acid, bicarbonate and phosphate into the urine. The proximal tubular damage can further progress to progressive glomerular damage and end-stage renal failure, eventually requiring renal replacement treatment.

Until now, the underlying mechanisms of nephropathic cystinosis remain unclear. An appropriate animal model resembling the features of human nephropathic cystinosis is crucial to understand this disease. Histopathologic features of human nephropathic cystinosis are: 1) Light microscopy: cystine crystal deposition in glomerular and tubular epithelial cells, and the interstitium; multinucleated glomerular and tubular epithelial cells, particularly involving podocytes; the unique “swan-neck” deformity in the proximal tubule. 2) Electron microscopy: cystine crystals (hexagonal, rhombohedral, or polymorphous in shape) within the interstitial macrophage and tubular epithelial cytoplasm<sup>135</sup>. Different animal models have been developed to recapitulate the features of human nephropathic cystinosis. The first *Ctns*<sup>-/-</sup> mouse model was generated in a mixed 129Sv x C57BL/6 strain<sup>136</sup>. In this *Ctns*<sup>-/-</sup> mouse model, cystine accumulation was found in kidney, liver, and muscle. However, these mice failed to develop renal proximal tubulopathy and glomerular dysfunction. Nevo and colleagues found that *Ctns*<sup>-/-</sup> mice with C57BL/6 background had an accumulation of cystine in tissues and pronounced histological renal lesions in the proximal tubules, and eventually developed chronic renal failure<sup>137</sup>. Recently, Shimizu et al. established a novel congenic *Ctns*<sup>ugl</sup> mutation on the F344 standard rat strain<sup>138</sup>. This *Ctns* mutant rat presented with renal lesions and cystine accumulation in renal tissue. Moreover, the cystine crystals in the lysosomes of the renal cortex were observed. These murine models are beneficial in revealing the pathogenic aspects of nephropathic cystinosis. However, murine models are usually time-consuming, expensive, and limited to a small number of experimental subjects. Therefore, generating less time- and cost-consuming animal models would be helpful to investigate the underlying molecular mechanism and find novel treatments for nephropathic cystinosis. In our previous study, we generated *ctns* mutant zebrafish which displayed glomerular and tubular dysfunction at the larvae stage and had significantly increased cystine levels in the kidney at the adult stage<sup>139</sup>.

### **Animal models for chronic kidney disease**

The best model to study human diseases is man itself. Since most experiments cannot ethically and practically be carried out on humans, animal models are extensively used as a representative alternative. Animal models are essential components of medical research because they provide the opportunity to understand the underlying mechanisms of diseases and assess potential novel therapeutic targets before testing in humans. Utilization of the datasets and resources from both human and animal models can lead to a better understanding of human diseases, including chronic kidney disease. A good animal disease model should meet several conditions. For instance, it has representative features of the particular human disease, is time-effective and cost-effective, and is easy to handle. Besides, the availability of molecular and genetic tools for this animal model also should be considered. Different animal models facilitate studying various aspects of a given disease since no perfect animal model for each disease exists. Choosing an optimal animal model is highly dependent on the specific hypotheses of the research.

Lacking reliable preclinical models is the major obstacle in dissecting the pathogenesis of disease and developing novel therapies for chronic kidney disease. Hence, developing new animal models of chronic kidney disease remains highly needed. Nowadays, murine models have been most widely used in studying chronic kidney disease. Since zebrafish are becoming a promising disease model <sup>140</sup>, in this thesis, we investigate whether zebrafish can be used as a disease model for chronic kidney disease.

### ***Murine models***

The genome's similarity to the human genome (99% of human and mouse genomes are conserved) makes murine models extensively used in modelling human diseases for decades <sup>141</sup>. Human and murine have many similar aspects, including anatomy, cell biology and physiology. The genetics and biology in murine models are well known, and numerous diverse tools for studying the murine models have been established. It is also possible to replace a particular mouse gene with its human counterpart, which allows the specific transgenic mouse to produce the human version of the protein <sup>142</sup>.

To date, the murine models are widely used to study the genetics and pathophysiology of chronic kidney disease (**Figure. 4A-4A''**) <sup>143</sup>. For instance, a diabetic murine model can nicely mimic many features of human diabetic nephropathy<sup>144</sup>. The albuminuria, serum creatinine, and creatinine clearance can be measured in those murine models. Based on the latest criteria published by the nephropathy subcommittee of the Animal Models of Diabetic Complications

Consortium, desirable rodent models of diabetic nephropathy should meet the following criteria:

1) The decline in GFR is greater than 50%. 2) The increase in albuminuria compared with controls for that strain at the same age and gender is greater than 10-fold. 3) Pathological features in the kidneys, advanced mesangial matrix expansion (with or without nodular sclerosis), arteriolar hyalinosis, tubulointerstitial fibrosis, podocyte loss, and demonstration of thickening of GBM by electron microscopy <sup>145-147</sup>.

However, the promising findings in murine models cannot always effectively translate into clinical trials <sup>148</sup>. Hence, developing new animal models of chronic kidney disease remains highly needed.

### ***Zebrafish model***

In 1930, zebrafish (*Danio rerio*) were used as a classical developmental and embryological model due to their rapid development and optical clarity of the embryos and larvae. Nowadays, zebrafish are gaining popularity for modelling several human diseases. Approximately 70% of human genes have orthologs in zebrafish <sup>149</sup>. Furthermore, a lot of critical molecular pathways are highly conserved between humans and zebrafish <sup>150</sup>. Therefore, zebrafish can theoretically be utilized to understand the pathogenic mechanisms of many human diseases. Zebrafish eggs are laid and fertilized externally. Therefore, they can be efficiently manipulated with various gene-editing tools. For instance, microinjection of early fertilized embryos with antisense morpholino or mRNA to change gene expression, or using CRISPR/Cas9 approach to generate knock-out or knock-in zebrafish <sup>151</sup>. Besides, zebrafish have a high fecundity; 50~300 eggs can be produced at a time <sup>152</sup>. Lower requests on space and cost for maintenance are the advantages of zebrafish compared to murine models. Another advantage of zebrafish is that they are ideal for large-scale genetic and therapeutic screening, which is limited in murine models. Naturally, mammals can form three distinct excretory organs during renal development, called pronephros, mesonephros and metanephros. Like other fish, zebrafish only develop the pronephros and mesonephros. However, the segmental anatomy of the nephron is conserved among vertebrates (**Figure. 4B-4B''**) <sup>153</sup>, which offers the possibility to study kidney diseases in zebrafish. Until now, there are not many studies using adult zebrafish as an animal model for chronic kidney disease. Considering that zebrafish might help get insights into the mechanisms and potential therapies for chronic kidney disease, a better understanding of the renal pathology of adult zebrafish is required.

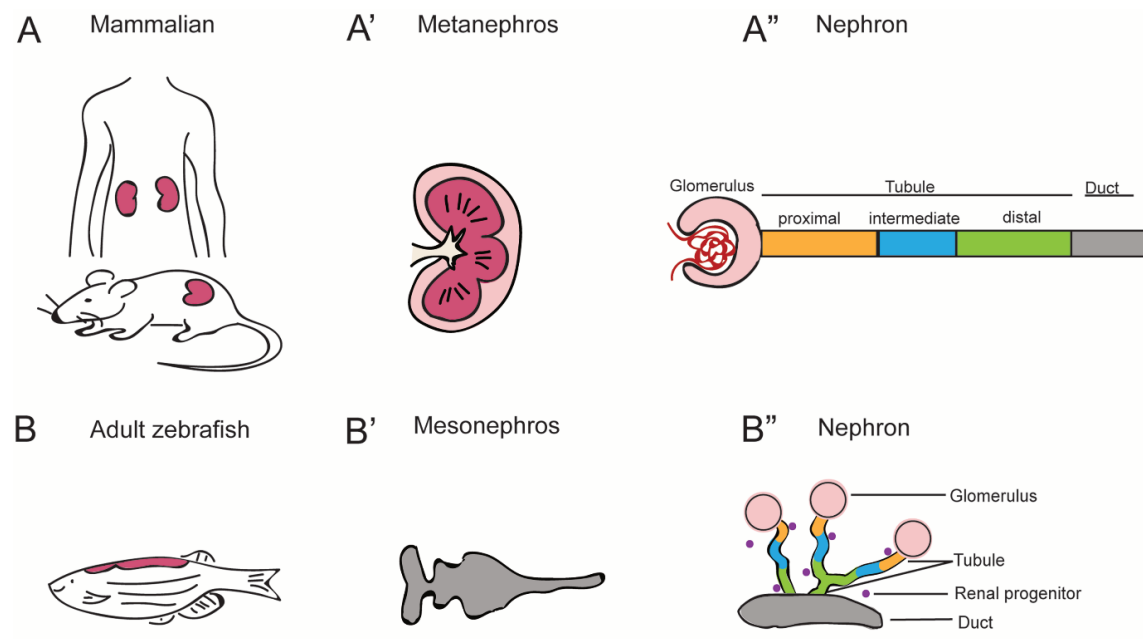


**Figure 4. The segmental composition of the nephron is conserved between vertebrates**



## Aims and outline of this thesis

The aim of this thesis is to evaluate the role of protective factors in the development of diabetic nephropathy both in clinical studies and in animal models. Understanding the role of these factors is vital for developing prevention and treatment strategies for diabetic nephropathy. Moreover, generating good animal models could provide the opportunity to understand the underlying mechanisms of chronic kidney diseases and assess potential novel therapeutic targets before clinical testing in humans. We are the first who investigate whether the *lepb* mutant and *ctns* mutant adult zebrafish model can be used for chronic kidney disease studies.

Clusterin, a glycoprotein, is upregulated in the glomeruli of patients with various forms of kidney disease. Using microarray analysis, our group found that glomerular *CLU* mRNA expression is significantly higher in diabetic nephropathy patients than in healthy individuals<sup>69</sup>. Several *in vitro* studies have demonstrated that clusterin could protect against oxidative stress-induced apoptosis. Therefore, we hypothesized that increased glomerular clusterin might protect podocytes against oxidative stress-induced damage in diabetic nephropathy. In the study described in **Chapter 2**, we examined glomerular clusterin expression in both a large cohort of patients with diabetic nephropathy and a diabetic mouse model. Also, we examined the regulation of clusterin expression in a human podocyte cell line cultured under various diabetic conditions. Finally, we investigated whether the recombinant clusterin protein can protect the podocytes against oxidative stress *in vitro*.

Carnosinase is an enzyme that hydrolyses carnosine. Previous studies have revealed an association between the variants of the *CNDPI* (*CNI*) gene and the susceptibility for diabetic nephropathy. The supplementation of carnosine has been shown to protect against the progression of diabetic nephropathy in different diabetic animal models. Compared to non-transgenic *db/db* mice, hCN1 transgenic *db/db* mice have higher human carnosinase-1 levels and lower L-carnosine levels in the serum, and significant renal hypertrophy. A higher carnosine content in the circulation was also found in the animals when physically active. Based on these findings, we hypothesized that 1) overexpressing the hCN1 or 2) chronic aerobic exercise training would have effects on the development of diabetic nephropathy. BTBR *ob/ob* mice develop pronounced diabetic nephropathy rapidly, compared to *db/db* mice<sup>154</sup>. In the study described in **Chapter 3**, we investigated the impact of these two interventions on the development of diabetic nephropathy in BTBR *ob/ob* mice.

Leptin is a hormone, which functions in the regulation of energy homeostasis via suppression of appetite. In humans, patients lacking leptin have evident obesity and glucose tolerance impairments, the hallmarks of type 2 diabetes. In a previous study, our group found that the *lepb* gene, but not the *lepa* gene, is significantly downregulated in zebrafish larvae in an insulin-resistance state caused by acute hyperinsulinemia, suggesting that *lepb* might play a crucial role in insulin homeostasis in zebrafish <sup>131</sup>. Based on mouse studies of leptin- or leptin receptor-deficient mice, we hypothesized that *lepb*-deficient zebrafish develop the pathogenic features of diabetes and diabetic nephropathy. In the study described in **Chapter 4**, we investigated whether deletion of *lepb* via CRISPR-CAS9 techniques influences the glucose homeostasis and adiposity in zebrafish and whether *lepb* deficiency contributes to the development of type 2 diabetes and diabetic nephropathy in adult zebrafish.

Cystinosis is a rare and incurable lysosomal storage disease. Mutations in the *CTNS* gene encoding for cystinosin cause defective function in lysosomal cystine transport. Some cystinosis murine models have been regenerated; however, no one resembles all the features of human nephropathic cystinosis. A *ctns* mutant zebrafish displayed glomerular and tubular dysfunction at the larvae stage and had significantly increased cystine levels in the kidney at the adult stage <sup>139</sup>. We hypothesized that the renal histopathological features of *ctns* mutant adult zebrafish resemble that of human nephropathic cystinosis. In the study described in **Chapter 5**, we characterized the *ctns* mutant adult zebrafish' renal features and compared them with the age-matched control adult zebrafish by performing histopathological examinations, including HE and PAS staining, immunohistochemistry, toluidine blue staining and transmission electron microscopy.

## References

- 1 Levey, A. S. & Coresh, J. Chronic kidney disease. *Lancet* **379**, 165-180, doi:10.1016/S0140-6736(11)60178-5 (2012).
- 2 National Kidney, F. K/DOQI clinical practice guidelines for chronic kidney disease: evaluation, classification, and stratification. *Am J Kidney Dis* **39**, S1-266 (2002).
- 3 Collaboration, G. B. D. C. K. D. Global, regional, and national burden of chronic kidney disease, 1990-2017: a systematic analysis for the Global Burden of Disease Study 2017. *Lancet* **395**, 709-733, doi:10.1016/S0140-6736(20)30045-3 (2020).
- 4 Bertram, J. F., Douglas-Denton, R. N., Diouf, B., Hughson, M. D. & Hoy, W. E. Human nephron number: implications for health and disease. *Pediatr Nephrol* **26**, 1529-1533, doi:10.1007/s00467-011-1843-8 (2011).
- 5 Satchell, S. C. & Braet, F. Glomerular endothelial cell fenestrations: an integral component of the glomerular filtration barrier. *Am J Physiol Renal Physiol* **296**, F947-956, doi:10.1152/ajprenal.90601.2008 (2009).
- 6 Singh, A. *et al.* Glomerular endothelial glycocalyx constitutes a barrier to protein permeability. *J Am Soc Nephrol* **18**, 2885-2893, doi:10.1681/ASN.2007010119 (2007).
- 7 Friden, V. *et al.* The glomerular endothelial cell coat is essential for glomerular filtration. *Kidney Int* **79**, 1322-1330, doi:10.1038/ki.2011.58 (2011).
- 8 Salmon, A. H. & Satchell, S. C. Endothelial glycocalyx dysfunction in disease: albuminuria and increased microvascular permeability. *J Pathol* **226**, 562-574, doi:10.1002/path.3964 (2012).
- 9 Nieuwdorp, M. *et al.* Endothelial glycocalyx damage coincides with microalbuminuria in type 1 diabetes. *Diabetes* **55**, 1127-1132, doi:10.2337/diabetes.55.04.06.db05-1619 (2006).
- 10 Nieuwdorp, M. *et al.* Loss of endothelial glycocalyx during acute hyperglycemia coincides with endothelial dysfunction and coagulation activation in vivo. *Diabetes* **55**, 480-486, doi:10.2337/diabetes.55.02.06.db05-1103 (2006).
- 11 Timpl, R. Structure and biological activity of basement membrane proteins. *Eur J Biochem* **180**, 487-502, doi:10.1111/j.1432-1033.1989.tb14673.x (1989).
- 12 Hudson, B. G. *et al.* The pathogenesis of Alport syndrome involves type IV collagen molecules containing the alpha 3(IV) chain: evidence from anti-GBM nephritis after renal transplantation. *Kidney Int* **42**, 179-187, doi:10.1038/ki.1992.276 (1992).
- 13 Poschl, E. *et al.* Collagen IV is essential for basement membrane stability but dispensable for initiation of its assembly during early development. *Development* **131**, 1619-1628, doi:10.1242/dev.01037 (2004).
- 14 Matejas, V. *et al.* Mutations in the human laminin beta2 (LAMB2) gene and the associated phenotypic spectrum. *Hum Mutat* **31**, 992-1002, doi:10.1002/humu.21304 (2010).
- 15 Shannon, M. B., Patton, B. L., Harvey, S. J. & Miner, J. H. A hypomorphic mutation in the mouse laminin alpha5 gene causes polycystic kidney disease. *J Am Soc Nephrol* **17**, 1913-1922, doi:10.1681/ASN.2005121298 (2006).
- 16 Miner, J. H. The glomerular basement membrane. *Exp Cell Res* **318**, 973-978, doi:10.1016/j.yexcr.2012.02.031 (2012).
- 17 Kanwar, Y. S., Danesh, F. R. & Chugh, S. S. Contribution of proteoglycans towards the integrated functions of renal glomerular capillaries: a historical perspective. *Am J Pathol* **171**, 9-13, doi:10.2353/ajpath.2007.070356 (2007).
- 18 Harvey, S. J. *et al.* Disruption of glomerular basement membrane charge through podocyte-specific mutation of agrin does not alter glomerular permselectivity. *Am J Pathol* **171**, 139-152, doi:10.2353/ajpath.2007.061116 (2007).
- 19 Goldberg, S., Harvey, S. J., Cunningham, J., Tryggvason, K. & Miner, J. H. Glomerular filtration is normal in the absence of both agrin and perlecan-heparan sulfate from the glomerular basement membrane. *Nephrol Dial Transplant* **24**, 2044-2051, doi:10.1093/ndt/gfn758 (2009).
- 20 van den Hoven, M. J. *et al.* Reduction of anionic sites in the glomerular basement membrane by heparanase does not lead to proteinuria. *Kidney Int* **73**, 278-287, doi:10.1038/sj.ki.5002706 (2008).

- 21 Kriz, W. *et al.* A role for podocytes to counteract capillary wall distension. *Kidney Int* **45**, 369-376, doi:10.1038/ki.1994.47 (1994).
- 22 Kawachi, H. *et al.* Role of podocyte slit diaphragm as a filtration barrier. *Nephrology (Carlton)* **11**, 274-281, doi:10.1111/j.1440-1797.2006.00583.x (2006).
- 23 Grahammer, F., Schell, C. & Huber, T. B. The podocyte slit diaphragm--from a thin grey line to a complex signalling hub. *Nat Rev Nephrol* **9**, 587-598, doi:10.1038/nrneph.2013.169 (2013).
- 24 Stockand, J. D. & Sansom, S. C. Glomerular mesangial cells: electrophysiology and regulation of contraction. *Physiol Rev* **78**, 723-744, doi:10.1152/physrev.1998.78.3.723 (1998).
- 25 Floege, J. *et al.* Increased synthesis of extracellular matrix in mesangial proliferative nephritis. *Kidney Int* **40**, 477-488, doi:10.1038/ki.1991.235 (1991).
- 26 Cove-Smith, A. & Hendry, B. M. The regulation of mesangial cell proliferation. *Nephron Exp Nephrol* **108**, e74-79, doi:10.1159/000127359 (2008).
- 27 Fioretto, P. & Mauer, M. Histopathology of diabetic nephropathy. *Semin Nephrol* **27**, 195-207, doi:10.1016/j.semnephrol.2007.01.012 (2007).
- 28 Webster, A. C., Nagler, E. V., Morton, R. L. & Masson, P. Chronic Kidney Disease. *Lancet* **389**, 1238-1252, doi:10.1016/S0140-6736(16)32064-5 (2017).
- 29 Malyszko, J. Mechanism of endothelial dysfunction in chronic kidney disease. *Clin Chim Acta* **411**, 1412-1420, doi:10.1016/j.cca.2010.06.019 (2010).
- 30 Zoccali, C. Endothelial dysfunction and the kidney: emerging risk factors for renal insufficiency and cardiovascular outcomes in essential hypertension. *J Am Soc Nephrol* **17**, S61-63, doi:10.1681/ASN.2005121344 (2006).
- 31 Yau, J. W., Teoh, H. & Verma, S. Endothelial cell control of thrombosis. *BMC Cardiovasc Disord* **15**, 130, doi:10.1186/s12872-015-0124-z (2015).
- 32 Siddiqi, F. S. & Advani, A. Endothelial-podocyte crosstalk: the missing link between endothelial dysfunction and albuminuria in diabetes. *Diabetes* **62**, 3647-3655, doi:10.2337/db13-0795 (2013).
- 33 Sol, M. *et al.* Glomerular Endothelial Cells as Instigators of Glomerular Sclerotic Diseases. *Front Pharmacol* **11**, 573557, doi:10.3389/fphar.2020.573557 (2020).
- 34 Tufro, A. & Veron, D. VEGF and podocytes in diabetic nephropathy. *Semin Nephrol* **32**, 385-393, doi:10.1016/j.semnephrol.2012.06.010 (2012).
- 35 Eremina, V. *et al.* Glomerular-specific alterations of VEGF-A expression lead to distinct congenital and acquired renal diseases. *The Journal of clinical investigation* **111**, 707-716, doi:10.1172/JCI17423 (2003).
- 36 Maynard, S. E. *et al.* Excess placental soluble fms-like tyrosine kinase 1 (sFlt1) may contribute to endothelial dysfunction, hypertension, and proteinuria in preeclampsia. *The Journal of clinical investigation* **111**, 649-658, doi:10.1172/JCI17189 (2003).
- 37 Alsaad, K. O. & Herzenberg, A. M. Distinguishing diabetic nephropathy from other causes of glomerulosclerosis: an update. *J Clin Pathol* **60**, 18-26, doi:10.1136/jcp.2005.035592 (2007).
- 38 Hodgkins, K. S. & Schnaper, H. W. Tubulointerstitial injury and the progression of chronic kidney disease. *Pediatr Nephrol* **27**, 901-909, doi:10.1007/s00467-011-1992-9 (2012).
- 39 Abbate, M., Zoja, C. & Remuzzi, G. How does proteinuria cause progressive renal damage? *J Am Soc Nephrol* **17**, 2974-2984, doi:10.1681/ASN.2006040377 (2006).
- 40 Nathan, C. F. Secretory products of macrophages. *The Journal of clinical investigation* **79**, 319-326, doi:10.1172/JCI112815 (1987).
- 41 Genovese, F., Manresa, A. A., Leeming, D. J., Karsdal, M. A. & Boor, P. The extracellular matrix in the kidney: a source of novel non-invasive biomarkers of kidney fibrosis? *Fibrogenesis Tissue Repair* **7**, 4, doi:10.1186/1755-1536-7-4 (2014).
- 42 Bulow, R. D. & Boor, P. Extracellular Matrix in Kidney Fibrosis: More Than Just a Scaffold. *J Histochem Cytochem* **67**, 643-661, doi:10.1369/0022155419849388 (2019).
- 43 Hewitson, T. D. Fibrosis in the kidney: is a problem shared a problem halved? *Fibrogenesis Tissue Repair* **5**, S14, doi:10.1186/1755-1536-5-S1-S14 (2012).
- 44 Eddy, A. A. Molecular basis of renal fibrosis. *Pediatr Nephrol* **15**, 290-301, doi:10.1007/s004670000461 (2000).
- 45 Giacco, F. & Brownlee, M. Oxidative stress and diabetic complications. *Circ Res* **107**, 1058-1070, doi:10.1161/CIRCRESAHA.110.223545 (2010).

- 46 Martindale, J. L. & Holbrook, N. J. Cellular response to oxidative stress: signaling for suicide and survival. *J Cell Physiol* **192**, 1-15, doi:10.1002/jcp.10119 (2002).
- 47 Cross, C. E. *et al.* Oxygen radicals and human disease. *Ann Intern Med* **107**, 526-545, doi:10.7326/0003-4819-107-4-526 (1987).
- 48 Droge, W. Free radicals in the physiological control of cell function. *Physiol Rev* **82**, 47-95, doi:10.1152/physrev.00018.2001 (2002).
- 49 Gross, J. L. *et al.* Diabetic nephropathy: diagnosis, prevention, and treatment. *Diabetes Care* **28**, 164-176, doi:10.2337/diacare.28.1.164 (2005).
- 50 Mogensen, C. E., Christensen, C. K. & Vittinghus, E. The stages in diabetic renal disease. With emphasis on the stage of incipient diabetic nephropathy. *Diabetes* **32 Suppl 2**, 64-78, doi:10.2337/diab.32.2.s64 (1983).
- 51 Tervaert, T. W. *et al.* Pathologic classification of diabetic nephropathy. *J Am Soc Nephrol* **21**, 556-563, doi:10.1681/ASN.2010010010 (2010).
- 52 Klessens, C. Q. *et al.* An autopsy study suggests that diabetic nephropathy is underdiagnosed. *Kidney Int* **90**, 149-156, doi:10.1016/j.kint.2016.01.023 (2016).
- 53 Krolewski, A. S., Warram, J. H., Rand, L. I. & Kahn, C. R. Epidemiologic approach to the etiology of type I diabetes mellitus and its complications. *N Engl J Med* **317**, 1390-1398, doi:10.1056/NEJM198711263172206 (1987).
- 54 Seaquist, E. R., Goetz, F. C., Rich, S. & Barbosa, J. Familial clustering of diabetic kidney disease. Evidence for genetic susceptibility to diabetic nephropathy. *N Engl J Med* **320**, 1161-1165, doi:10.1056/NEJM198905043201801 (1989).
- 55 Pettitt, D. J., Saad, M. F., Bennett, P. H., Nelson, R. G. & Knowler, W. C. Familial predisposition to renal disease in two generations of Pima Indians with type 2 (non-insulin-dependent) diabetes mellitus. *Diabetologia* **33**, 438-443, doi:10.1007/BF00404096 (1990).
- 56 Freedman, B. I., Bostrom, M., Daeihagh, P. & Bowden, D. W. Genetic factors in diabetic nephropathy. *Clin J Am Soc Nephrol* **2**, 1306-1316, doi:10.2215/CJN.02560607 (2007).
- 57 Mooyaart, A. L. *et al.* Genetic associations in diabetic nephropathy: a meta-analysis. *Diabetologia* **54**, 544-553, doi:10.1007/s00125-010-1996-1 (2011).
- 58 Kim, B. M. *et al.* Clusterin induces differentiation of pancreatic duct cells into insulin-secreting cells. *Diabetologia* **49**, 311-320, doi:10.1007/s00125-005-0106-2 (2006).
- 59 de Silva, H. V. *et al.* A 70-kDa apolipoprotein designated ApoJ is a marker for subclasses of human plasma high density lipoproteins. *J Biol Chem* **265**, 13240-13247 (1990).
- 60 Heo, J. Y. *et al.* Clusterin deficiency induces lipid accumulation and tissue damage in kidney. *The Journal of endocrinology* **237**, 175-191, doi:10.1530/JOE-17-0453 (2018).
- 61 Jenne, D. E. & Tschopp, J. Molecular structure and functional characterization of a human complement cytotoxicity inhibitor found in blood and seminal plasma: identity to sulfated glycoprotein 2, a constituent of rat testis fluid. *Proc Natl Acad Sci U S A* **86**, 7123-7127 (1989).
- 62 Jones, S. E. & Jomary, C. Clusterin. *Int J Biochem Cell Biol* **34**, 427-431 (2002).
- 63 Pereira, R. M. *et al.* Protective molecular mechanisms of clusterin against apoptosis in cardiomyocytes. *Heart Fail Rev* **23**, 123-129, doi:10.1007/s10741-017-9654-z (2018).
- 64 Koltai, T. Clusterin: a key player in cancer chemoresistance and its inhibition. *Onco Targets Ther* **7**, 447-456, doi:10.2147/OTT.S58622 (2014).
- 65 Trougakos, I. P. & Gonos, E. S. Clusterin/apolipoprotein J in human aging and cancer. *Int J Biochem Cell Biol* **34**, 1430-1448, doi:10.1016/s1357-2725(02)00041-9 (2002).
- 66 Jeong, S. *et al.* Interaction of clusterin and matrix metalloproteinase-9 and its implication for epithelial homeostasis and inflammation. *Am J Pathol* **180**, 2028-2039, doi:10.1016/j.ajpath.2012.01.025 (2012).
- 67 Foster, E. M., Dangla-Valls, A., Lovestone, S., Ribe, E. M. & Buckley, N. J. Clusterin in Alzheimer's Disease: Mechanisms, Genetics, and Lessons From Other Pathologies. *Front Neurosci* **13**, 164, doi:10.3389/fnins.2019.00164 (2019).
- 68 Daimon, M. *et al.* Association of the clusterin gene polymorphisms with type 2 diabetes mellitus. *Metabolism* **60**, 815-822, doi:10.1016/j.metabol.2010.07.033 (2011).
- 69 Baelde, H. J. *et al.* Gene expression profiling in glomeruli from human kidneys with diabetic nephropathy. *Am J Kidney Dis* **43**, 636-650 (2004).

- 70 Nakatani, S. *et al.* Proteome analysis of laser microdissected glomeruli from formalin-fixed paraffin-embedded kidneys of autopsies of diabetic patients: nephronectin is associated with the development of diabetic glomerulosclerosis. *Nephrol Dial Transplant* **27**, 1889-1897, doi:10.1093/ndt/gfr682 (2012).
- 71 Asmat, U., Abad, K. & Ismail, K. Diabetes mellitus and oxidative stress-A concise review. *Saudi Pharm J* **24**, 547-553, doi:10.1016/j.jsps.2015.03.013 (2016).
- 72 Schwochau, G. B., Nath, K. A. & Rosenberg, M. E. Clusterin protects against oxidative stress in vitro through aggregative and nonaggregative properties. *Kidney Int* **53**, 1647-1653, doi:10.1046/j.1523-1755.1998.00902.x (1998).
- 73 Kim, J. H., Kim, J. H., Yu, Y. S., Min, B. H. & Kim, K. W. The role of clusterin in retinal development and free radical damage. *Br J Ophthalmol* **91**, 1541-1546, doi:10.1136/bjo.2007.115220 (2007).
- 74 Kim, J. H. *et al.* Protective effect of clusterin from oxidative stress-induced apoptosis in human retinal pigment epithelial cells. *Invest Ophthalmol Vis Sci* **51**, 561-566, doi:10.1167/iovs.09-3774 (2010).
- 75 Jun, H. O. *et al.* Clusterin protects H9c2 cardiomyocytes from oxidative stress-induced apoptosis via Akt/GSK-3 $\beta$  signaling pathway. *Exp Mol Med* **43**, 53-61, doi:10.3858/emmm.2011.43.1.006 (2011).
- 76 Pagtalunan, M. E. *et al.* Podocyte loss and progressive glomerular injury in type II diabetes. *The Journal of clinical investigation* **99**, 342-348, doi:10.1172/JCI119163 (1997).
- 77 Dalla Vestra, M. *et al.* Is podocyte injury relevant in diabetic nephropathy? Studies in patients with type 2 diabetes. *Diabetes* **52**, 1031-1035, doi:10.2337/diabetes.52.4.1031 (2003).
- 78 Weil, E. J. *et al.* Podocyte detachment and reduced glomerular capillary endothelial fenestration promote kidney disease in type 2 diabetic nephropathy. *Kidney Int* **82**, 1010-1017, doi:10.1038/ki.2012.234 (2012).
- 79 Zheng, S. *et al.* Podocyte-specific overexpression of the antioxidant metallothionein reduces diabetic nephropathy. *J Am Soc Nephrol* **19**, 2077-2085, doi:10.1681/ASN.2007080967 (2008).
- 80 Rastaldi, M. P. *et al.* Glomerular clusterin is associated with PKC- $\alpha$ / $\beta$  regulation and good outcome of membranous glomerulonephritis in humans. *Kidney Int* **70**, 477-485, doi:10.1038/sj.ki.5001563 (2006).
- 81 Boldyrev, A. A., Stvolinsky, S. L., Fedorova, T. N. & Suslina, Z. A. Carnosine as a natural antioxidant and geroprotector: from molecular mechanisms to clinical trials. *Rejuvenation Res* **13**, 156-158, doi:10.1089/rej.2009.0923 (2010).
- 82 Hipkiss, A. R. Glycation, ageing and carnosine: are carnivorous diets beneficial? *Mech Ageing Dev* **126**, 1034-1039, doi:10.1016/j.mad.2005.05.002 (2005).
- 83 Aldini, G. *et al.* The carbonyl scavenger carnosine ameliorates dyslipidaemia and renal function in Zucker obese rats. *J Cell Mol Med* **15**, 1339-1354, doi:10.1111/j.1582-4934.2010.01101.x (2011).
- 84 Teufel, M. *et al.* Sequence identification and characterization of human carnosinase and a closely related non-specific dipeptidase. *J Biol Chem* **278**, 6521-6531, doi:10.1074/jbc.M209764200 (2003).
- 85 Vardarli, I. *et al.* Gene for susceptibility to diabetic nephropathy in type 2 diabetes maps to 18q22.3-23. *Kidney Int* **62**, 2176-2183, doi:10.1046/j.1523-1755.2002.00663.x (2002).
- 86 Janssen, B. *et al.* Carnosine as a protective factor in diabetic nephropathy: association with a leucine repeat of the carnosinase gene CNDP1. *Diabetes* **54**, 2320-2327, doi:10.2337/diabetes.54.8.2320 (2005).
- 87 Ahluwalia, T. S., Lindholm, E. & Groop, L. C. Common variants in CNDP1 and CNDP2, and risk of nephropathy in type 2 diabetes. *Diabetologia* **54**, 2295-2302, doi:10.1007/s00125-011-2178-5 (2011).
- 88 Margolis, F. L. & Grillo, M. Inherited differences in mouse kidney carnosinase activity. *Biochem Genet* **22**, 441-451, doi:10.1007/BF00484515 (1984).
- 89 Sauerhofer, S. *et al.* L-carnosine, a substrate of carnosinase-1, influences glucose metabolism. *Diabetes* **56**, 2425-2432, doi:10.2337/db07-0177 (2007).

- 90 Martinez, R. *et al.* Aerobic interval exercise improves renal functionality and affects mineral metabolism in obese Zucker rats. *Am J Physiol Renal Physiol* **316**, F90-F100, doi:10.1152/ajprenal.00356.2018 (2019).
- 91 Ward, K. M., Mahan, J. D. & Sherman, W. M. Aerobic training and diabetic nephropathy in the obese Zucker rat. *Ann Clin Lab Sci* **24**, 266-277 (1994).
- 92 Rodrigues, A. M. *et al.* Effects of training and nitric oxide on diabetic nephropathy progression in type I diabetic rats. *Exp Biol Med (Maywood)* **236**, 1180-1187, doi:10.1258/ebm.2011.011005 (2011).
- 93 Tufescu, A. *et al.* Combination of exercise and losartan enhances renoprotective and peripheral effects in spontaneously type 2 diabetes mellitus rats with nephropathy. *J Hypertens* **26**, 312-321, doi:10.1097/HJH.0b013e3282f2450b (2008).
- 94 Calle-Pascual, A. L., Martin-Alvarez, P. J., Reyes, C. & Calle, J. R. Regular physical activity and reduced occurrence of microalbuminuria in type 2 diabetic patients. *Diabete Metab* **19**, 304-309 (1993).
- 95 Lazarevic, G. *et al.* Effects of aerobic exercise on microalbuminuria and enzymuria in type 2 diabetic patients. *Ren Fail* **29**, 199-205, doi:10.1080/08860220601098870 (2007).
- 96 Culbertson, J. Y., Kreider, R. B., Greenwood, M. & Cooke, M. Effects of beta-alanine on muscle carnosine and exercise performance: a review of the current literature. *Nutrients* **2**, 75-98, doi:10.3390/nu2010075 (2010).
- 97 Dunnett, M., Harris, R. C., Dunnett, C. E. & Harris, P. A. Plasma carnosine concentration: diurnal variation and effects of age, exercise and muscle damage. *Equine Vet J Suppl*, 283-287, doi:10.1111/j.2042-3306.2002.tb05434.x (2002).
- 98 Nagai, K. *et al.* Possible role of L-carnosine in the regulation of blood glucose through controlling autonomic nerves. *Exp Biol Med (Maywood)* **228**, 1138-1145, doi:10.1177/153537020322801007 (2003).
- 99 Albrecht, T. *et al.* Carnosine Attenuates the Development of both Type 2 Diabetes and Diabetic Nephropathy in BTBR ob/ob Mice. *Sci Rep* **7**, 44492, doi:10.1038/srep44492 (2017).
- 100 Peters, V. *et al.* Carnosine treatment in combination with ACE inhibition in diabetic rats. *Regul Pept* **194-195**, 36-40, doi:10.1016/j.regpep.2014.09.005 (2014).
- 101 Peters, V. *et al.* Carnosine treatment largely prevents alterations of renal carnosine metabolism in diabetic mice. *Amino Acids* **42**, 2411-2416, doi:10.1007/s00726-011-1046-4 (2012).
- 102 Zhang, Y. *et al.* Positional cloning of the mouse obese gene and its human homologue. *Nature* **372**, 425-432, doi:10.1038/372425a0 (1994).
- 103 Ahima, R. S. & Flier, J. S. Leptin. *Annu Rev Physiol* **62**, 413-437, doi:10.1146/annurev.physiol.62.1.413 (2000).
- 104 Lord, G. M. *et al.* Leptin modulates the T-cell immune response and reverses starvation-induced immunosuppression. *Nature* **394**, 897-901, doi:10.1038/29795 (1998).
- 105 Matarese, G., Moschos, S. & Mantzoros, C. S. Leptin in immunology. *J Immunol* **174**, 3137-3142, doi:10.4049/jimmunol.174.6.3137 (2005).
- 106 Meier, U. & Gressner, A. M. Endocrine regulation of energy metabolism: review of pathobiochemical and clinical chemical aspects of leptin, ghrelin, adiponectin, and resistin. *Clin Chem* **50**, 1511-1525, doi:10.1373/clinchem.2004.032482 (2004).
- 107 Caprio, M., Fabbri, E., Isidori, A. M., Aversa, A. & Fabbri, A. Leptin in reproduction. *Trends Endocrinol Metab* **12**, 65-72, doi:10.1016/s1043-2760(00)00352-0 (2001).
- 108 Licinio, J. *et al.* Phenotypic effects of leptin replacement on morbid obesity, diabetes mellitus, hypogonadism, and behavior in leptin-deficient adults. *Proc Natl Acad Sci U S A* **101**, 4531-4536, doi:10.1073/pnas.0308767101 (2004).
- 109 Prieur, X. *et al.* Leptin regulates peripheral lipid metabolism primarily through central effects on food intake. *Endocrinology* **149**, 5432-5439, doi:10.1210/en.2008-0498 (2008).
- 110 Hackl, M. T. *et al.* Brain leptin reduces liver lipids by increasing hepatic triglyceride secretion and lowering lipogenesis. *Nat Commun* **10**, 2717, doi:10.1038/s41467-019-10684-1 (2019).
- 111 Farooqi, I. S. *et al.* Effects of recombinant leptin therapy in a child with congenital leptin deficiency. *N Engl J Med* **341**, 879-884, doi:10.1056/NEJM199909163411204 (1999).
- 112 Funcke, J. B. *et al.* Monogenic forms of childhood obesity due to mutations in the leptin gene. *Mol Cell Pediatr* **1**, 3, doi:10.1186/s40348-014-0003-1 (2014).

- 113 Coleman, D. L. Obese and diabetes: two mutant genes causing diabetes-obesity syndromes in mice. *Diabetologia* **14**, 141-148, doi:10.1007/BF00429772 (1978).
- 114 Pellemounter, M. A. *et al.* Effects of the obese gene product on body weight regulation in ob/ob mice. *Science* **269**, 540-543, doi:10.1126/science.7624776 (1995).
- 115 Chen, H. *et al.* Evidence that the diabetes gene encodes the leptin receptor: identification of a mutation in the leptin receptor gene in db/db mice. *Cell* **84**, 491-495, doi:10.1016/s0092-8674(00)81294-5 (1996).
- 116 Argiles, J. M. The obese Zucker rat: a choice for fat metabolism 1968-1988: twenty years of research on the insights of the Zucker mutation. *Prog Lipid Res* **28**, 53-66, doi:10.1016/0163-7827(89)90007-6 (1989).
- 117 Levi, J. *et al.* Acute disruption of leptin signaling in vivo leads to increased insulin levels and insulin resistance. *Endocrinology* **152**, 3385-3395, doi:10.1210/en.2011-0185 (2011).
- 118 Yu, X., Park, B. H., Wang, M. Y., Wang, Z. V. & Unger, R. H. Making insulin-deficient type 1 diabetic rodents thrive without insulin. *Proc Natl Acad Sci U S A* **105**, 14070-14075, doi:10.1073/pnas.0806993105 (2008).
- 119 Shimomura, I., Hammer, R. E., Ikemoto, S., Brown, M. S. & Goldstein, J. L. Leptin reverses insulin resistance and diabetes mellitus in mice with congenital lipodystrophy. *Nature* **401**, 73-76, doi:10.1038/43448 (1999).
- 120 German, J. *et al.* Hypothalamic leptin signaling regulates hepatic insulin sensitivity via a neurocircuit involving the vagus nerve. *Endocrinology* **150**, 4502-4511, doi:10.1210/en.2009-0445 (2009).
- 121 Paz-Filho, G., Mastronardi, C., Wong, M. L. & Licinio, J. Leptin therapy, insulin sensitivity, and glucose homeostasis. *Indian J Endocrinol Metab* **16**, S549-S555, doi:10.4103/2230-8210.105571 (2012).
- 122 Morton, G. J. *et al.* Leptin regulates insulin sensitivity via phosphatidylinositol-3-OH kinase signaling in mediobasal hypothalamic neurons. *Cell Metab* **2**, 411-420, doi:10.1016/j.cmet.2005.10.009 (2005).
- 123 Denver, R. J., Bonett, R. M. & Boorse, G. C. Evolution of leptin structure and function. *Neuroendocrinology* **94**, 21-38, doi:10.1159/000328435 (2011).
- 124 Volkoff, H., Eykelbosh, A. J. & Peter, R. E. Role of leptin in the control of feeding of goldfish *Carassius auratus*: interactions with cholecystokinin, neuropeptide Y and orexin A, and modulation by fasting. *Brain Res* **972**, 90-109, doi:10.1016/s0006-8993(03)02507-1 (2003).
- 125 Murashita, K., Uji, S., Yamamoto, T., Ronnestad, I. & Kurokawa, T. Production of recombinant leptin and its effects on food intake in rainbow trout (*Oncorhynchus mykiss*). *Comp Biochem Physiol B Biochem Mol Biol* **150**, 377-384, doi:10.1016/j.cbpb.2008.04.007 (2008).
- 126 Aguilar, A. J., Conde-Sieira, M., Lopez-Patino, M. A., Miguez, J. M. & Soengas, J. L. In vitro leptin treatment of rainbow trout hypothalamus and hindbrain affects glucosensing and gene expression of neuropeptides involved in food intake regulation. *Peptides* **32**, 232-240, doi:10.1016/j.peptides.2010.11.007 (2011).
- 127 Campfield, L. A., Smith, F. J., Guisez, Y., Devos, R. & Burn, P. Recombinant mouse OB protein: evidence for a peripheral signal linking adiposity and central neural networks. *Science* **269**, 546-549, doi:10.1126/science.7624778 (1995).
- 128 Olsen, A. S., Sarras, M. P., Jr. & Intine, R. V. Limb regeneration is impaired in an adult zebrafish model of diabetes mellitus. *Wound Repair Regen* **18**, 532-542, doi:10.1111/j.1524-475X.2010.00613.x (2010).
- 129 Zang, L., Shimada, Y. & Nishimura, N. Development of a Novel Zebrafish Model for Type 2 Diabetes Mellitus. *Sci Rep* **7**, 1461, doi:10.1038/s41598-017-01432-w (2017).
- 130 Gorissen, M., Bernier, N. J., Nabuurs, S. B., Flik, G. & Huising, M. O. Two divergent leptin paralogues in zebrafish (*Danio rerio*) that originate early in teleostean evolution. *The Journal of endocrinology* **201**, 329-339, doi:10.1677/JOE-09-0034 (2009).
- 131 Marin-Juez, R., Jong-Raadsen, S., Yang, S. & Spaink, H. P. Hyperinsulinemia induces insulin resistance and immune suppression via Ptpn6/Shp1 in zebrafish. *The Journal of endocrinology* **222**, 229-241, doi:10.1530/JOE-14-0178 (2014).
- 132 Nesterova, G. & Gahl, W. A. Cystinosis: the evolution of a treatable disease. *Pediatr Nephrol* **28**, 51-59, doi:10.1007/s00467-012-2242-5 (2013).



- 133 Town, M. *et al.* A novel gene encoding an integral membrane protein is mutated in nephropathic cystinosis. *Nat Genet* **18**, 319-324, doi:10.1038/ng0498-319 (1998).
- 134 Cherqui, S. & Courtoy, P. J. The renal Fanconi syndrome in cystinosis: pathogenic insights and therapeutic perspectives. *Nat Rev Nephrol* **13**, 115-131, doi:10.1038/nrneph.2016.182 (2017).
- 135 Lusco, M. A., Najafian, B., Alpers, C. E. & Fogo, A. B. AJKD Atlas of Renal Pathology: Cystinosis. *Am J Kidney Dis* **70**, e23-e24, doi:10.1053/j.ajkd.2017.10.002 (2017).
- 136 Cherqui, S. *et al.* Intralysosomal cystine accumulation in mice lacking cystinosis, the protein defective in cystinosis. *Mol Cell Biol* **22**, 7622-7632, doi:10.1128/mcb.22.21.7622-7632.2002 (2002).
- 137 Nevo, N. *et al.* Renal phenotype of the cystinosis mouse model is dependent upon genetic background. *Nephrol Dial Transplant* **25**, 1059-1066, doi:10.1093/ndt/gfp553 (2010).
- 138 Shimizu, Y. *et al.* A deletion in the Ctns gene causes renal tubular dysfunction and cystine accumulation in LEA/Tohm rats. *Mamm Genome* **30**, 23-33, doi:10.1007/s00335-018-9790-3 (2019).
- 139 Elmonem, M. A. *et al.* Cystinosis (ctns) zebrafish mutant shows pronephric glomerular and tubular dysfunction. *Sci Rep* **7**, 42583, doi:10.1038/srep42583 (2017).
- 140 Dooley, K. & Zon, L. I. Zebrafish: a model system for the study of human disease. *Curr Opin Genet Dev* **10**, 252-256, doi:10.1016/s0959-437x(00)00074-5 (2000).
- 141 Guenet, J. L. The mouse genome. *Genome Res* **15**, 1729-1740, doi:10.1101/gr.3728305 (2005).
- 142 Birmingham, D. J., Rovin, B. H., Yu, C. Y. & Hebert, L. A. Of mice and men: the relevance of the mouse to the study of human SLE. *Immunol Res* **24**, 211-224, doi:10.1385/IR.24:2:211 (2001).
- 143 Korstanje, R. & DiPetrillo, K. Unraveling the genetics of chronic kidney disease using animal models. *Am J Physiol Renal Physiol* **287**, F347-352, doi:10.1152/ajprenal.00159.2004 (2004).
- 144 Betz, B. & Conway, B. R. An Update on the Use of Animal Models in Diabetic Nephropathy Research. *Curr Diab Rep* **16**, 18, doi:10.1007/s11892-015-0706-2 (2016).
- 145 Breyer, M. D. *et al.* Mouse models of diabetic nephropathy. *J Am Soc Nephrol* **16**, 27-45, doi:10.1681/ASN.2004080648 (2005).
- 146 Brosius, F. C., 3rd *et al.* Mouse models of diabetic nephropathy. *J Am Soc Nephrol* **20**, 2503-2512, doi:10.1681/ASN.2009070721 (2009).
- 147 Alpers, C. E. & Hudkins, K. L. Mouse models of diabetic nephropathy. *Curr Opin Nephrol Hypertens* **20**, 278-284, doi:10.1097/MNH.0b013e3283451901 (2011).
- 148 Mak, I. W., Evaniew, N. & Ghert, M. Lost in translation: animal models and clinical trials in cancer treatment. *Am J Transl Res* **6**, 114-118 (2014).
- 149 Howe, K. *et al.* The zebrafish reference genome sequence and its relationship to the human genome. *Nature* **496**, 498-503, doi:10.1038/nature12111 (2013).
- 150 Shehwana, H. & Konu, O. Comparative Transcriptomics Between Zebrafish and Mammals: A Roadmap for Discovery of Conserved and Unique Signaling Pathways in Physiology and Disease. *Front Cell Dev Biol* **7**, 5, doi:10.3389/fcell.2019.00005 (2019).
- 151 Liu, K., Petree, C., Requena, T., Varshney, P. & Varshney, G. K. Expanding the CRISPR Toolbox in Zebrafish for Studying Development and Disease. *Front Cell Dev Biol* **7**, 13, doi:10.3389/fcell.2019.00013 (2019).
- 152 Hill, A. J., Teraoka, H., Heideman, W. & Peterson, R. E. Zebrafish as a model vertebrate for investigating chemical toxicity. *Toxicol Sci* **86**, 6-19, doi:10.1093/toxsci/kfi110 (2005).
- 153 McCampbell, K. K. & Wingert, R. A. New tides: using zebrafish to study renal regeneration. *Transl Res* **163**, 109-122, doi:10.1016/j.trsl.2013.10.003 (2014).
- 154 Hudkins, K. L. *et al.* BTBR Ob/Ob mutant mice model progressive diabetic nephropathy. *J Am Soc Nephrol* **21**, 1533-1542, doi:10.1681/ASN.2009121290 (2010).



## Chapter 2

### Glomerular clusterin expression is increased in diabetic nephropathy and protects against oxidative stress–induced apoptosis in podocytes

Junling He, Kyra L Dijkstra, Kim Bakker, Pascal Bus, Jan A. Bruijn, Marion

Scharpfenecker, Hans J. Baelde.

*Sci Rep.* 2020; 10(1):14888.



## Abstract

Clusterin, a glycoprotein encoded by the *CLU* gene, is expressed in many tissues, including the kidney, and clusterin expression is upregulated in the glomeruli of patients with various forms of kidney disease. Here, we investigated the role of clusterin in diabetic nephropathy (DN).

In this study, we found that glomerular clusterin expression was increased in both patients with DN and streptozotocin-induced diabetic mice and that it co-localised with the podocyte marker WT1, indicating clusterin is expressed in podocytes. In our *in vitro* analysis, we found no significant change in *CLU* mRNA expression in podocytes following stimulation with high glucose and angiotensin II; in contrast, *CLU* mRNA expression was significantly upregulated following methylglyoxal stimulation. Methylglyoxal treatment also significantly decreased the mRNA expression of the slit diaphragm markers *ZO-1* and *NEPH1* and significantly increased the mRNA expression of the oxidative stress marker *HO-1*. Lastly, we showed that pre-incubating podocytes with recombinant human clusterin protein increased podocyte survival, prevented slit diaphragm damage, and reduced oxidative stress-induced apoptosis following methylglyoxal stimulation. Taken together, our results indicate that glomerular clusterin is upregulated in DN, and this increase in clusterin expression may protect against oxidative stress-induced apoptosis in podocytes, providing a possible new therapeutic target for DN and other kidney diseases.

## Introduction

Diabetic nephropathy (DN) is a major complication of diabetes and the leading cause of end-stage renal disease. Although the incidence of DN is increasing <sup>1</sup>, the mechanisms underlying the pathophysiology of DN are unclear, and no effective treatment for DN is currently available. However, one of the hallmarks of DN is a loss of podocytes, which are terminally differentiated and highly specialised epithelial cells in the glomerulus that serve as a critical component of the glomerular filtration barrier. Specifically, reduced numbers of podocytes are associated with the development of DN in patients with type 2 diabetes <sup>2</sup>, and changes in the structure and density of podocytes occur in the early stages of DN <sup>3</sup>. Moreover, Weil *et al.* reported that podocyte detachment is correlated with increasing albuminuria in these patients <sup>4</sup>. Therefore, new therapeutic strategies designed to prevent podocyte loss might slow or even prevent the progression of DN.

Clusterin (also known as Apolipoprotein J) is a disulphide-linked heterodimeric protein expressed in a wide range of tissues, including the kidney. Clusterin is a molecular chaperone that participates in a variety of biological processes, including lipid transport <sup>5,6</sup>, complement inhibition <sup>7</sup>, and regulation of apoptosis <sup>8,9</sup>. In addition, a number of studies have shown that clusterin can protect against oxidative stress. For example, Kim *et al.* reported that clusterin protects retinal pigment epithelial cells against oxidative stress via the PI3K/Akt pathway <sup>10</sup>. Besides, Jun *et al.* found that clusterin can protect cardiomyocytes from oxidative stress-induced apoptosis by inhibiting the Akt/GSK-3beta signalling pathway <sup>11</sup>, and Schwochau *et al.* found that clusterin protects cultured porcine proximal tubular cells against H<sub>2</sub>O<sub>2</sub>-induced damage <sup>12</sup>. In addition to playing a role in protecting against oxidative stress, biotinylated clusterin can bind to podocytes via the LDL receptor, thereby preventing complement-induced cellular damage in membranous glomerulonephritis (also known as membranous nephropathy) <sup>13</sup>. These findings collectively suggest that glomerular clusterin may protect podocytes from cellular damage.

Experimental studies also support the notion that clusterin may play a protective role in various forms of kidney disease. For example, reduced levels of clusterin have been associated with accelerated kidney fibrosis and aggravated tubular damage in a renal ischaemia-reperfusion injury model, thereby increasing kidney dysfunction <sup>14,15</sup>. Moreover, Jung *et al.* found that overexpressing clusterin reduces renal fibrosis in a unilateral ureteral obstruction model <sup>16</sup>, and Rosenberg *et al.* found that ageing clusterin-deficient mice develop moderate to severe mesangial lesions and have deposits of immune complex in the mesangium, compared to relatively few or no glomerular lesions in age-matched wild-type controls <sup>17</sup>. Finally, data from

our group and others also suggest that clusterin may play a role in DN. Using microarray analysis, we found that glomerular *CLU* mRNA expression is significantly higher in two patients with DN compared to healthy individuals <sup>18</sup>. Moreover, using an autopsy cohort Nakatani *et al.* found that glomerular clusterin protein levels are 2.42-fold higher in ten diabetic patients compared to non-diabetic controls <sup>19</sup>. However, as these studies involved a relatively small number of patients, the role that increased glomerular clusterin expression plays in DN patients remains poorly understood.

To address this question, we examined glomerular clusterin expression in both a large cohort of patients with DN and a diabetic mouse model. In addition, we examined clusterin expression in a human podocyte cell line cultured under diabetic conditions. Finally, we examined whether treating podocytes with recombinant clusterin protein can protect the cells under diabetic conditions.

## **Methods**

### **Human renal tissue**

Two patient cohorts were used in this study. First, *CLU* mRNA was measured in microdissected glomeruli from a frozen biopsy cohort that included kidney tissue obtained from patients with DN (n=24) and healthy subjects (n=11); this cohort has been described previously <sup>20</sup>. Because no tissues were left from the biopsy cohort described above, we measured clusterin protein using a separate human biopsy cohort obtained from patients with histologically confirmed DN (n=12); normal renal tissue samples obtained from healthy transplant donor kidney biopsies (n=10) were used as a control group. The clinical parameters of these DN patients and healthy transplant donors can be founded in the Supplementary Table 1. The samples selected for this cohort were retrieved from the pathology archives of the Leiden University Medical Center (LUMC) in Leiden, the Netherlands, and were coded and treated anonymously in accordance with institutional guidelines and the code of conduct regarding the responsible use of human tissues from the Dutch Federa.

### **Mouse model of type 1 diabetes**

Diabetes was induced in 8-week-old female C57BL/6J mice (Harlan Laboratories, Indianapolis, IN) by three intraperitoneal injections of streptozotocin (STZ; 75 mg/kg body weight; Sigma-Aldrich, St Louis, MO) given at two-day intervals. Seven days after the first STZ injection, blood glucose levels were measured, and mice with a blood glucose level >15 mmol/L were considered diabetic. Fifteen weeks after the induction of diabetes, diabetic mice (n=5) were

sacrificed, and the kidneys were harvested; age-matched control C57BL/6J mice (n=5) were sacrificed at the same time points. The clinical biochemical parameters of these mice have been described previously <sup>21</sup>. All experiments were conducted in accordance with national guidelines regarding the care and use of experimental animals (DEC license 13163) approved by the Animal Experiments Committee (DEC) of the LUMC, the Netherlands.

### **Immunohistochemistry**

Paraffin-embedded human and mouse kidney tissues were sectioned at four  $\mu$ m thickness using a Leica microtome (Leica, Wetzlar, Germany), and the sections were subjected to heat-induced antigen retrieval using citrate (pH 6). Mouse kidney sections were stained with the following primary antibodies: rabbit anti-mouse clusterin (1:800, H-330, Santa Cruz Biotechnology, Santa Cruz, CA) or rabbit anti-mouse Wilms' tumour protein (1:1000, WT1, Santa Cruz Biotechnology); human kidney sections were stained with mouse anti-human clusterin (1:9000, clone B-5, Santa Cruz Biotechnology). The anti-rabbit or anti-mouse Envision HRP-conjugated secondary antibody (Dako, Glostrup, Denmark) were used to visualise the primary antibodies, and diaminobenzidine (DAB+, Dako) was used for chromogenic detection. The sections were visualised using a Philips Ultra-Fast Scanner 1.6 RA (Philips, the Netherlands) for immunohistochemical analysis.

### **Glomerular clusterin immunohistochemistry staining score**

A semi-quantitative score was used to analyse glomerular clusterin protein expression in the human kidney tissues. Specifically, glomerular clusterin expression was scored as 1, 2, or 3, corresponding to negative staining, weak staining, and moderate/strong staining, respectively. All glomeruli included in the human kidney biopsies were scored, and a mean was calculated. Glomerular clusterin protein expression scores can be found in the Supplementary Table 1. Quantitative measurements were used to measure glomerular clusterin expression in the mouse kidney tissues. A total of 25 glomeruli per sample were randomly selected and measured quantitatively using ImageJ software (National Institutes of Health, Bethesda, MD).

### **Cell culture**

Conditionally immortalised human podocytes <sup>22</sup>, kindly provided by Moin Saleem (Bristol, UK), were cultured in RPMI 1640 medium (Gibco, Paisley, Scotland) supplemented with 10% foetal bovine serum (Sigma-Aldrich), 1% Insulin-Transferrin-Selenium (Invitrogen, the Netherlands), and 1% penicillin/streptomycin (Sigma-Aldrich). Podocytes were cultured at

33°C (5% CO<sub>2</sub>) for proliferation and were differentiated by culturing in non-permissive conditions at 37°C (5% CO<sub>2</sub>). Podocytes were used for experiments after 14 days of differentiation at 37°C (5% CO<sub>2</sub>). All cells used in this study tested negative for mycoplasma infection.

### **Incubation of podocytes with various compounds**

After starving the cells in serum-free RPMI 1640 medium for 24 h, differentiated podocytes were treated as follows: puromycin aminonucleoside (PAN, 30 µg/ml) for 24, 48, or 72 h; normal glucose (5 mM) or high glucose (25 mM) for 24, 48, or 72 h; angiotensin II (1 µM) for 24, 48, or 72 h; methylglyoxal (0, 0.5, 1.0, or 1.5 mM) for 24 h; or N-acetyl-L-cysteine (NAC, 150 µmol/L) for 24 h. All compounds were obtained from Sigma-Aldrich, and all experiments were performed in triplicate.

### **Quantitative real-time PCR analysis**

RNA was extracted and analysed using quantitative real-time PCR (qPCR) as previously described<sup>21</sup> using the following forward (FW) and reverse (RV) primers. The sequences of the primers used for the qPCR analysis can be found in Supplementary Table 2. PCR products were confirmed by sequencing. The *CLU*, *TJPI/ZO-1*, *NEPH1*, *HMOX1/HO-1*, *BAX*, and *BCL2* mRNA levels were normalised to the housekeeping gene *HPRT1*.

### **Cell viability assay**

Fully differentiated human podocytes were seeded in 96-well plates (5000 cells per well), with three wells per condition. After starving in serum-free RPMI 1640 medium for 24 h, the podocytes were incubated with 1.5 mM methylglyoxal for 24 h either with or without pre-incubation for 4 h with 0, 0.25, 0.5, 1.0, or 2.0 µg/ml recombinant human clusterin protein dissolved in PBS (R&D Systems, the Netherlands). Twenty-four hours after the addition of methylglyoxal, the medium was replaced with PrestoBlue Cell Viability Reagent (Invitrogen); 1 h later, fluorescence (570 nm) was measured using a Victor Multilabel plate reader (PerkinElmer, Waltham, MA). All experiments were performed in triplicate.

### **Caspase 3/7 assay**

Fully differentiated human podocytes were seeded in white 96-well plates. After starving in serum-free RPMI 1640 medium for 24 h, the podocytes were incubated with 1.5 mM methylglyoxal for 12 h either with or without pre-incubation for 4 h with 2.0 µg/ml recombinant



human clusterin protein. Then, an equal volume of Caspase-Glo 3/7 reagent (Promega) was added to the samples, and the plate was left in the dark at room temperature for 1 hour on a shaker. Luminescence was measured with a TECAN- Infinite 200PRO (Switzerland).

### **DCFDA/ H2DCFDA staining**

Intracellular ROS generation was detected using a 2',7' -dichlorofluorescein diacetate (DCFDA, also known as H2DCFDA) fluorescent probe (Abcam, the Netherlands). Podocytes seeded on glass slides in 24-well plates. The podocytes treated with Milli-Q water or methylglyoxal (1.5 mM) for 2 h with or without pre-treated with 2.0 µg/ml recombinant human clusterin protein for 4 h, followed by incubating with DCFDA (10 µmol/L) at 37 °C for 30 minutes in the dark and then washed with DFCDA kit buffer. The cell fluorescence was observed under a fluorescence microscope (Ex/Em=485/535nm).

### **MitoSOX Red staining of mitochondrial superoxide**

Podocytes seeded on glass slides were treated as described above, followed by staining with 2.5 µM MitoSOX Red (Thermo Fisher Scientific, Waltham, MA) for 10 minutes. After rinsing with cold phosphate-buffered saline, the podocytes were fixed with 4% PFA for 5 minutes, followed by ice-cold 100% methanol for 10 minutes. Images were then captured using a Zeiss confocal microscope with ZEN software (Zeiss, Germany).

### **Statistical analysis**

Data were analysed using SPSS, version 25 (IBM, Armonk, NY). Summary data are presented as the mean  $\pm$  SD of three independent experiments. Differences between two groups were analysed using the Student's *t*-test, and differences between more than two groups were analysed using a one-way ANOVA. Differences with a *P*-value <0.05 were considered statistically significant.

## **Results**

### **Glomerular clusterin expression is upregulated in patients with DN**

First, we performed immunohistochemistry to examine kidney biopsies obtained from patients with DN and healthy kidney transplant donors and found little or no clusterin protein in the glomeruli of healthy subjects (Fig. 1a, 1c and 1e). In contrast, robust clusterin staining was present in the mesangial area and in podocytes in the kidney sections of DN patients (Fig. 1b, 1d, 1f and supplementary Figure S1). Quantitative analysis revealed that glomerular clusterin

protein expression was significantly higher in DN patient samples compared to controls (Fig. 1g).

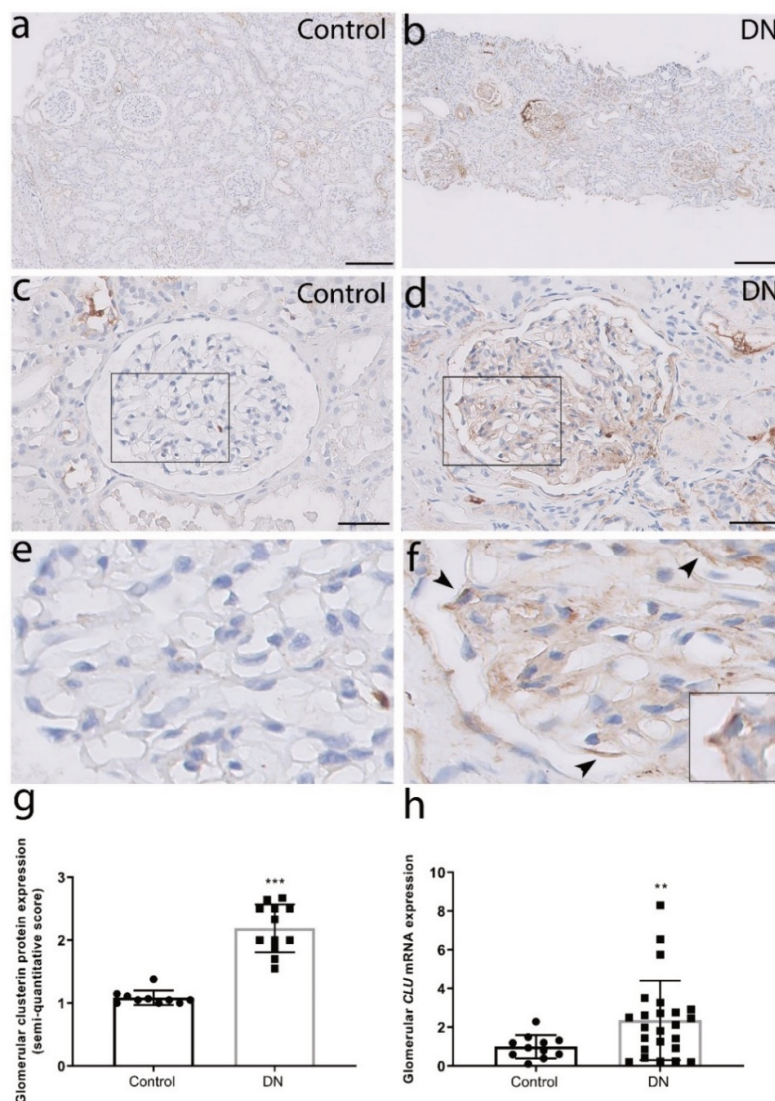


**Figure 1. Glomerular clusterin expression is increased in patients with DN**

(a-b) Representative images of kidney sections obtained from a healthy subject (Control; a) and a patient with DN (DN; b) stained for clusterin; the scale bars represent 200  $\mu\text{m}$ . (c-d) Representative high-magnification images of a and b; the scale bars represent 50  $\mu\text{m}$ . (e-f) The high-magnification views of the rectangles in c and d. Clusterin staining was present along the outer side of the GBM at the place where the podocytes are located (arrowheads; the square shows a zoomed in image of a clusterin-positive podocyte). (g) Summary of clusterin staining (semi-quantitative score) in the glomeruli of healthy subjects (Control; n=10) and patients with DN (DN; n=12); \*\*\* $P$ <0.001 vs. control (Student's t-test). (h) Summary of CLU mRNA measured in isolated glomeruli from healthy subjects (Control; n=11) and patients with DN (DN; n=24); \*\* $P$ <0.01 vs. control (Student's t-test).

These results were supported by analysing *CLU* mRNA expression in another cohort, which showed significantly higher levels of *CLU* mRNA in the glomeruli of DN patient samples compared to controls (Fig. 1h).

### **Glomerular clusterin expression is increased in a mouse model of type 1 diabetes and co-localises with podocytes**

Next, we used immunohistochemistry to measure clusterin protein in the glomeruli of mice with STZ-induced type 1 diabetes and age-matched control mice. Clusterin staining was visible in the mouse glomeruli as a granular pattern (Fig. 2a-d). Compared to control mice, the STZ-treated mice had significantly higher glomerular clusterin staining (Fig. 2g). Furthermore, we stained adjacent sections for clusterin and the podocyte marker WT1 and found that clusterin co-localised with WT1, confirming that clusterin is expressed specifically in podocytes (Fig. 2e and 2f).

### **Altered expression of human clusterin in podocytes cultured under diabetic conditions**

Next, we investigated whether clusterin expression is altered in diabetes by measuring *CLU* mRNA in a human podocyte cell line under various diabetic conditions. First, we measured *CLU* mRNA in podocytes stimulated with puromycin aminonucleoside (PAN, 30 µg/ml), a toxic compound commonly used to induce podocyte cellular damage, and found significantly increased clusterin expression in stimulated cells (Fig. 3a). We then stimulated cells with either high glucose (Fig. 3b) or angiotensin II (Fig. 3c), but neither treatment significantly affected clusterin expression. Lastly, we stimulated podocytes with methylglyoxal, a major precursor in the formation of advanced glycated end products, which can increase ROS production and induce oxidative stress. Importantly, increased plasma levels of methylglyoxal have been reported in diabetic patients<sup>23,24</sup>. We found that culturing podocytes with 1.5 mM methylglyoxal for 24 h significantly increased clusterin expression compared to non-stimulated cells (Fig. 3d).

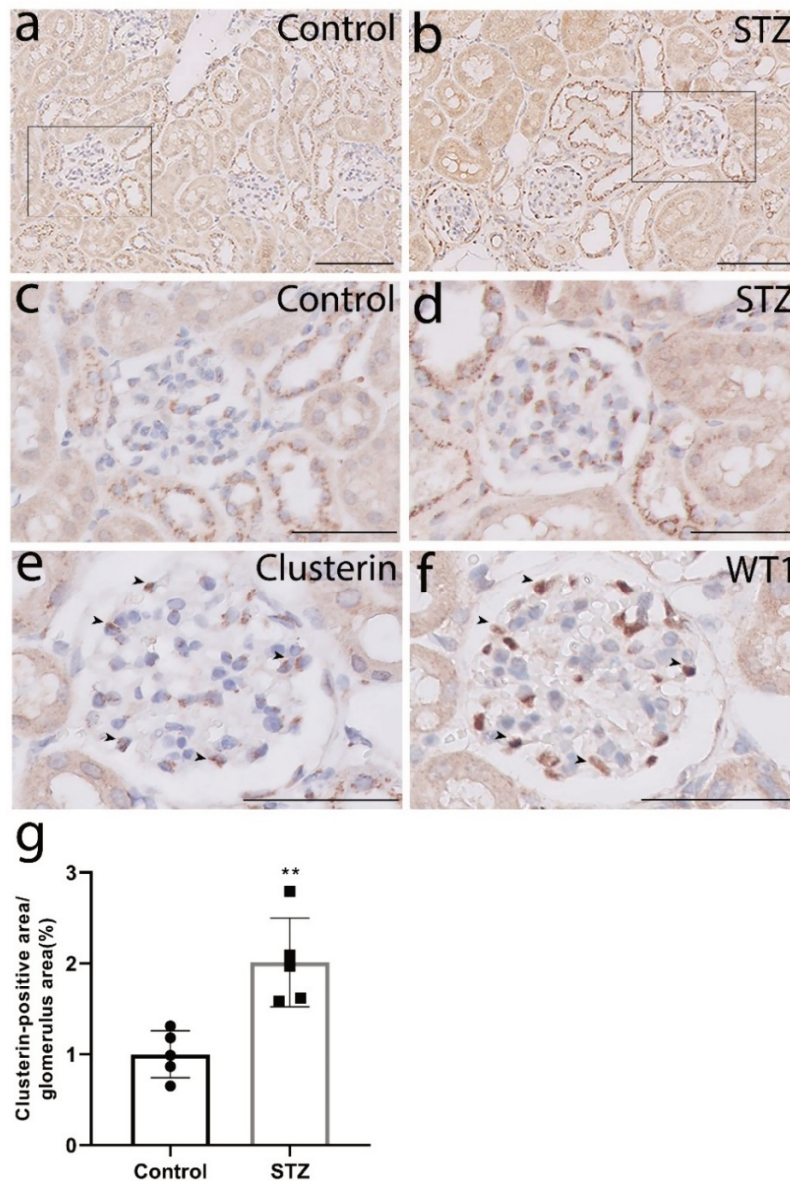


**Figure 2. Clusterin expression is increased in the glomeruli of mice with type 1 diabetes and co-localises with podocytes**

(a-b) Representative images of mouse kidney sections obtained from control mice and STZ-treated mice 15 weeks after diabetes was induced; the scale bars represent 100  $\mu$ m. (c-d) The high-magnification views of a and b; the scale bars represent 50  $\mu$ m. (e-f) Representative images of the adjacent sections stained for clusterin and WT1, showing co-localisation of clusterin with WT1 in the glomeruli (arrowheads). (g) Averaged clusterin-positive area (measured by using ImageJ) in the glomeruli of control and STZ-treated mice 15 weeks after diabetes was induced; \*\* $P < 0.01$  vs. control (Student's t-test).

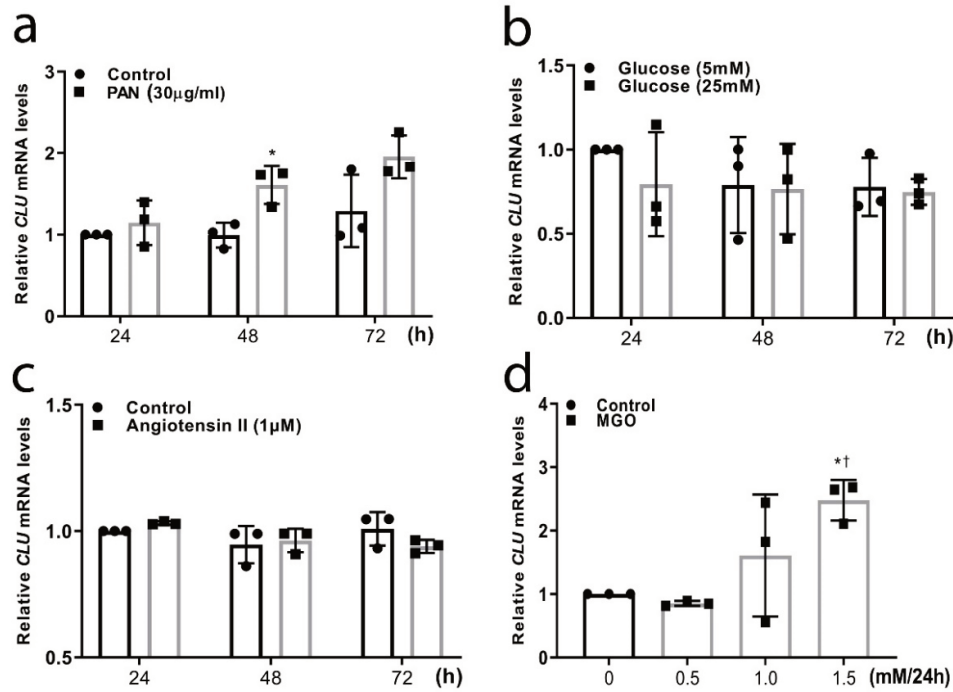


**Figure 3. Clusterin expression in podocytes cultured under various diabetic conditions**

Human podocytes were cultured for the indicated times in PAN (30 μg/ml) (a), Glucose (5 mM or 25 mM) (b), Angiotensin II (1 μM) (c), or the indicated concentrations of MGO for 24 h (d). The *CLU* mRNA expression after these treatments was measured, the mRNA levels were normalised to the respective control. In a-c, \* $P < 0.05$  vs. the respective control at the same time point (Student's t-test); in d, \* $P < 0.05$  vs. control, and † $P < 0.05$  vs. 0.5 mM MGO (one-way ANOVA). PAN: puromycin aminonucleoside; MGO: methylglyoxal.

### Methylglyoxal increases oxidative stress and damages podocytes

To investigate the consequences of methylglyoxal stimulation, we measured cell viability in podocytes cultured for 24 h in increasing concentrations of methylglyoxal. We found that methylglyoxal reduced cell viability in a dose-dependent manner (Fig. 4a). Moreover, we found that methylglyoxal significantly decreased expression of tight junction protein 1 (*Tjp1/ZO-1*) and nephrin-like protein 1 (*NEPH1*), both of which are involved in maintaining slit diaphragm integrity in podocytes (Fig. 4b and 4c).

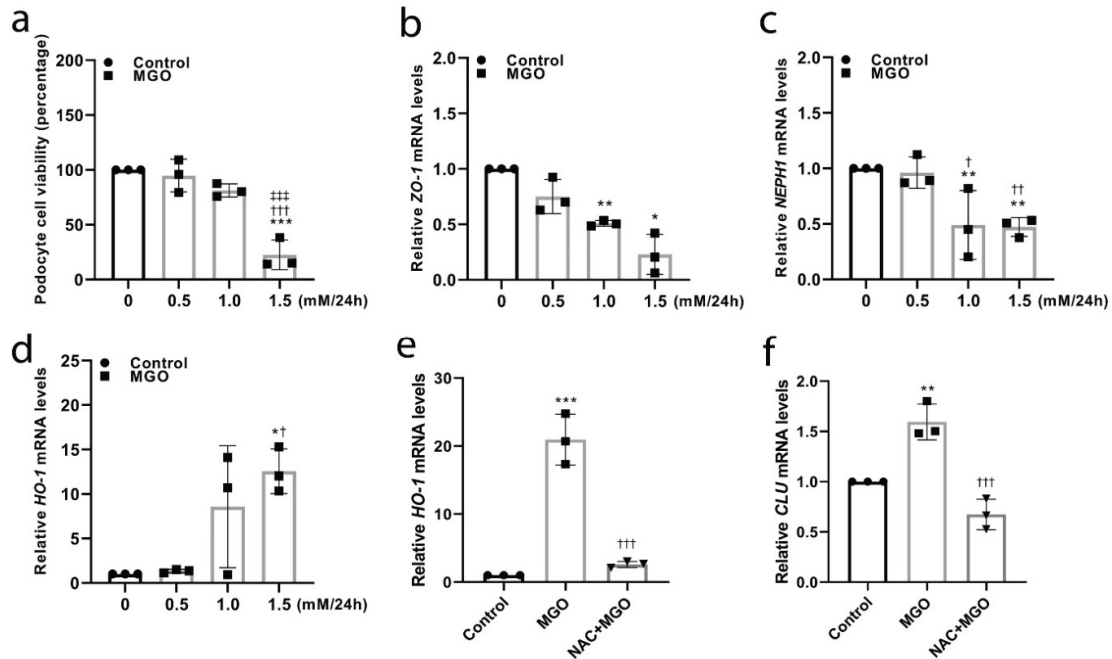


**Figure 4. Methylglyoxal reduces podocyte viability, down-regulates *ZO-1* and *NEPH1* expression, and up-regulates *HO-1* expression**

(a) Cell viability was measured in podocytes incubated with the indicated concentrations of methylglyoxal for 24 h; \*\*\* $P < 0.001$  vs. control, ††† $P < 0.001$  vs. 0.5 mM MGO, and ‡‡‡ $P < 0.001$  vs. 1.0 mM MGO (one-way ANOVA). (b-d) Podocytes were incubated with the indicated concentrations of MGO for 24 h, followed by measuring *ZO-1* (b), *NEPH1* (c), and *HO-1* (d) mRNA expression; the mRNA levels were normalised to the respective control; \* $P < 0.05$  vs. control, \*\* $P < 0.01$  vs. control, \*\*\* $P < 0.001$  vs. control, † $P < 0.05$  vs. 0.5 mM MGO, †† $P < 0.01$  vs. 0.5 mM MGO, and ††† $P < 0.001$  vs. 0.5 mM MGO (one-way ANOVA). (e-f) Podocytes were incubated with MGO (1.5 mM) for 24 h, with or without pre-treatment with NAC (150  $\mu\text{mol/L}$ ) for 1 h, followed by measuring *HO-1* (e) and *CLU* (f) mRNA expression; the mRNA levels were normalised to the respective control; \*\* $P < 0.01$  vs. control, \*\*\* $P < 0.001$  vs. control, and ††† $P < 0.001$  vs. MGO (one-way ANOVA). MGO: methylglyoxal; NAC: N-acetyl-L-cysteine.

Finally, as discussed above, methylglyoxal can increase ROS production and cause oxidative stress. Consistent with this, we found that methylglyoxal significantly upregulated mRNA expression of Heme oxygenase 1 (HO-1), an oxidative stress marker (Fig. 4d). We also found that N-acetyl-L-cysteine (NAC), an anti-oxidant, can ameliorate the effect on HO-1 in methylglyoxal-treated podocytes (Fig. 4e). In addition, NAC was able to inhibit the methylglyoxal-induced increase of clusterin expression at the mRNA level (Fig. 4f). Taken

together, these data suggest that oxidative stress might play an important role in up-regulating clusterin expression in podocytes under diabetic conditions.

### **Clusterin protects against methylglyoxal-induced apoptosis in podocytes by reducing oxidative stress**

Next, we examined whether clusterin can protect podocytes during methylglyoxal stimulation. We therefore added recombinant human clusterin protein to podocytes and measured cell viability. We found that although culturing podocytes with recombinant human clusterin protein for 24 h had no effect on cell viability (Fig. 5a), pre-incubating podocytes with recombinant human clusterin protein (2.0  $\mu\text{g/ml}$ ) for 4 h significantly reduced methylglyoxal-induced cell death (Fig. 5b).

We then stained podocytes with MitoSOX Red to measure mitochondrial superoxide in order to test whether incubating cells with recombinant human clusterin protein reduced methylglyoxal-induced oxidative stress (Fig. 5c). We found that stimulating podocytes with 1.5 mM methylglyoxal for 2 h caused a substantial increase in MitoSOX Red staining in the cell cytoplasm, which was considerably reduced by pre-incubating cells with recombinant human clusterin protein (2.0  $\mu\text{g/ml}$ ). We also found that control podocytes and podocytes which were treated with rhCLU show a weak DCFDA staining. This staining was increased after methylglyoxal (1.5 mM) stimulation for 2 h. Pre-treatment with recombinant human clusterin protein (2.0  $\mu\text{g/ml}$ ) for 4 h considerably reduced the DCFDA staining in methylglyoxal-treated podocytes (Fig. 5d). These data suggest that clusterin can reduce methylglyoxal-induced oxidative stress in podocytes.

Furthermore, we examined whether methylglyoxal-induced cell death is mediated by apoptosis and whether clusterin can reduce apoptotic signalling in podocytes. We found an increased caspase 3/7 activity in methylglyoxal-treated podocytes compared to the control podocytes. Pre-incubation with recombinant human clusterin protein (2.0  $\mu\text{g/ml}$ ) for 4 h reduced the caspase 3/7 activity in methylglyoxal-treated podocytes compared to the podocytes treated with methylglyoxal only (Fig. 5e). Bax and Bcl-2 (encoded by the *BAX* and *BCL2* genes, respectively) are two major members of the Bcl-2 family and play a vital role in the apoptotic signalling pathway, as the balance between pro-apoptotic Bax and anti-apoptotic Bcl-2 determines the cells' susceptibility to apoptosis<sup>25</sup>. We therefore measured the ratio between *BAX* mRNA and *BCL2* mRNA, and found that this ratio was significantly increased in methylglyoxal-stimulated podocytes; moreover, pre-incubating cells with recombinant human clusterin protein prevented this increase (Fig. 5f).



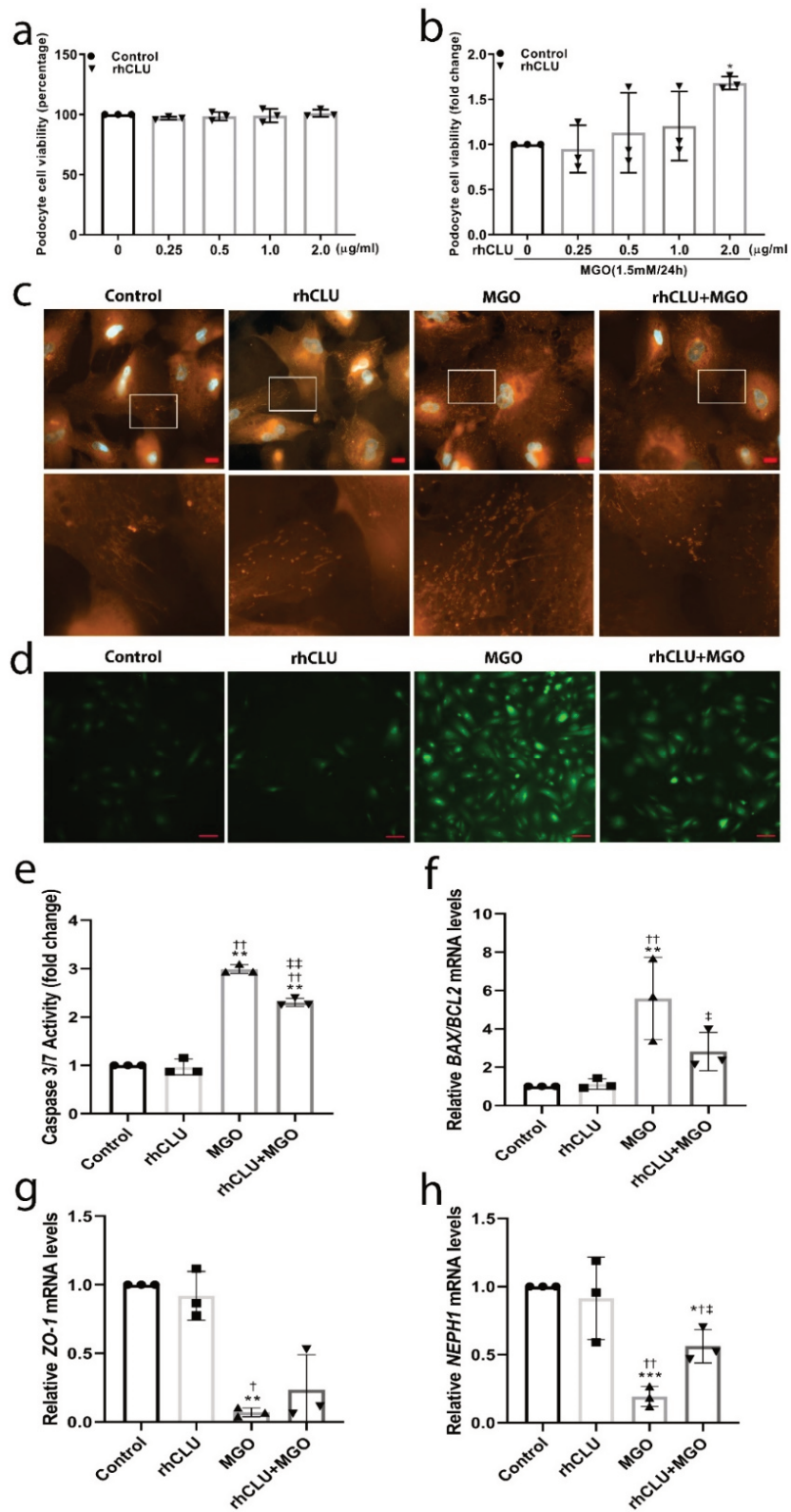


**Figure 5. Recombinant human clusterin protein protects podocytes against methylglyoxal-induced oxidative stress and apoptosis**



(a) Cell viability was measured in podocytes incubated with the indicated concentrations of rhCLU for 24 h. (b) Cell viability was measured in podocytes pre-incubated for 4 h with the indicated concentrations of rhCLU, followed by 24 h in the presence or absence of 1.5 mM MGO. Cell viability in the presence of MGO was normalised to cells stimulated in the absence of rhCLU; \* $P < 0.05$  vs. 0  $\mu\text{g/ml}$  rhCLU+ 1.5 mM MGO (one-way ANOVA). (c) Representative images of untreated podocytes (Control) and podocytes pre-treated for 4 h with 2.0  $\mu\text{g/ml}$  rhCLU, 2 h with 1.5 mM MGO, or both, followed by MitoSOX Red staining. The scale bars indicate 20  $\mu\text{m}$  and the boxed areas are shown at higher magnification in the bottom row. (d) Representative images of untreated podocytes (Control) and podocytes treated as described in c, followed by DCFDA staining. The scale bars indicate 100  $\mu\text{m}$ . (e) Caspase3/7 activity in podocytes treated with Milli-Q water (Control) or MGO (1.5 mM) for 12 h with or without pre-treated with 2.0  $\mu\text{g/ml}$  rhCLU for 4 h. The measurement was normalized to the untreated control podocytes; \*\* $P < 0.01$  vs. control,  $\dagger\dagger P < 0.01$  vs. rhCLU, and  $\ddagger\ddagger P < 0.01$  vs. MGO (one-way ANOVA). (f) Podocytes treated with Milli-Q water (Control) or MGO (1.5 mM) for 2 h with or without pre-treatment with 2.0  $\mu\text{g/ml}$  rhCLU for 4 h, followed by measuring BAX and BCL2 mRNA expression. The BAX/BCL2 ratio was calculated and normalised to control; \*\* $P < 0.01$  vs. control,  $\dagger\dagger P < 0.01$  vs. rhCLU, and  $\ddagger P < 0.05$  vs. MGO (one-way ANOVA). (g-h) Podocytes treated with Milli-Q water (Control) or MGO (1.5 mM) for 2 h with or without pre-treated with 2.0  $\mu\text{g/ml}$  rhCLU for 4 h, followed by measuring *ZO-1* (g) and *NEPH1* (h) mRNA expression; the mRNA levels were normalised to the respective control; \* $P < 0.05$  vs. control, \*\* $P < 0.01$  vs. control \*\*\* $P < 0.001$  vs. control,  $\dagger P < 0.05$  vs. rhCLU,  $\dagger\dagger P < 0.01$  vs. rhCLU, and  $\ddagger P < 0.05$  vs. MGO (one-way ANOVA). MGO: methylglyoxal; rhCLU: recombinant human clusterin protein.

These data indicate that clusterin prevents methylglyoxal-induced apoptosis in podocytes by reducing oxidative stress. Lastly, and consistent with our previous results, we found that pre-incubating podocytes with recombinant human clusterin protein for 4 h prevented the methylglyoxal (1.5 mM, 2 h)-induced downregulation of both *ZO-1* (Fig. 5g) and *NEPH1* (Fig. 5h).

## Discussion

Here, we report that glomerular clusterin expression was increased in patients with DN and a mouse model of STZ-induced diabetes. Moreover, we found that methylglyoxal significantly increased clusterin expression in cultured human podocytes, and that pre-treating podocytes with recombinant human clusterin protein protected against methylglyoxal-induced oxidative stress and apoptosis.

Urinary clusterin (uCLU) levels have been used as a biomarker for detecting kidney damage<sup>26</sup>. For example, Kim *et al.* recently reported that uCLU levels are significantly increased in patients with type 2 diabetes compared to non-diabetic subjects; the authors also found that uCLU is associated with the annual decline in estimated glomerular filtration rate (eGFR) and the progression of DN stage in patients with type 2 diabetes<sup>27</sup>. Moreover, Zeng *et al.* performed a consecutive cohort study and found that uCLU levels are higher in type 2 diabetic patients with DN compared to control subjects, and that this increase is positively correlated with the urinary albumin-creatinine ratio<sup>28</sup>. Interestingly, studies suggest that changes in uCLU levels may be due – at least in part – to changes in renal *CLU* expression. For example, Nakatani *et al.* performed a proteomics analysis in an autopsy cohort and found that clusterin protein is significantly increased in the glomeruli of patients with DN<sup>19</sup>. Similarly, using microarray analysis, we previously found that *CLU* mRNA expression is significantly increased in isolated glomeruli of two patients with DN compared to healthy individuals<sup>18</sup>. In the present study, we found that *CLU* mRNA expression was increased in micro-dissected glomeruli of DN patients, and we found increased clusterin protein expression in the mesangium and podocytes in DN patient biopsies. Importantly, this cohort consists of kidney samples taken from patients with DN ranging from class 2 to class 4; thus, a larger biopsy cohort would be helpful in determining whether clusterin expression is correlated with the class and/or severity of DN.

To support our findings in patients with DN, we also measured glomerular clusterin protein expression in a mouse model of type 1 diabetes and observed increased glomerular clusterin protein expression in mice with STZ-induced type 1 diabetes compared to control mice. This finding is consistent with a previous report by Tunçdemir *et al.* showing increased glomerular clusterin expression in a rat model of type 1 diabetes<sup>29</sup>. Our finding that clusterin co-localised with the podocyte marker WT1 in mice is also consistent with our clusterin immunostaining results in renal biopsies obtained from patients with DN, indicating that podocytes are the clusterin-expressing cell type in glomeruli, which is consistent with reports that clusterin expression is upregulated in various epithelial cells during stress<sup>30,31</sup>.

The clusterin protein is post-translationally modified to produce a secreted isoform and a nuclear isoform, which play opposite roles in apoptosis <sup>8</sup>. Our mouse data show that the clusterin staining in the glomeruli of diabetic mice had a granular pattern, which suggests that this is the secreted, anti-apoptotic isoform. Several experimental studies support the notion that clusterin has protective properties in various kidney diseases. For example, clusterin deficiency accelerates renal fibrosis and increases renal inflammation in a mouse model of renal ischaemia-reperfusion injury <sup>15</sup>. Moreover, overexpressing clusterin reduces renal fibrosis in the mouse unilateral ureteral obstruction model <sup>16</sup>. Rosenberg *et al.* found that aged clusterin-deficient mice, but not aged control mice, have moderate to severe mesangial matrix expansion <sup>17</sup>. In addition, Ghiggeri *et al.* illustrated that low levels of clusterin in serum negatively affect the clinical outcome in patients with nephrotic syndrome <sup>32</sup>. However, whether clusterin plays a protective role in DN remains elusive.

It is still controversial whether glomerular clusterin is derived from the circulation or synthesized by resident glomerular cells. Yamada *et al.* found that clusterin is upregulated in glomerular mesangial cells during the course of immune-mediated injuries <sup>33</sup>. Laping *et al.* demonstrated that thrombin increases clusterin expression in mesangial cells and glomerular epithelial cells at the mRNA level <sup>34</sup>. In the present study, we focussed on the podocytes according to our findings from human biopsies and mice tissue. In *in vitro* experiments using a human podocyte cell line, we found that PAN, a compound commonly used to induce cell damage in podocytes, significantly increased *CLU* mRNA expression. In contrast, exposing cells to either high glucose or angiotensin II had no significant effect on clusterin expression. However, we demonstrate that treating podocytes with methylglyoxal to mimic diabetes-related oxidative stress increased *CLU* mRNA expression. Methylglyoxal is a major precursor in the formation of advanced glycosylated end products, which can increase ROS production and cause oxidative stress. Interestingly, studies have shown elevated levels of methylglyoxal in diabetic patients <sup>23,24</sup>. Moreover, Kim *et al.* reported that methylglyoxal-induced oxidative stress might play a role in podocyte apoptosis in DN <sup>35</sup>. Here, we found that stimulating podocytes with methylglyoxal for 24 h increased *CLU* mRNA expression, as well as expression of the oxidative stress marker (HO-1) at the mRNA level. We did not find a difference between *HO-1* mRNA expression in control podocytes and in angiotensin II-treated podocytes with the concentration we used (data not shown). Furthermore, we show that methylglyoxal treatment increased mitochondrial superoxide and intracellular ROS regeneration in podocytes. In addition, we found that NAC, an anti-oxidant, ameliorated the effect on HO-1 in methylglyoxal-treated podocytes and inhibited the methylglyoxal-induced increase of clusterin expression at the

mRNA level. Taken together, these data suggest that oxidative stress, but not hyperglycemia or the renin-angiotensin system, is the principal factor underlying the upregulation of clusterin expression in podocytes under diabetic conditions.

Our findings also show that pre-treating podocytes with recombinant clusterin protein can help to protect podocytes against methylglyoxal-induced apoptosis. We observed that pre-incubating podocytes with recombinant human clusterin protein (2.0 µg/ml) for 4 h significantly reduced methylglyoxal-induced cell death. Pre-incubating podocytes with recombinant human clusterin protein prevented an increase of the *BAX/BCL2* ratio, as well as of caspase 3/7 activity. The protective function of clusterin may have clinical relevance. Evidence suggesting how clusterin might exert this protective role comes from several *in vitro* studies. For example, Rastaldi *et al.* found that biotinylated clusterin can bind to podocytes via the LDL receptor and can protect podocytes from complement-induced injury in membranous glomerulonephritis <sup>13</sup>. Kim *et al.* found that clusterin can protect human retinal pigment epithelial cells from oxidative stress via the PI3K/Akt pathway <sup>10</sup>, and Jun *et al.* showed that clusterin protects cardiomyocytes from oxidative stress-induced apoptosis by inhibiting the Akt/GSK-3beta signalling pathway <sup>11</sup>. Yu *et al.* demonstrated that *p*-Akt expression is upregulated in mesenchymal stem cells following pre-treatment with clusterin, and that the Akt inhibitor LY29440236 partially abrogated the protective function of clusterin <sup>36</sup>. Therefore, clusterin may modulate Akt-related pathways to slow or even halt the progression of DN. The mechanism of how cytoprotection is mediated by clusterin in the different pathways needs to be further elucidated. Further *in vivo* studies are also needed to confirm our hypothesis that clusterin may slow or even halt the progression of DN.

In summary, we provide evidence that glomerular clusterin is upregulated in DN and that experimentally-induced oxidative stress up-regulates clusterin expression in podocytes. Moreover, pre-treating podocytes with recombinant human clusterin protein protects against apoptosis by reducing oxidative stress-induced under diabetic conditions, suggesting a possible therapeutic target for treating DN.

### **Acknowledgements**

The first author (J.He) was supported by the China Scholarship Council (CSC).

### **Competing interests**

The authors declare no competing interests.

## References

- 1 Ingelfinger, J. R. & Jarcho, J. A. Increase in the Incidence of Diabetes and Its Implications. *N Engl J Med* **376**, 1473-1474, doi:10.1056/NEJMe1616575 (2017).
- 2 Pagtalunan, M. E. *et al.* Podocyte loss and progressive glomerular injury in type II diabetes. *The Journal of clinical investigation* **99**, 342-348, doi:10.1172/JCI119163 (1997).
- 3 Dalla Vestra, M. *et al.* Is podocyte injury relevant in diabetic nephropathy? Studies in patients with type 2 diabetes. *Diabetes* **52**, 1031-1035, doi:10.2337/diabetes.52.4.1031 (2003).
- 4 Weil, E. J. *et al.* Podocyte detachment and reduced glomerular capillary endothelial fenestration promote kidney disease in type 2 diabetic nephropathy. *Kidney Int* **82**, 1010-1017, doi:10.1038/ki.2012.234 (2012).
- 5 de Silva, H. V. *et al.* A 70-kDa apolipoprotein designated ApoJ is a marker for subclasses of human plasma high density lipoproteins. *J Biol Chem* **265**, 13240-13247 (1990).
- 6 Heo, J. Y. *et al.* Clusterin deficiency induces lipid accumulation and tissue damage in kidney. *The Journal of endocrinology* **237**, 175-191, doi:10.1530/JOE-17-0453 (2018).
- 7 Jenne, D. E. & Tschopp, J. Molecular structure and functional characterization of a human complement cytotoxicity inhibitor found in blood and seminal plasma: identity to sulfated glycoprotein 2, a constituent of rat testis fluid. *Proc Natl Acad Sci U S A* **86**, 7123-7127 (1989).
- 8 Jones, S. E. & Jomary, C. Clusterin. *Int J Biochem Cell Biol* **34**, 427-431 (2002).
- 9 Pereira, R. M. *et al.* Protective molecular mechanisms of clusterin against apoptosis in cardiomyocytes. *Heart Fail Rev* **23**, 123-129, doi:10.1007/s10741-017-9654-z (2018).
- 10 Kim, J. H. *et al.* Protective effect of clusterin from oxidative stress-induced apoptosis in human retinal pigment epithelial cells. *Invest Ophthalmol Vis Sci* **51**, 561-566, doi:10.1167/iovs.09-3774 (2010).
- 11 Jun, H. O. *et al.* Clusterin protects H9c2 cardiomyocytes from oxidative stress-induced apoptosis via Akt/GSK-3 $\beta$  signaling pathway. *Exp Mol Med* **43**, 53-61, doi:10.3858/emmm.2011.43.1.006 (2011).
- 12 Schwochau, G. B., Nath, K. A. & Rosenberg, M. E. Clusterin protects against oxidative stress in vitro through aggregative and nonaggregative properties. *Kidney Int* **53**, 1647-1653, doi:10.1046/j.1523-1755.1998.00902.x (1998).
- 13 Rastaldi, M. P. *et al.* Glomerular clusterin is associated with PKC- $\alpha$ / $\beta$  regulation and good outcome of membranous glomerulonephritis in humans. *Kidney Int* **70**, 477-485, doi:10.1038/sj.ki.5001563 (2006).
- 14 Zhou, W. *et al.* Loss of clusterin expression worsens renal ischemia-reperfusion injury. *Am J Physiol Renal Physiol* **298**, F568-578, doi:10.1152/ajprenal.00399.2009 (2010).
- 15 Guo, J. *et al.* Relationship of clusterin with renal inflammation and fibrosis after the recovery phase of ischemia-reperfusion injury. *BMC Nephrol* **17**, 133, doi:10.1186/s12882-016-0348-x (2016).
- 16 Jung, G. S. *et al.* Clusterin attenuates the development of renal fibrosis. *J Am Soc Nephrol* **23**, 73-85, doi:10.1681/ASN.2011010048 (2012).
- 17 Rosenberg, M. E. *et al.* Apolipoprotein J/clusterin prevents a progressive glomerulopathy of aging. *Mol Cell Biol* **22**, 1893-1902 (2002).
- 18 Baelde, H. J. *et al.* Gene expression profiling in glomeruli from human kidneys with diabetic nephropathy. *Am J Kidney Dis* **43**, 636-650 (2004).
- 19 Nakatani, S. *et al.* Proteome analysis of laser microdissected glomeruli from formalin-fixed paraffin-embedded kidneys of autopsies of diabetic patients: nephrin is associated with the development of diabetic glomerulosclerosis. *Nephrol Dial Transplant* **27**, 1889-1897, doi:10.1093/ndt/gfr682 (2012).
- 20 Baelde, H. J. *et al.* Reduction of VEGF-A and CTGF expression in diabetic nephropathy is associated with podocyte loss. *Kidney Int* **71**, 637-645, doi:10.1038/sj.ki.5002101 (2007).
- 21 Bus, P. *et al.* The VEGF-A inhibitor sFLT-1 improves renal function by reducing endothelial activation and inflammation in a mouse model of type 1 diabetes. *Diabetologia* **60**, 1813-1821, doi:10.1007/s00125-017-4322-3 (2017).
- 22 Ni, L., Saleem, M. & Mathieson, P. W. Podocyte culture: tricks of the trade. *Nephrology (Carlton)* **17**, 525-531, doi:10.1111/j.1440-1797.2012.01619.x (2012).

- 23 McLellan, A. C., Thornalley, P. J., Benn, J. & Sonksen, P. H. Glyoxalase system in clinical diabetes mellitus and correlation with diabetic complications. *Clin Sci (Lond)* **87**, 21-29 (1994).
- 24 Lapolla, A. *et al.* Glyoxal and methylglyoxal levels in diabetic patients: quantitative determination by a new GC/MS method. *Clin Chem Lab Med* **41**, 1166-1173, doi:10.1515/CCLM.2003.180 (2003).
- 25 Raisova, M. *et al.* The Bax/Bcl-2 ratio determines the susceptibility of human melanoma cells to CD95/Fas-mediated apoptosis. *J Invest Dermatol* **117**, 333-340, doi:10.1046/j.0022-202x.2001.01409.x (2001).
- 26 Dieterle, F. *et al.* Urinary clusterin, cystatin C, beta2-microglobulin and total protein as markers to detect drug-induced kidney injury. *Nat Biotechnol* **28**, 463-469, doi:10.1038/nbt.1622 (2010).
- 27 Kim, S. S. *et al.* Urine clusterin/apolipoprotein J is linked to tubular damage and renal outcomes in patients with type 2 diabetes mellitus. *Clin Endocrinol (Oxf)* **87**, 156-164, doi:10.1111/cen.13360 (2017).
- 28 Zeng, X. F. *et al.* Performance of urinary neutrophil gelatinase-associated lipocalin, clusterin, and cystatin C in predicting diabetic kidney disease and diabetic microalbuminuria: a consecutive cohort study. *BMC Nephrol* **18**, 233, doi:10.1186/s12882-017-0620-8 (2017).
- 29 Tuncdemir, M. & Ozturk, M. The effects of ACE inhibitor and angiotensin receptor blocker on clusterin and apoptosis in the kidney tissue of streptozotocin-diabetic rats. *J Mol Histol* **39**, 605-616, doi:10.1007/s10735-008-9201-2 (2008).
- 30 Itahana, Y. *et al.* Regulation of clusterin expression in mammary epithelial cells. *Exp Cell Res* **313**, 943-951, doi:10.1016/j.yexcr.2006.12.010 (2007).
- 31 Cochrane, D. R., Wang, Z., Muramaki, M., Gleave, M. E. & Nelson, C. C. Differential regulation of clusterin and its isoforms by androgens in prostate cells. *J Biol Chem* **282**, 2278-2287, doi:10.1074/jbc.M608162200 (2007).
- 32 Ghiggeri, G. M. *et al.* Depletion of clusterin in renal diseases causing nephrotic syndrome. *Kidney Int* **62**, 2184-2194, doi:10.1046/j.1523-1755.2002.00664.x (2002).
- 33 Yamada, K. *et al.* Clusterin is up-regulated in glomerular mesangial cells in complement-mediated injury. *Kidney Int* **59**, 137-146, doi:10.1046/j.1523-1755.2001.00474.x (2001).
- 34 Laping, N. J., Olson, B. A., Short, B. & Albrightson, C. R. Thrombin increases clusterin mRNA in glomerular epithelial and mesangial cells. *J Am Soc Nephrol* **8**, 906-914 (1997).
- 35 Kim, J., Sohn, E., Kim, C. S. & Kim, J. S. Renal podocyte apoptosis in Zucker diabetic fatty rats: involvement of methylglyoxal-induced oxidative DNA damage. *J Comp Pathol* **144**, 41-47, doi:10.1016/j.jcpa.2010.04.008 (2011).
- 36 Yu, B. *et al.* Clusterin/Akt Up-Regulation Is Critical for GATA-4 Mediated Cytoprotection of Mesenchymal Stem Cells against Ischemia Injury. *PLoS One* **11**, e0151542, doi:10.1371/journal.pone.0151542 (2016).

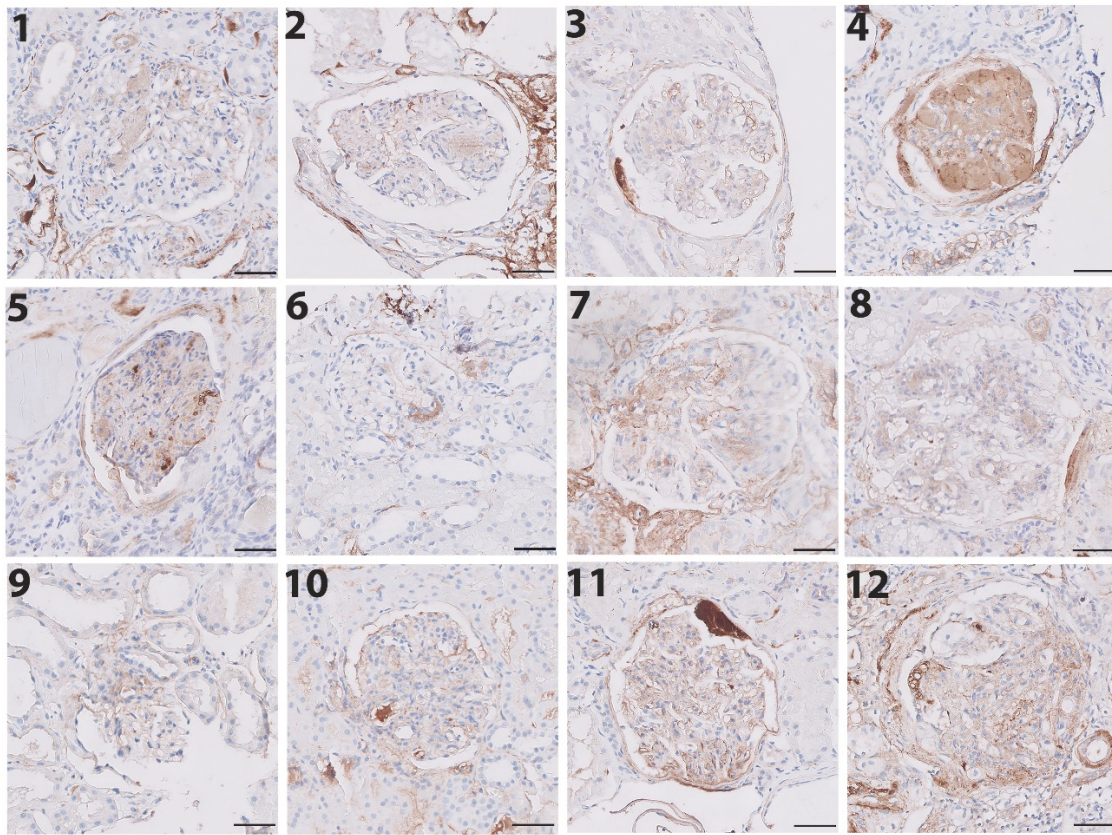
## Supplementary data

Supplementary Table 1. Clinic parameters of DN patients and Healthy subjects

| No.                     | Age | Sex    | DM  | DN class | HTN | Creatinine (μmol/L) | Proteinuria (g/24h) | HbA1c(%) | Clusterin protein expression score |
|-------------------------|-----|--------|-----|----------|-----|---------------------|---------------------|----------|------------------------------------|
| <b>DN patients</b>      |     |        |     |          |     |                     |                     |          |                                    |
| 1                       | 52  | Male   | DM2 | Class 3  | Yes | 96                  | 8.5                 | Missing  | 1.88                               |
| 2                       | 32  | Female | DM1 | Class 3  | Yes | 97                  | 6.2                 | Missing  | 2.00                               |
| 3                       | 51  | Male   | DM2 | Class 3  | Yes | 193                 | 5.3                 | 5.7      | 2.00                               |
| 4                       | 83  | Female | DM1 | Class 2  | No  | 440                 | 6.61                | 7.5      | 2.50                               |
| 5                       | 58  | Male   | DM  | Unclear  | Yes | 160                 | 7.0                 | Missing  | 2.50                               |
| 6                       | 70  | Male   | DM2 | Class 2  | No  | 186                 | 0.06                | 6.6      | 1.55                               |
| 7                       | 46  | Female | DM  | Class 3  | Yes | 300                 | 6.0                 | Missing  | 2.50                               |
| 8                       | 49  | Male   | DM2 | Class 4  | Yes | 183                 | 1.4                 | 6.0      | 2.64                               |
| 9                       | 67  | Female | DM2 | Class 3  | Yes | 613                 | 3.4                 | 6.6      | 2.00                               |
| 10                      | 35  | Male   | DM1 | Class 2  | No  | 95                  | 3.1                 | 8.3      | 1.70                               |
| 11                      | 41  | Male   | DM2 | Class 3  | Yes | 215                 | 3.8                 | 7.7      | 2.67                               |
| 12                      | 53  | Male   | DM2 | Class 4  | Yes | 275                 | 10                  | Missing  | 2.33                               |
| <b>Healthy subjects</b> |     |        |     |          |     |                     |                     |          |                                    |
| 1                       | 42  | Male   | No  | No       | No  | 97                  | 0.09                | 5.2      | 1.05                               |
| 2                       | 41  | Male   | No  | No       | No  | 89                  | 0.14                | 4.6      | 1.05                               |
| 3                       | 56  | Male   | No  | No       | No  | 83                  | 0.14                | 5.1      | 1.38                               |
| 4                       | 49  | Female | No  | No       | No  | 64                  | 0.1                 | 5.1      | 1.00                               |
| 5                       | 63  | Female | No  | No       | No  | 69                  | 0.11                | 5.6      | 1.00                               |
| 6                       | 69  | Female | No  | No       | No  | 71                  | 0.13                | 5.5      | 1.15                               |
| 7                       | 33  | Female | No  | No       | No  | 65                  | 0.11                | 5.5      | 1.11                               |
| 8                       | 46  | Male   | No  | No       | No  | 81                  | 0.08                | 5.4      | 1.05                               |
| 9                       | 62  | Female | No  | No       | No  | 68                  | 0.24                | 5.6      | 1.00                               |
| 10                      | 49  | Male   | No  | No       | No  | 92                  | 0.14                | 5.9      | 1.07                               |

Abbreviations: DM: diabetes mellitus; DN: diabetic nephropathy; HTN: hypertension; HbA1c: glycated haemoglobin.

### Supplementary Figure 1



**Supplementary Figure 1. Clusterin immunohistochemistry on biopsies from patients with diabetic nephropathy**

Representative pictures of clusterin staining on paraffin-embedded sections of the biopsies of 12 individual patients with diabetic nephropathy; the scale bars represent 50  $\mu$ m.



**Supplementary Table 2. Primer sequences used for the qPCR analysis**

| <b>Gene name</b>          | <b>Forward (5'-3')</b>     | <b>Reverse (5'-3')</b>       |
|---------------------------|----------------------------|------------------------------|
| <i>CLU</i> (human)        | AATGCTGTCAACGGGGTGA<br>A   | TGGGAGCTCCTTCAGCTTTG         |
| <i>TJP1/ZO-1</i> (human)  | GAACGAGGCATCATCCCTA<br>A   | CCAGCTTCTCGAAGAACCAC         |
| <i>NEPH1</i> (human)      | GAATAAGACACCTCCTCCT<br>G   | GACTGCTTAGGAGAAGAGAG         |
| <i>HMOX1/HO-1</i> (human) | CCGATGGGTCCTTACACTC<br>AG  | AAAGTTCATGGCCCTGGGAG         |
| <i>BAX</i> (human)        | TGCTTCAGGGTTTCATCCA<br>G   | GGCGGCAATCATCCTCTG           |
| <i>BCL2</i> (human)       | AGGAAGTGAACATTTCCGT<br>GAC | GCTCAGTTCCAGGACCAGGC         |
| <i>HPRT1</i> (human)      | AGATGGTCAAGGTCGCAAG<br>C   | TCAAGGGCATATCCTACAAC<br>AAAC |



## Chapter 3

### Carnosinase-1 overexpression, but not aerobic exercise training, affects the development of advanced diabetic nephropathy in BTBR *ob/ob* mice

Inge Everaert\*, Junling He\*, Maxime Hanssens\*, Jan Stautemas, Kim Bakker, Thomas Albrecht, Shiqi Zhang, Thibaux Van der Stede, Kenneth Vanhove, David Hoetker, Michael Howsam, Frédéric J Tessier, Benito Yard, Shahid Baba, Hans Baelde, Wim Derave.

\*These authors contributed equally to this work

*Am J Physiol Renal Physiol.* 2020 Apr 1;318(4):F1030-F1040.



## Abstract

Manipulation of circulating histidine-containing dipeptides (HCD) has been shown to affect the development of diabetes and early-stage diabetic nephropathy (DN). The aim of the present study was to investigate whether such interventions, which potentially alter levels of circulating HCD, also affect the development of advanced-stage DN. Two interventions, aerobic exercise training and overexpression of the human carnosinase-1 (hCN1) enzyme, were tested. BTBR *ob/ob* mice were either subjected to aerobic exercise training (20 wk) or genetically manipulated to overexpress hCN1, and different diabetes- and DN- related markers were compared with control *ob/ob* and healthy (wild-type) mice. An acute exercise study was performed to elucidate the effect of obesity, acute running, and hCN1 overexpression on plasma HCD levels. Chronic aerobic exercise training did not affect the development of diabetes or DN, but hCN1 overexpression accelerated hyperlipidemia and aggravated the development of albuminuria, mesangial matrix expansion, and glomerular hypertrophy of *ob/ob* mice. In line, plasma, kidney, and muscle HCD were markedly lower in *ob/ob* versus wild-type mice, and plasma and kidney HCD in particular were lower in *ob/ob* hCN1 versus *ob/ob* mice but were unaffected by aerobic exercise. In conclusion, advanced glomerular damage is accelerated in mice overexpressing the hCN1 enzyme but not protected by chronic exercise training. Interestingly, we showed, for the first time, that the development of DN is closely linked to renal HCD availability. Further research will have to elucidate whether the stimulation of renal HCD levels can be a therapeutic strategy to reduce the risk for developing DN.

## Introduction

Twenty to forty percent of patients with type 2 diabetes develop diabetic nephropathy (DN). As no optimal treatment for DN is currently available, this frequently results in end-stage renal disease and dependence on dialysis. A growing body of evidence suggests a protective role of carnosine against DN. Carnosine and its methylated analog anserine are histidine-containing dipeptides (HCD), consisting of amino acids  $\beta$ -alanine and histidine and  $\pi$ -methylhistidine, respectively, which are available in the diet of omnivorous subjects. They possess some beneficial biochemical properties, such as antioxidative, metal chelating, and antiglycation properties, which enable them to attenuate the development of DN (for a review, see Ref. <sup>1</sup>).

Genetic studies have revealed an association of a polymorphism in the carnosinase-1 gene (*CNDP1*), the enzyme responsible for the hydrolysis of carnosine in the circulation, and the prevalence of DN, especially in female patients with type 2 diabetes<sup>2-4</sup>. Although carnosine is only present in the low nanomolar range in the fasted state (because of the very active carnosinase-1 enzyme)<sup>5</sup>, it has been hypothesized that a higher circulating carnosine content upon dietary intake was the underlying mechanism for protection against DN<sup>6,7</sup>.

Long-term supplementation of carnosine in drinking water has repeatedly been shown to protect against early signs of DN in different diabetic rodent models (*db/db* mice<sup>8</sup>, obese Zucker rats<sup>9</sup>, and streptozotocin-induced diabetic rats<sup>10,11</sup>) and recently also in BTBR *ob/ob* mice, which have DN with severe glomerular lesions<sup>12</sup>. Reducing the amount of circulating carnosine levels, on the other hand, has been achieved by overexpressing the human carnosinase-1 (hCN1) enzyme, which is only present in humans and not in rodents. This resulted in a more pronounced diabetic state (as reflected by hyperglycemia, HbA1c, and insulin) in *db/db* mice<sup>7</sup>. However, since *db/db* mice are slow to develop advanced DN, the effect of reduced circulating carnosine levels on DN in a model with more pronounced DN (BTBR *ob/ob*) was investigated in the present study.

HCD are mainly present in skeletal muscle but also in lower amounts in kidney tissue. Owing to its high concentration in skeletal muscles and their total volume, it is estimated that ~99% of the carnosine body burden is stored in skeletal muscle. Therefore, a potential alternative way to manipulate circulating carnosine levels is hypothesized to be the release of carnosine from skeletal muscle as a result of physical exercise. Both mice and horses were characterized by higher carnosine content in their circulation when being physically active<sup>13,14</sup>. Human evidence is scarce, but muscle interstitium carnosine levels were increased in response to submaximal leg exercise<sup>15</sup>.

Interestingly, it has been established that prolonged aerobic exercise training could protect different diabetic rodent models against the increase in urinary albumin and other pathophysiological characteristics of DN <sup>16-18</sup>. Intervention studies investigating the effects of exercise training on the development of DN in patients with diabetes are lacking <sup>19</sup>; however, one prospective study revealed that moderate- and high- intensity leisure-time physical activity attenuate the initiation and progression of DN <sup>20</sup>. We thus hypothesized that part of the protective effect of exercise training on DN is mediated by enhanced circulating carnosine and/or anserine, which are released from muscular storage sites upon muscle contractile activity. This could be a novel therapeutic insight on the benefits of exercise, in addition to the more commonly proposed mechanism that exercise training can improve glycemic control <sup>21</sup>.

The aim of the present study was to investigate whether overexpression of the hCN1 enzyme or chronic aerobic exercise training, interventions potentially resulting in decreased and increased circulating HCD levels, respectively, could affect the development of DN in mice that develop glomerular lesions that closely resemble an advanced stage of human DN (BTBR *ob/ob* mice <sup>22</sup>). An acute study was performed to evaluate the effect of obesity, acute exercise, and hCN1 overexpression on plasma and muscle HCD levels. A chronic study further examined the development of diabetes and DN in *ob/ob* mice compared with that in 1) *ob/ob* mice that underwent a treadmill-based aerobic exercise training protocol for 20 wk and 2) *ob/ob* mice that were genetically manipulated to overexpress the hCN1 enzyme.

## Methods

The experimental protocol was approved by the Ethics Committee for Animal Research at Ghent University and followed the Principles of Laboratory Animal Care.

### Generation and genotyping of experimental mice

Human carnosine dipeptidase 1 (*hCNDP1*) transgenic mice were generated in the BTBR *wt/ob* (Black and Tan, BRachyuric) background as previously described in *db/db* mice <sup>7</sup>. Briefly, The cDNA of *hCNDP1* including the endogenous signal peptide of six leucines was amplified from IMAGE clone Accession No. BX094414 with the primers 5'-PCACCATGGATCCCAAACCTCGGGA-3' (*CNDP1* forward) and 5'-PTCAATGGAGCTGGGCCATCT-3' (*CNDP1* reverse). PCR products were ligated behind the transthyretin promoter into the *StuI* site of plasmid pTTR1ExV3. Thereafter, DH5 $\alpha$ -competent *Escherichia coli* were transformed with *hCNDP1* containing pTTR1ExV3.

Transformed *E. coli* were propagated with standard protocols. For isolation of the hCNDP1-pTTR1ExV3 plasmid, a Maxi-Prep plasmid purification kit (Qiagen, Hilden, Germany) was used. Thereafter, the fragment containing hCNDP1 and the TTR1 promoter was cut from the plasmid by HindIII digestion. The purified fragment was injected into the pronuclei of the fertilized ovum of BTBR *ob/wt* female mouse (stock no. 004824, Jackson Laboratories, Bar Harbor, ME). All animal procedures were approved by the Regierungspräsidium Karlsruhe (AZ 35-9185.81/G-116/14 and G-108/13). The fertilized ovum was transplanted into the oviduct of a pseudopregnant mouse that had been induced to act as a recipient by mating with a vasectomized male mouse. In separate experiments from our research group, we previously observed that hCN1 overexpression in *ob/wt* mice did not result in metabolic disturbances, reflected by similar levels of HbA1c and the albumin-to-creatinine ratio in transgenic versus nontransgenic *ob/wt* mice (B. Yard et al., unpublished data).

hCN1 transgenic BTBR mice were crossbred with BTBR *ob/wt* mice (line 004824, The Jackson Laboratory). The *Lep<sup>ob</sup>* point mutation and overexpression with hCN1 was checked by quantitative PCR (high-resolution melting analysis, based on Ref.<sup>23</sup>). DNA was isolated from tails of 7- to 11-day-old pups with the Invisorb Spin tissue mini kit (Strattec Molecular). DNA content was quantified with NanoDrop (ThermoFisher Scientific) and diluted with elution buffer to a final concentration of 25 ng/μL. For the *ob* point mutation, primer mix (0.4 μL, final concentration: 2 μM, forward: 5'- CAGATAGCCAATGACCTGGAG-3' and reverse: 5'- TCTTGGAGAAGGCCAGCAGAT-3'), JumpStart Taq ReadyMix (6 μL, Sigma-Aldrich), SYBR Green PCR Master Mix (1.2 μL, Life Technologies), and DNA (0.5 μL) were added to a LightCycler 480 multiwell plate. For CN1 transgene, primer mix (0.4 μL, final concentration: 2 μM, forward 5'-CCTCGCTTCAGACAAGAGCTCTTCAGAATGA-3' and reverse 5'- GCTCTGAAGGCGCTCACAGCATTGATCCAA-3', JumpStart Taq ReadyMix (3.6 μL, Sigma-Aldrich), SYBR Green PCR Master Mix (3.6 μL, Life Technologies) and DNA (0.5 μL) were used. Amplification and melt curve analysis was performed on a Roche LightCycler 480 instrument using the following parameters: detection format: SYBR Green I, preincubation (95°C for 3 min), amplification/quantification (95°C for 30 s, 58°C for 30 s, 72°C for 1 min with single acquisition; 38 cycles), high-resolution melting (95°C for 1 min, 40°C for 1 min, 65°C for 1 s, and 90°C with 25 acquisitions per °C). The genotyping was validated by evaluating the phenotypes, i.e., obesity and plasma CN1 activity, respectively.

## Experimental design

### Acute study

Four- to six-week-old wild-type (WT;  $n = 17$ ), *ob/ob* ( $n = 29$ ), and *ob/ob* hCN1 ( $n = 5$ ) mice were included in these experiments (Table 1). After five familiarization sessions (in 2 wk), mice were placed on either a running treadmill (*ob/ob* EX; 10 m/min,  $n = 14$ ) or a stationary treadmill (*ob/ob*;  $n = 14$ ) for 1 h. Mice were immediately sedated (80% Ketalar -20% Rompun) after 1 h, blood was collected as quickly as possible in precooled EDTA tubes and centrifuged at 14,000 g for 5 min, and collected plasma was stored, after deproteinization with sulfosalicylic acid (SSA), at -20°C. Gastrocnemius muscle was immediately collected after cervical dislocation, snap frozen in liquid nitrogen, and stored at -80°C.

### Chronic study

Four-week-old BTBR mice were randomly allocated to the following four experimental groups: WT ( $n = 15$ ), *ob/ob* ( $n = 19$ ), *ob/ob* with exercise training (EX-T;  $n = 19$ ), and *ob/ob* hCN1 ( $n = 16$ ) (Table 2). Male and female mice were included equally. Exercise training, on a Columbus Exer-3/6 open treadmill, was initiated at the age of 4 wk with a familiarization period of 2 wk, in which running time and intensity were gradually increased up to 10m/min for 1 h. Mice were closely monitored during running and were removed from the treadmill when they refused (e.g., because of injury) to leave the electrical grid. At the age of 4 and 24 wk, daily food and water intake (mean value per cage, mice having been placed in separate cages per group, sex, and age) and body weight were monitored. At *weeks 4, 14* and 24, fasted (4-6 h) serum was collected via the tail vein and diluted with 0.9% NaCl for further analysis. Fasted (4-6 h) spot urine was collected at *weeks 4, 8, 12, 14* and 24. Euthanasia took place at the age of 24 wk. One kidney was removed (snap frozen and stored at -80°C) under isoflurane anesthesia, after which whole body perfusion (heart left ventricle) with saline was performed. The remaining, perfused kidney was placed in formalin solution (neutral buffered, 10%, Sigma-Aldrich) for 24 h, after which it was stored in 70% ethanol at room temperature and embedded in paraffin. The perfused gastrocnemius was further dissected and stored at -80°C until analysis. Fasted serum glucose, triglycerides, and cholesterol were measured in the Clinical Laboratory of University Hospital UZ Ghent with a Roche/Hitachi Cobas C according to the manufacturer's procedures. Serum protein levels were evaluated by means of the Total Protein Kit Micro-Lowry, Onishi & Barr Modification (catalog no.TP0200, Sigma).



**Histological analysis**

Paraffin-embedded kidney tissue was cut on a Leica microtome (Wetzlar). Sections (4- $\mu\text{m}$  thickness) were deparaffinized and rehydrated according to a standard protocol. Sections were stained with periodic acid-Schiff as well as haematoxylin and eosin. Stained slides were digitalized with the Philips Ultra Fast Scanner 1.6 RA (Philips Electronics) for morphological measurement. The surface areas ( $\mu\text{m}^2$ ) of the whole glomerulus, Bowman's space, and glomerular tuft of 25 randomly chosen glomeruli were measured with ImageJ software to examine glomerular hypertrophy. Periodic acid-Schiff -stained kidney tissue was graded in a blinded manner by two independent observers on a scale of 0 -3, depending on the amount of mesangial matrix( 0: 0-25%, 1: 25-50%, 2: 50-75%, and 3: >75%), in 25 randomly chosen glomeruli. Interstitial fibrosis was determined by Sirius red staining.

**Immunohistochemistry**

Sections were deparaffinized, rehydrated, and thereafter stained for Wilms' tumor-1 protein. Antigen retrieval was performed with Tris/EDTA buffer. Sections were incubated with rabbit anti-Wilms' tumor-1 (1:1000, Santa Cruz Biotechnology, Santa Cruz, CA) followed by an anti-rabbit-Envision, horseradish peroxidase-labeled secondary antibody (Dako, Denmark). As a negative control, a normal rabbit serum was used as the primary antibody. Immunostaining was visualized with diaminobenzidine (DAB+; Dako, Denmark) as the chromogen. Thereafter, sections were counterstained with haematoxylin and eosin, dehydrated, and mounted. Sections were imaged with a Philips Ultra-Fast Scanner 1.6 RA (Philips Electronics). The number of podocytes in each sample was determined by counting the number of Wilms' tumor-1-positive nuclei per glomerulus in 25 randomly chosen glomeruli.

**Urinary albumin**

Urine albumin levels were measured using the rocket immunoelectrophoresis against rabbit anti-mouse albumin, and purified mouse serum albumin (Sigma-Aldrich, USA) was used as the standard. Urine creatinine levels were measured with a creatinine assay with picric acid, sodium hydroxide, and creatinine standards (Sigma-Aldrich, USA). Thereafter, the albumin-to-creatinine ratio was calculated. The rabbit anti-mouse albumin antibody was produced in our laboratory and tested by Western Blot for specificity.

### **Kidney Carboxymethyllysine**

Carboxymethyllysine (CML), a widely studied marker of advanced glycation, was analyzed in kidneys with the method described by Niquet-Léridon and Tessier <sup>24</sup> with the instrument parameters detailed by Guilbaud et al. <sup>25</sup>.

### **Carnosine and anserine determination**

Carnosine and anserine were quantified based on the protocol of Ref. <sup>26</sup>. Deproteinized plasma (acute exercise study) and spot urine (chronic exercise study) were diluted 1:20 and 1:25, respectively, in a 75% acetonitrile-25% water solution containing 10  $\mu$ M tyrosine-histidine (mass-to-charge ratio: 319 Da) as an internal standard. Samples were centrifuged at 13,000 g for 10 min to eliminate excessive precipitate. The supernatant was used for further analysis. Gastrocnemius muscle (acute study) and kidney tissue (chronic study) were homogenized in extraction solution containing 10 mM HCl, 100  $\mu$ M phenanthroline (specific CN1 inhibitor), and tyrosine-histidine internal standard (25  $\mu$ M for muscle tissue and 2  $\mu$ M for kidney tissue) with a BeadBug D1030 tissue homogenizer. Homogenates were sonicated on ice for 10 s and centrifuged at 13,000 g for 10 min. The supernatant was diluted 1:1,500 (muscle homogenate) and 1:100 (kidney homogenate) in a 75% acetonitrile-25% water solution before further analysis.

High-resolution ultraperformance liquid chromatography (UPLC; Waters ACQUITY UPLC H-Class System) coupled with a Xevo TQ-S micro triple quadrupole MS (LC-MS/MS) was used to identify and quantify carnosine, anserine, and carnosine-aldehyde conjugate levels. Carnosine, anserine and carnosine-aldehyde conjugates were separated with a Waters ACQUITY BEH HILIC column (1.7  $\mu$ m, 2.1 x 50 mm) equipped with an in-line frit filter unit. The elution of analytes was achieved with a binary solvent system consisting of 10 mM ammonium formate and 0.125 % formic acid in 5% acetonitrile-95% water for *mobile phase A* and 10 mM ammonium formate and 0.125% formic acid in 95% acetonitrile-5% water for *mobile phase B* at a flow rate of 0.55 mL/min. Initial conditions were 0.1:99.9 A:B ramping to 99.9:0.1 A:B over 5 min before rapidly returning to 0.1:99.9 A:B over 0.5 min. This mobile phase composition was held from 5.5 min to 8 min to equilibrate the column for the next injection (5  $\mu$ L). Dipeptides were quantified with external standard curves, and carnosine-aldehyde conjugates were quantified with the peak ratio of histidyl-dipeptide to the tyrosine-histidine internal standard.

### **CN1 activity**

CN1 activity was quantified by fluorometric determination of liberated histidine after carnosine addition (based on Teufel et al. <sup>27</sup>). Briefly, the reaction was initiated by the addition of 10 mM carnosine (Flamma) to serum and stopped after 10 min incubation at 37°C by the addition of 600 mM trichloroacetic acid (TCA). For controls, TCA was added before carnosine. After centrifugation (4,500g, 15 min), supernatant was added to a mixture of *o*-phthalal-dehyde (OPA; incomplete phthalaldehyde with 0.2% 2-mercaptoethanol) and 4M sodium hydroxide, and fluorescence was determined after 40 min (excitation: 360 nm and emission: 465 nm).

### **Citrate synthase activity**

Citrate synthase activity assay was based on the binding of coenzyme A (CoA-SH) to 5,5'-dithiobis (2-nitrobenzoic acid) (DTNB), after initiation by oxaloacetic acid, and absorbance measured at 450nm. In short, gastrocnemius muscle was homogenized in ice-cold buffer consisting of 250 mM sucrose, 2 mM Na-EDTA, and 5 mM Tris base (pH 7.4) and centrifuged for 10 min at 10,000 rpm. Protein content was measured with a Total Protein Kit (Merck, Micro-Lowry, Onishi & Barr modification). Reagent solution (100 mM Tris base, 100  $\mu$ M DTNB, and 0.05 mM acetyl CoA, pH 8, 250  $\mu$ L) was added to the samples (5  $\mu$ L, ~ 0.5 g/L protein) or standards (5  $\mu$ L CoA-SH), after which the reaction was initiated by the addition of 5  $\mu$ L of 25 mM oxaloacetic acid. The linear part of the enzymatic reaction was used to calculate, with a standard curve, the amount of CoA-SH that was formed.

### **Statistical analysis**

All data are expressed as means  $\pm$  SD. For the acute study, one-way ANOVA was performed to evaluate the effect of the interventions on plasma and muscle carnosine and anserine. Significant results were further evaluated by means of independent *t* tests. For the chronic study, body weight and water intake were analyzed by means of repeated measures with time <sup>9</sup> as within-subject and group <sup>28</sup> as between-subjects factor. The evolution over time of serum CN1 activity of the hCN1 group was evaluated by means of a paired *t* test. Repeated-measured parameters were evaluated with time as within-factor <sup>28,29</sup> and group <sup>28</sup> as between factor. In case of significant interaction effects, the test was repeated per two groups and an independent *t* test was performed per time point. Parameters measured at week 24 were checked with one-way ANOVA with group <sup>28</sup> as between factor and post hoc analysis when

necessary. Correlations were evaluated by means of Pearson correlations. Differences were considered statistically significant at  $P < 0.05$ .

## Results

### Acute study

Because CN1 hydrolyzes carnosine and anserine, we first determined whether hCN1 overexpression in *ob/ob* mice enhanced the CN1 activity and affected circulating and skeletal muscle HCD levels. As expected, no CN1 activity was detected in the serum of WT or *ob/ob* mice, whereas CN1 hydrolyzing activity was significantly enhanced in the *ob/ob* hCN1 mice ( $6.04 \pm 0.94 \mu\text{mol}\cdot\text{mL}^{-1}\cdot\text{h}^{-1}$ ; Table 1). This CN1 activity was higher compared with the CN1 activity of healthy subjects (mean:  $\sim 1.5 \mu\text{mol}\cdot\text{mL}^{-1}\cdot\text{h}^{-1}$ , unpublished data). Analysis of the plasma by LC-MS/MS showed that HCD levels were significantly decreased in the *ob/ob* mice ( $0.28 \pm 0.16 \mu\text{M}$ ) compared with WT mice ( $0.65 \pm 0.38 \mu\text{M}$ ;  $P < 0.05$ ). This decrease can be attributed to both carnosine (WT:  $0.36 \pm 0.32 \mu\text{M}$  vs. *ob/ob*:  $0.11 \pm 0.08 \mu\text{M}$ ) and anserine (WT:  $0.29 \pm 0.15 \mu\text{M}$  vs. *ob/ob*:  $0.16 \pm 0.08 \mu\text{M}$ ). As expected, overexpression of hCN1 in *ob/ob* mice resulted in a >100-fold decrease in circulating HCD ( $0.003 \pm 0.007 \mu\text{M}$ ,  $P < 0.05$ ) compared with *ob/ob* mice. Acute running did not significantly affect circulating carnosine and anserine levels in *ob/ob* mice ( $P > 0.1$ ; Fig. 1A). Circulating carnosine-propanal levels (carnosine bounded to the reactive carbonyl acrolein) were significantly higher in *ob/ob* mice ( $7.73 \pm 2.10 \text{ nM}$ ) versus WT mice ( $5.03 \pm 1.22 \text{ nM}$ ) and tended ( $0.05 > P < 0.1$ ) to be higher in exercising *ob/ob* mice ( $8.83 \pm 1.45 \text{ nM}$ ) compared with the resting ( $6.63 \pm 2.18 \text{ nM}$ ) obese control mice (data not shown).

In these young animals, carnosine and anserine gastrocnemius levels were not dependent on obesity (Fig. 1B). Further, acute exercise or overexpression of hCN1 had no effect on the skeletal muscle HCD levels in these BTBR *ob/ob* mice (Fig. 1B).

**Table 1. Acute study: basic group characteristics**

|                   | Number of Mice<br>(Male/Female) | Age, wk       | Body Weight, g | Carnosinase-1 Activity, $\mu\text{mol}\cdot\text{mL}^{-1}\cdot\text{h}^{-1}$ |
|-------------------|---------------------------------|---------------|----------------|--|
| WT                | 17 (8/9)                        | $8.3 \pm 0.7$ | $28.1 \pm 3.0$ | <LOD   |
| <i>ob/ob</i>      | 15 (6/9)                        | $7.5 \pm 1.5$ | $47.3 \pm 6.5$ | <LOD   |
| <i>ob/ob</i> EX   | 14 (7/7)                        | $7.0 \pm 1.3$ | $47.7 \pm 8.3$ | <LOD   |
| <i>ob/ob</i> hCN1 | 5 (2/3)                         | $6.6 \pm 1.1$ | $44.2 \pm 8.7$ | $6.04 \pm 0.94$  |

Values are means  $\pm$  SD for the numbers of mice indicated. The following groups are shown: wild type (WT) mice, *ob/ob* mice, *ob/ob* mice with acute exercise (EX), and *ob/ob* human carnosinase-1 transgenic (hCN1) mice. LOD, limit of detection.

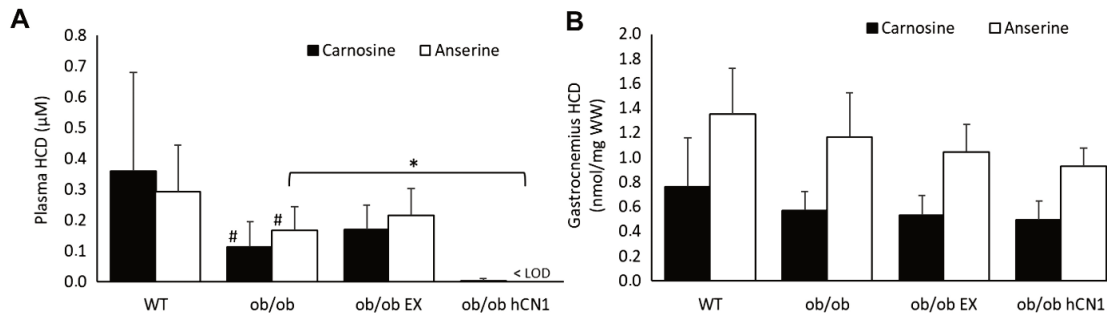


**Figure 1. Acute study: metabolism of histidine-containing dipeptides (HCD)**

A and B: plasma (A) and gastrocnemius (B) carnosine and anserine content in wild-type (WT) mice, *ob/ob* mice, *ob/ob* mice with acute exercise (EX), and *ob/ob* human carnosinase-1 (hCN1) transgenic mice. LOD, limit of detection; WW, wet weight. Values are means  $\pm$  SD. <sup>#</sup> $P \leq 0.05$ , *ob/ob* vs. WT mice; \* $P \leq 0.05$  vs. *ob/ob* mice.

### Chronic study

To determine the effect of exercise training, *ob/ob* mice were exercised at an aerobic intensity for 20 wk, running 5 days/wk for 1 h at 10 m/min. The body weight gain after 20 wk was more than twofold higher in *ob/ob* versus WT mice. Exercise training or hCN1 overexpression did not influence the evolution of body weight over time (Table 2). Serum carnosinase activity (week 24) was markedly higher in hCN1 transgenic mice ( $145.8 \pm 61.5 \mu\text{mol}\cdot\text{mL}^{-1}\cdot\text{h}^{-1}$ ) versus nontransgenic mice ( $0.54 \pm 0.75 \mu\text{mol}\cdot\text{mL}^{-1}\cdot\text{h}^{-1}$ ) and increased approximately fourfold from 4 to 24 wk in transgenic mice (Table 2).

**Table 2. Chronic study: basic group characteristics**

|                   | Number of Mice<br>(Male/Female) | Body Weight, g    | Water Intake,<br>mL/day | Carnosinase-1 Activity,<br>$\mu\text{mol}\cdot\text{mL}^{-1}\cdot\text{h}^{-1}$ |
|-------------------|---------------------------------|-------------------|-------------------------|---|
| <i>Week 4</i>     |                                 |                   |                         |   |
| WT                | 15 (7/8)                        | $19.9 \pm 4.6$    | $12.7 \pm 9.4$          | ND  |
| <i>ob/ob</i>      | 19 (10/9)                       | $28.8 \pm 5.0^*$  | $13.0 \pm 3.7$          | ND  |
| <i>ob/ob</i> EX-T | 19 (9/10)                       | $27.2 \pm 2.9$    | $15.1 \pm 4.3$          | ND  |
| <i>ob/ob</i> hCN1 | 16 (7/9)                        | $26.4 \pm 7.9$    | $15.1 \pm 5.8$          | $33.4 \pm 20.2$   |
| <i>Week 24</i>    |                                 |                   |                         |   |
| WT                | 14 (7/7)                        | $38.8 \pm 6.8$    | $15.7 \pm 5.2$          | $0.15 \pm 0.15$   |
| <i>ob/ob</i>      | 17 (9/8)                        | $74.0 \pm 10.8^*$ | $29.4 \pm 15.3^*$       | $0.54 \pm 0.75$   |
| <i>ob/ob</i> EX-T | 16 (7/9)                        | $67.7 \pm 7.4$    | $25.0 \pm 14.1$         | $0.62 \pm 0.75$   |
| <i>ob/ob</i> hCN1 | 14 (6/8)                        | $72.2 \pm 12.2$   | $30.6 \pm 11.7$         | $145.8 \pm 61.5^\dagger$  |

Values are means  $\pm$  SD for the numbers of mice indicated. The following groups are shown: wild type (WT) mice, *ob/ob* mice, *ob/ob* mice with chronic exercise training (EX-T), and *ob/ob* human carnosinase-1 transgenic (hCN1) mice. ND, not determined. \* $P \leq 0.05$ , *ob/ob* vs. WT mice;  $^\dagger P > 0.05$  and  $< 0.1$  vs. *ob/ob* mice.

### Development of diabetes in BTBR *ob/ob* mice

To determine the effect of exercise training and hCN1 overexpression on the development of diabetes, we measured fasting serum glucose levels. The results showed that serum glucose levels were three- to four- fold higher in *ob/ob* mice at *weeks 14* and *24* compared with WT mice (*week 14*:  $674.02 \pm 297.54$  mg/dL vs.  $170.76 \pm 40.49$  mg/dL; *week 24*:  $724.90 \pm 502.58$  mg/dL vs.  $265.67 \pm 66.75$  mg/dL; Fig. 2A), but were not affected by exercise training or hCN1 overexpression.

Plasma fructosamine content, a long-term biomarker of glucose overload, was significantly higher at *weeks 14* (+57%) and *24* (+48%) in *ob/ob* versus WT mice. Fructosamine levels returned to baseline levels from *week 14* to *24* in *ob/ob* mice ( $P < 0.05$ ; Fig. 2B). The increase in fructosamine levels was independent of exercise training or hCN1 overexpression (Fig. 2B). Total serum protein levels were higher in *ob/ob* mice ( $71.58 \pm 21.92$  g/L) compared with WT mice at *week 24* ( $61.90 \pm 8.48$  g/L; data not shown). Therefore, it is suggested that reduced circulating protein levels were not the cause of the decline in serum fructosamine levels between *weeks 14* and *24*.

In contrast to the glucose-based markers, serum triglycerides and cholesterol levels were significantly affected by hCN1 overexpression. Serum triglycerides evolved differentially over time in *ob/ob* versus *ob/ob* hCN1 mice, with a trend to significant higher values at *week 14* (+57%) but not at *week 24* (Fig. 2C). Similar to triglycerides, cholesterol levels were significantly increased (+ 109%) at 14 wk of age in the *ob/ob* hCN1 mice compared with the *ob/ob* mice but not at 24 wk. No effect of exercise training on the evolution over time of serum triglycerides and cholesterol was observed (Fig. 2C and 2D).

The effect of the interventions (hCN1 and exercise training) on the different diabetes-related parameters were not dependent on sex (data not shown) except for the development of hyperglycemia. The development of hyperglycemia was more pronounced in male (*week 24*:  $1001.41 \pm 309.48$  mg/dL) versus female (*week 24*:  $462.55 \pm 253.30$  mg/dL,  $P < 0.05$ ) obese mice. Furthermore, male *ob/ob* EX-T and *ob/ob* hCN1 mice had significantly lower serum glucose levels (-20% and -18%, respectively) compared with male *ob/ob* mice at *week 14*, whereas no differences were found between different obese groups in female mice (data not shown).

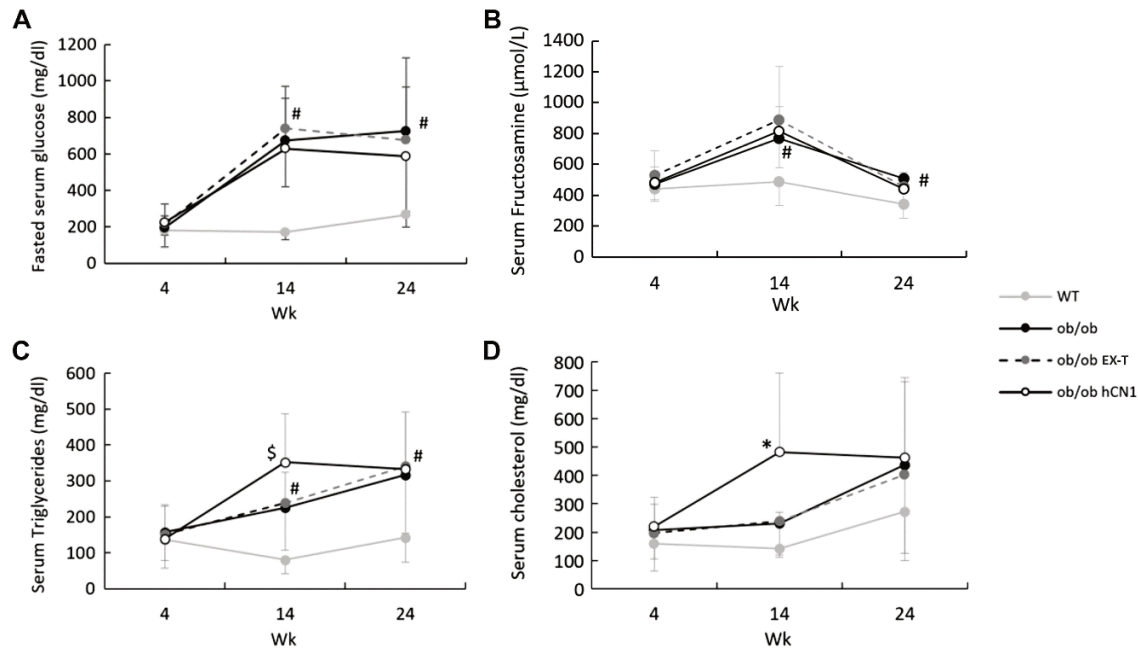


**Figure 2. Development of diabetes in BTBR *ob/ob* mice**

A-D: fasted serum glucose (A), fructosamine (B), triglycerides (C), and cholesterol (D) were quantified at 4, 14, and 24 wk of age in wild-type (WT) mice, *ob/ob* mice, *ob/ob* mice with exercise training (EX-T), and *ob/ob* human carnosinase-1 (hCN1) transgenic mice. Values are means  $\pm$  SD. # $P \leq 0.05$ , *ob/ob* vs. WT mice; \* $P \leq 0.05$  vs. *ob/ob* mice; \$ $P > 0.05$  and  $< 0.1$  vs. *ob/ob* mice at the same time point.

### Development of diabetic nephropathy in BTBR *ob/ob* mice

The development of DN was evaluated by measuring the urinary albumin-to-creatinine ratio. At the end of the intervention, the albumin-to-creatinine ratio of *ob/ob* mice was  $1194.62 \pm 963.86$   $\mu\text{g}/\text{mg}$ , i.e. ~25-fold higher in *ob/ob* versus WT mice ( $47.86 \pm 21.87$   $\mu\text{g}/\text{mg}$ ), which corresponds with a stage of advanced DN. The albumin-to-creatinine ratio was not affected by the exercise intervention, but *ob/ob* hCN1 mice ( $2,182.24 \pm 1,667.66$   $\mu\text{g}/\text{mg}$ ) had significantly higher levels (+82%) compared with *ob/ob* mice (Fig. 3B).

Renal lesions were evaluated by scoring the degree of mesangial matrix expansion. This expansion was 3.8-fold more pronounced in *ob/ob* versus WT mice and was further aggravated by hCN1 overexpression (+22%,  $P < 0.05$ ; Fig. 3C). Representative images of a WT, an *ob/ob*, and an *ob/ob* hCN1 mouse are shown in Fig. 3A. The number of podocytes was not affected by obesity or by hCN1 overexpression ( $P > 0.1$ ; Fig. 3D). Also, weak to mild interstitial fibrosis was seen both in the *ob/ob* mouse and *ob/ob* hCN1 mouse.

Glomerular hypertrophy was evaluated by measuring the surface areas ( $\mu\text{m}^2$ ) of the glomerular tuft, Bowman's space and whole glomerulus (Fig. 3E-3G). The three different areas were expanded in *ob/ob* mice versus WT mice ( $P < 0.05$ ), and overexpression of hCN1 further aggravated the hypertrophy in glomerular tuft ( $P < 0.05$ ; Fig. 3E) and whole glomerulus ( $P < 0.05$ ; Fig. 3G), but not in Bowman's space ( $P > 0.1$ ; Fig. 3F).

None of the above-mentioned DN-related parameters was affected by the chronic aerobic exercise training protocol (Fig. 3).

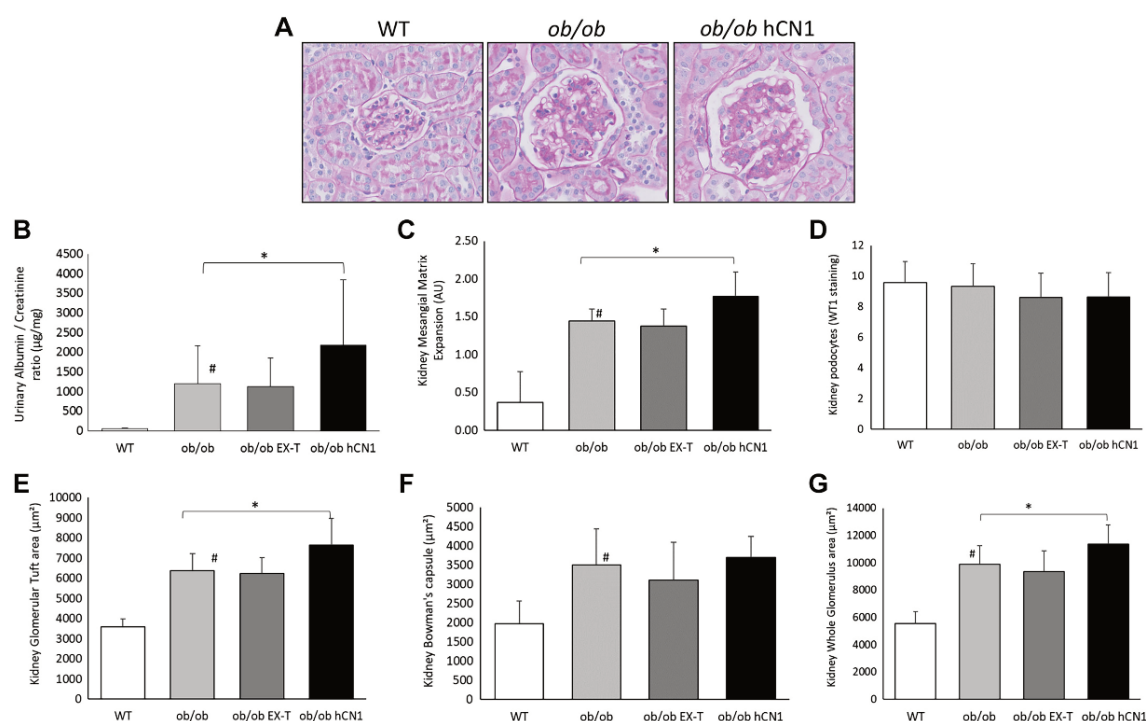


**Figure 3. Development of diabetic nephropathy in BTBR *ob/ob* mice**

A: representative images of glomeruli (periodic acid-Schiff-stained sections) of (from left to right) wild-type (WT) mice, *ob/ob* mice, and *ob/ob* human carnosinase-1 (hCN1) transgenic mice. B–G: urinary albumin-to-creatinine ratio (B), degree of mesangial matrix expansion (C), number of podocytes (D), and surface area of the glomerular tuft (E), Bowman's space (F), and whole glomerular area (G) at week 24 for WT mice, *ob/ob* mice, *ob/ob* mice with exercise training (EX-T), and *ob/ob* hCN1 mice. AU, arbitrary units; WT1, Wilms' tumor-1 protein. Values are means  $\pm$  SD. #  $P \leq 0.05$ , *ob/ob* vs. WT mice; \*  $P \leq 0.05$  vs. *ob/ob* mice.

### Metabolism of HCD and acrolein adducts

To further elucidate the effect of hCN1 overexpression, HCD levels were quantified in the kidney, skeletal muscle and urine in 24-wk-old mice. Carnosine and anserine were



remarkably lower in both the kidney (Fig. 4A) and muscle (Fig. 4B) in *ob/ob* versus WT mice ( $P < 0.05$ ). Kidney (-95%,  $P < 0.05$ ) and muscle (-20%,  $P < 0.1$ ) anserine were further declined in hCN1 transgenic *ob/ob* versus nontransgenic *ob/ob* mice (Fig. 4A and 4B).

The evolution of urinary excretion of HCD was not dependent on obesity or the different interventions ( $P > 0.1$ ; Fig. 4C). Urinary carnosine-propanal adducts were not detectable throughout the intervention period. In contrast, urinary carnosine-propanol levels were above the limit of detection and similar between WT and *ob/ob* mice at 4 and 24 wk of age and slightly higher at 14 wk of age in *ob/ob* versus WT mice. In *ob/ob* hCN1 mice, urinary carnosine-propanol levels were not different at 4 and 14 wk from *ob/ob* mice, however, were 20-fold lower in *ob/ob* hCN1 at 24 wk of age ( $P < 0.05$ ; Fig. 4D).

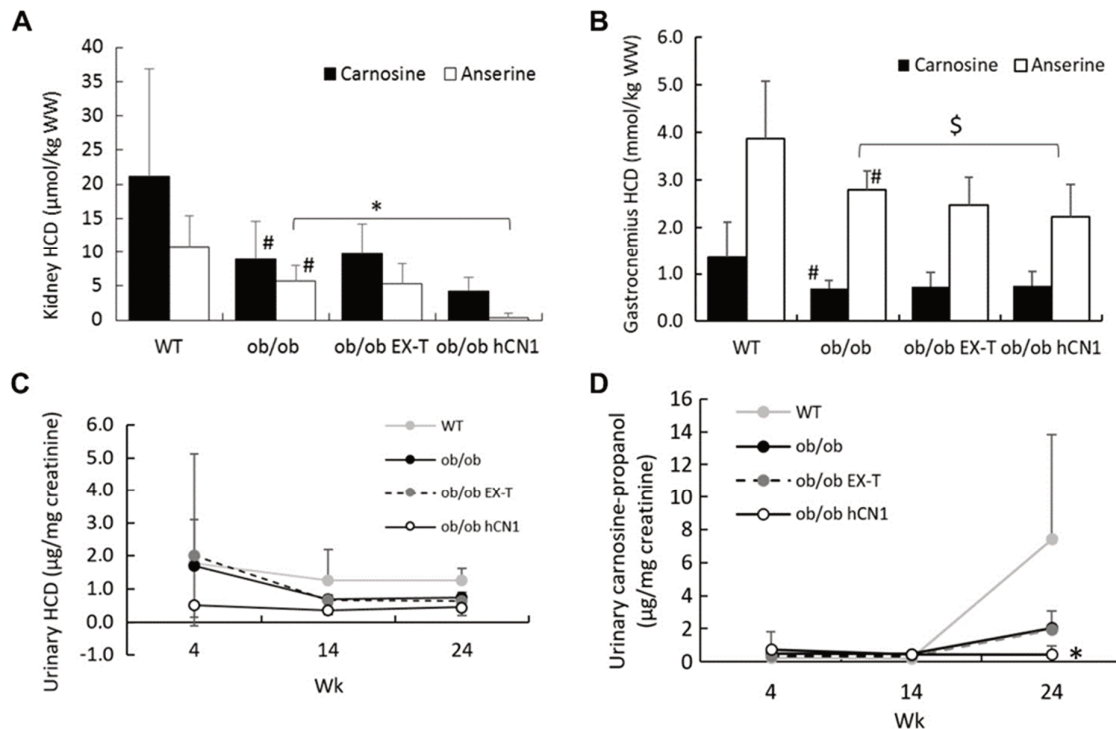


**Figure 4. Metabolism of histidine-containing dipeptides (HCD) in BTBR *ob/ob* mice**

A–C: kidney (A; week 24), gastrocnemius (B; week 24), and urinary (C; weeks 4, 14, and 24) HCD content in wild-type (WT) mice, *ob/ob* mice, *ob/ob* mice with exercise training (EX-T), and *ob/ob* human carnosinase-1 (hCN1) transgenic mice. Values are means  $\pm$  SD. <sup>#</sup> $P \leq 0.05$ , *ob/ob* vs. WT mice; <sup>\*</sup> $P \leq 0.05$  vs. *ob/ob* mice; <sup>\$</sup> $P > 0.05$  and  $< 0.1$  vs. *ob/ob* mice. D: urinary carnosine-propanol adducts (weeks 4, 14, and 24) in WT, *ob/ob*, *ob/ob* EX-T, and *ob/ob* hCN1 mice. WW, wet weight. Values are means  $\pm$  SD. <sup>\*</sup> $P \leq 0.05$  vs. *ob/ob* mice at the same time point.

Kidney carnosine-propanol levels were not detectable in any of the groups. In contrast, kidney carnosine-propanal levels were detectable (overall mean  $\pm$  SD:  $3.09 \pm 0.79$  pmol/mg wet weight) but not affected by obesity, hCN1 overexpression, or by the chronic exercise intervention (data not shown).

## Correlations

The amount of HCD in muscle ( $r = -0.38$  and  $r = -0.38$ ,  $P < 0.05$ ) and especially in the kidney ( $r = -0.76$  and  $r = -0.69$ ,  $P < 0.05$ ) was negatively correlated to mesangial matrix expansion (Fig. 5A) and glomerular hypertrophy (Fig. 5B), respectively.

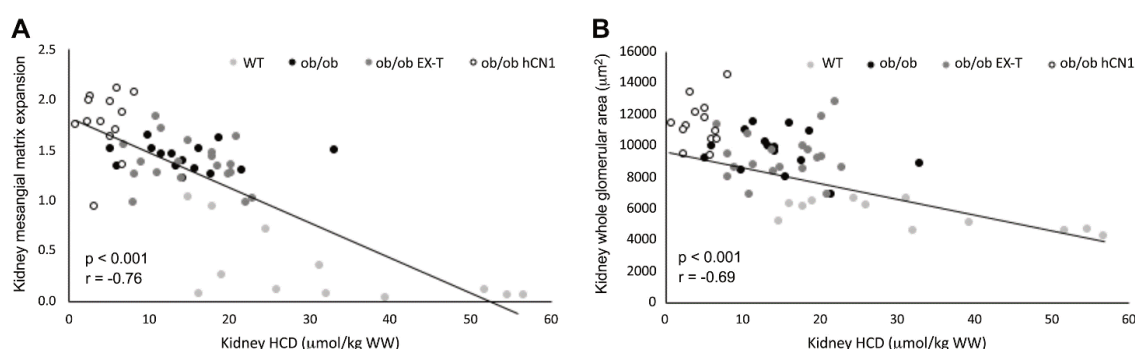


**Figure 5. Correlations**

A and B: correlations between kidney histidine-containing dipeptide (HCD) content and mesangial matrix expansion (A) and whole glomerular area (B) in wild-type (WT) mice, *ob/ob* mice, *ob/ob* mice with exercise training (EX-T), and *ob/ob* human carnosinase-1 (hCN1) transgenic mice. WW, wet weight.

## Carboxymethyllysine

The amount of protein-bound kidney CML was quantified as a marker of glycation damage in this mouse model. At the age of 24 wk, kidney CML levels (overall:  $203.77 \pm 39.33$   $\mu\text{mol/mol}$  lysine) were independent of obesity, exercise training, and hCN1 overexpression (data not shown).

## Citrate synthase activity

The activity of the citrate synthase enzyme was measured in gastrocnemius muscles to elucidate the effect of chronic exercise training on the aerobic capacity of the BTBR *ob/ob* mice. After 20 wk of aerobic exercise training, citrate synthase activity was approximately

twofold higher in *ob/ob* EX-T mice ( $132.9 \pm 61.1 \mu\text{mol}\cdot\text{min}^{-1}\cdot\text{g protein}^{-1}$ ) compared with control *ob/ob* mice ( $66.6 \pm 50.0 \mu\text{mol}\cdot\text{min}^{-1}\cdot\text{g protein}^{-1}$ ;  $P < 0.05$ ), and not affected by obesity (WT:  $45.2 \pm 46.6 \mu\text{mol}\cdot\text{min}^{-1}\cdot\text{g protein}^{-1}$ ;  $P > 0.1$ ) or hCN1 overexpression (*ob/ob* hCN1:  $75.7 \pm 56.6 \mu\text{mol}\cdot\text{min}^{-1}\cdot\text{g protein}^{-1}$ ;  $P > 0.1$ ).

## Discussion

The main finding of the present study is that changes in renal HCD availability are accompanied by variations in the development of DN in BTBR *ob/ob* mice. Kidney HCD content is already compromised in the diabetic state, and DN is significantly accelerated and aggravated when it is further reduced by hCN1 overexpression. The underlying mechanism seems lipid rather than sugar related, since biochemical markers indicate that this does not coincide with hyperglycemic state (Fig. 2A & B) or glycation damage but rather with an attenuation of hyperlipidemic state and a diminished capacity to quench, eliminate, and protect against lipid-derived reactive carbonyl species, such as acrolein. Interestingly, overexpression of hCN1 had opposite effects on the development of DN (albumin-to-creatinine ratio, glomerular hypertrophy) as carnosine supplementation, which has been investigated in the same mouse model by Albrecht et al.<sup>12</sup> The second hypothesis, i.e., that exercise training attenuates the development of DN through the release of HCD from muscular depots, was not supported by our findings. There was no substantial elevation of circulating HCD during acute exercise in this animal model, and there was no protective effect of exercise training on DN.

The results of the present study suggest that the amount of body burden of HCD determines the potential for scavenging reactive carbonyl species such as acrolein and thereby plays a (key) role in the development of DN. Diabetes in itself resulted in strongly reduced gastrocnemius (-48% and -28%, respectively; Fig. 4B), kidney (-58% and -47%, respectively; Fig. 4A) and plasma (-69% and -44%, respectively; Fig. 1A) carnosine and anserine levels. This is in accordance with reduced HCD levels in the kidney (from -90% to -98%)<sup>8,10,30</sup>, retina (-31%)<sup>31</sup>, liver (-78%)<sup>32</sup> and brain (-64%)<sup>33</sup> in different type 1 and type 2 diabetic models but not with increased levels in skeletal muscle of patients with type 2 diabetes (+39%)<sup>34</sup>. Different reports have suggested that carnosine can act as a sacrificial dipeptide by binding and eliminating deleterious agents such as reactive carbonyl species. A disproportional accumulation of reactive carbonyl species, which takes place, for example, during diabetes, can therefore result in a shortage of tissue carnosine or anserine. Compared with the reducing

effect of diabetes on carnosine and anserine levels, hCN1 overexpression resulted not only in lower circulating HCD levels (carnosine: -97% and anserine: more than -99%) but in strongly reduced whole body carnosine and anserine stores. Diminished levels of carnosine and anserine were observed in the kidney (*week 24*: -53% and -95%, respectively) and gastrocnemius tissue (*week 24*: anserine: -20%) in hCN1 transgenic versus nontransgenic *ob/ob* mice (Fig. 4A and 4B).

Importantly, there was a positive correlation between the amount of carnosine ( $r = 0.64$ ,  $P < 0.05$ ) and anserine ( $r = 0.33$ ,  $P < 0.05$ ) in the kidney and urinary carnosine-acrolein adducts. Kidney HCD were further also negatively correlated with different markers of DN (Fig. 5). Unfortunately, it is not known whether kidney HCD levels were enhanced after carnosine supplementation in BTBR *ob/ob* mice in the study of Albrecht et al.<sup>12</sup> and could therefore be the main underlying mechanism for an attenuated development of DN in carnosine-supplemented mice. However, as 1) different rodent studies have shown that kidney HCD are enhanced upon oral supplementation of carnosine<sup>10</sup>,  $\beta$ -alanine (unpublished data), D-carnosine<sup>9</sup>, and carnosinol<sup>29</sup> and as 2) the PEPT2 transporter is highly abundant in renal cells<sup>35,36</sup>, it is highly likely that kidney HCD levels were enhanced in the carnosine-supplemented BTBR *ob/ob* mice. Enhancing the dietary intake of HCD, which potentially maintains kidney carnosine and anserine during periods of increased exposure of reactive carbonyl species, should therefore be further explored as a promising therapeutic strategy to offset DN. Unfortunately, our study is limited by the lack of a direct comparison between the effect of hCN1 overexpression and carnosine supplementation on both kidney HCD levels and DN.

The observed effect of hCN1 overexpression on DN in mice confirms the genetic link between polymorphisms of the *CNDP1* gene, the gene encoding the CN1 enzyme, and the prevalence of DN in patients with diabetes<sup>3</sup>. The dramatic decline in kidney carnosine and anserine levels in hCN1 transgenic mice together with the strong correlation between kidney HCD levels and the degree of DN (Fig. 5), brings us to the hypothesis that the underlying protective mechanism of a low CN1 activity<sup>3</sup> could not only be higher circulating carnosine levels but also higher renal carnosine and anserine levels. Indeed, in this study, serum CN1 activity was negatively correlated with renal carnosine ( $r = -0.33$ ,  $P < 0.05$ ) and especially anserine ( $r = -0.70$ ,  $P < 0.05$ ) levels. These results can therefore be a start to further elucidating the exact role of renal HCD in (diabetic) kidney diseases. The development of a mouse model with a podocyte-specific CN1 overexpression, which would probably only results in a decline in the kidney and not full body HCD levels, would be able to further

unravel the contribution of renal HCD to the development of DN. Future research will have to elucidate whether serum CN1 activity and the risk for developing DN is also related to renal HCD levels in humans.

The present study is the first to document that overexpression of the hCN1 enzyme results in a faster development of hyperlipidemia in diabetic mice (as reflected by higher fasting triglycerides and cholesterol at *week 14*; Fig. 2C and 2D). These results are in line with an improved lipidemic profile in different diabetes or metabolic syndrome rodent models after long-term carnosine supplementation<sup>9,28,37,38</sup>. The levels of serum triglycerides were furthermore also significantly reduced in patients with type 2 diabetes who received oral supplements of 1g carnosine/day for 12 wk<sup>39</sup>. Although evidence is accumulating for an antihyperlipidemic effect of carnosine, no underlying mechanism has been reported so far. Novel approaches, such as lipidomics and proteomics, are needed to further explain this lipid regulation mechanism. Anyhow, it is likely that the favorable effects of carnosine (and adverse effects of CN1) on dyslipidemia and hypercholesteremia will contribute to a lower risk of developing diabetes-induced microvascular and macrovascular complications.

Different therapeutic approaches are currently being developed to encounter the negative effects of CN1 upon carnosine supplementation. The administration of carnosinol, a chemically synthesized carnosine analog that is well absorbed in the intestinal wall but not degraded by CN1, strongly and dose dependently counteracted several consequences of metabolic syndrome (inflammation, dyslipidemia, insulin resistance and steatohepatitis<sup>29</sup>). Anserine, a naturally occurring carnosine analogue that is also less vulnerable for degradation by CN1<sup>40</sup>, efficiently reduces fasting plasma glucose levels, proteinuria, and vascular permeability in *db/db* mice<sup>41</sup>. In parallel to the development of carnosinase-resistant carnosine analogs, CN1 blockers are also currently under investigation<sup>42</sup>.

Surprisingly, 20 wk of chronic aerobic exercise training did not retard the progression of diabetes or DN in the BTBR *ob/ob* mouse model. This is in contrast with previous reports on treadmill-trained *db/db* mice<sup>43,44</sup> and different high-fat<sup>45,46</sup>, heminephrectomized<sup>17</sup>, and streptozocin-induced<sup>47</sup> diabetic rat models. All studies reported a slower development of early DN (mostly based on the albumin-to-creatinine ratio and mesangial matrix expansion) following 5-12 wk of aerobic treadmill running. The lack of an exercise-induced amelioration of the development of DN is especially surprising as the chronic exercise training program enhanced the citrate synthase enzyme activity, a marker of mitochondrial content<sup>48</sup>. Our intervention doubled the citrate synthase activity, whereas others have reported increases of approximately ~30-50% following chronic exercise intervention in obese mice models<sup>43,49,50</sup>.

It can be concluded that a doubling in citrate synthase enzyme activity did not ameliorate the disturbance in glucose and lipid metabolism, or the development of DN, in our BTBR *ob/ob* model. A possible reason for the absence of a protective effect of chronic exercise in our study (Fig. 2 A and 2B) could be the very high glucose levels, possibly leading to severe ketoacidosis, lower exercise tolerance, or dehydration during exercise training. This is in accordance with the absence of an antihyperglycemic effect of exercise in *db/db* mice with very high circulating glucose levels<sup>43,51</sup> compared with *db/db* mice with lower glucose levels<sup>44</sup> and in accordance with absence of an exercise-induced improvement in glycemic control in subjects with high (> 13 mmol/L) fasting glucose levels<sup>52</sup>.

In contrast to previous reports<sup>13,14</sup>, circulating carnosine and anserine were not significantly enhanced after an acute bout of exercise in mice lacking the serum CN1 enzyme. The degree of release could be dependent on different exercise modalities, such as intensity and duration, but can also be dependent on other factors, such as perceived stress (treadmill vs. running wheel) or mouse strain. The lack of exercise-induced release of carnosine and anserine may also partially explain the absence of a protective effect of the chronic exercise program on diabetes and DN.

In conclusion, we have shown, for the first time, that overexpression of the hCN1 enzyme in BTBR *ob/ob* mice aggravates the development of advanced glomerular lesions. However, a chronic aerobic exercise training program did not affect diabetes or DN. Our data further suggest that the amount of renal HCD is closely linked to the severity of DN. Developing a supplementation regimen that efficiently enhances renal carnosine and anserine levels in humans should be explored as a potential therapeutic target to reduce the risk of developing DN.

## **Acknowledgements**

The technical assistance of the animal caretakers, the Clinical Laboratory of University Hospital UZ Ghent, and Anneke Volkaert is greatly acknowledged.

## **Grants**

This work was financially supported by grants of the Special Research Fund of Ghent University. I. Everaert is a recipient of a postdoctoral scholarship by the Research Foundation – Flanders (FWO).

## **Disclosures**

No conflicts of interest, financial or otherwise, are declared by the authors.

## References

- 1 Boldyrev, A. A., Aldini, G. & Derave, W. Physiology and pathophysiology of carnosine. *Physiol Rev* **93**, 1803-1845, doi:10.1152/physrev.00039.2012 (2013).
- 2 Freedman, B. I. *et al.* A leucine repeat in the carnosinase gene CNDP1 is associated with diabetic end-stage renal disease in European Americans. *Nephrol Dial Transplant* **22**, 1131-1135, doi:10.1093/ndt/gfl717 (2007).
- 3 Janssen, B. *et al.* Carnosine as a protective factor in diabetic nephropathy: association with a leucine repeat of the carnosinase gene CNDP1. *Diabetes* **54**, 2320-2327, doi:10.2337/diabetes.54.8.2320 (2005).
- 4 Mooyaart, A. L. *et al.* Association between CNDP1 genotype and diabetic nephropathy is sex specific. *Diabetes* **59**, 1555-1559, doi:10.2337/db09-1377 (2010).
- 5 Rohm, F., Skurk, T., Daniel, H. & Spanier, B. Appearance of Di- and Tripeptides in Human Plasma after a Protein Meal Does Not Correlate with PEPT1 Substrate Selectivity. *Mol Nutr Food Res* **63**, e1801094, doi:10.1002/mnfr.201801094 (2019).
- 6 Everaert, I. *et al.* Low plasma carnosinase activity promotes carnosinemia after carnosine ingestion in humans. *Am J Physiol Renal Physiol* **302**, F1537-1544, doi:10.1152/ajprenal.00084.2012 (2012).
- 7 Sauerhofer, S. *et al.* L-carnosine, a substrate of carnosinase-1, influences glucose metabolism. *Diabetes* **56**, 2425-2432, doi:10.2337/db07-0177 (2007).
- 8 Peters, V. *et al.* Carnosine treatment largely prevents alterations of renal carnosine metabolism in diabetic mice. *Amino Acids* **42**, 2411-2416, doi:10.1007/s00726-011-1046-4 (2012).
- 9 Aldini, G. *et al.* The carbonyl scavenger carnosine ameliorates dyslipidaemia and renal function in Zucker obese rats. *J Cell Mol Med* **15**, 1339-1354, doi:10.1111/j.1582-4934.2010.01101.x (2011).
- 10 Peters, V. *et al.* Carnosine treatment in combination with ACE inhibition in diabetic rats. *Regul Pept* **194-195**, 36-40, doi:10.1016/j.regpep.2014.09.005 (2014).
- 11 Yay, A. *et al.* Antioxidant effect of carnosine treatment on renal oxidative stress in streptozotocin-induced diabetic rats. *Biotech Histochem* **89**, 552-557, doi:10.3109/10520295.2014.913811 (2014).
- 12 Albrecht, T. *et al.* Carnosine Attenuates the Development of both Type 2 Diabetes and Diabetic Nephropathy in BTBR ob/ob Mice. *Sci Rep* **7**, 44492, doi:10.1038/srep44492 (2017).
- 13 Dunnett, M., Harris, R. C., Dunnett, C. E. & Harris, P. A. Plasma carnosine concentration: diurnal variation and effects of age, exercise and muscle damage. *Equine Vet J Suppl*, 283-287, doi:10.1111/j.2042-3306.2002.tb05434.x (2002).
- 14 Nagai, K. *et al.* Possible role of L-carnosine in the regulation of blood glucose through controlling autonomic nerves. *Exp Biol Med (Maywood)* **228**, 1138-1145, doi:10.1177/153537020322801007 (2003).
- 15 Nordsborg, N. *et al.* Muscle interstitial potassium kinetics during intense exhaustive exercise: effect of previous arm exercise. *Am J Physiol Regul Integr Comp Physiol* **285**, R143-148, doi:10.1152/ajpregu.00029.2003 (2003).
- 16 Rodrigues, A. M. *et al.* Effects of training and nitric oxide on diabetic nephropathy progression in type I diabetic rats. *Exp Biol Med (Maywood)* **236**, 1180-1187, doi:10.1258/ebm.2011.011005 (2011).
- 17 Tufescu, A. *et al.* Combination of exercise and losartan enhances renoprotective and peripheral effects in spontaneously type 2 diabetes mellitus rats with nephropathy. *J Hypertens* **26**, 312-321, doi:10.1097/HJH.0b013e3282f2450b (2008).
- 18 Ward, K. M., Mahan, J. D. & Sherman, W. M. Aerobic training and diabetic nephropathy in the obese Zucker rat. *Ann Clin Lab Sci* **24**, 266-277 (1994).
- 19 Colberg, S. R. *et al.* Exercise and type 2 diabetes: American College of Sports Medicine and the American Diabetes Association: joint position statement. Exercise and type 2 diabetes. *Med Sci Sports Exerc* **42**, 2282-2303, doi:10.1249/MSS.0b013e3181eeb61c (2010).
- 20 Waden, J. *et al.* Leisure-time physical activity and development and progression of diabetic nephropathy in type 1 diabetes: the FinnDiane Study. *Diabetologia* **58**, 929-936, doi:10.1007/s00125-015-3499-6 (2015).

- 21 Sigal, R. J. *et al.* Effects of aerobic training, resistance training, or both on glycemic control in type 2 diabetes: a randomized trial. *Ann Intern Med* **147**, 357-369, doi:10.7326/0003-4819-147-6-200709180-00005 (2007).
- 22 Hudkins, K. L. *et al.* BTBR Ob/Ob mutant mice model progressive diabetic nephropathy. *J Am Soc Nephrol* **21**, 1533-1542, doi:10.1681/ASN.2009121290 (2010).
- 23 Sutter, A. G., Palanisamy, A. P., Kurtz, N., Spyropoulos, D. D. & Chavin, K. D. Efficient method of genotyping ob/ob mice using high resolution melting analysis. *PLoS One* **8**, e78840, doi:10.1371/journal.pone.0078840 (2013).
- 24 Niquet-Léridon, C. & Tessier, F. J. Quantification of N  $\epsilon$ -carboxymethyl-lysine in selected chocolate-flavoured drink mixes using high-performance liquid chromatography-linear ion trap tandem mass spectrometry. *Food chemistry* **126**, 655-663, doi:10.1016/j.foodchem.2010.10.111 (2011).
- 25 Guilbaud, A. *et al.* The LepR(db/db) mice model for studying glycation in the context of diabetes. *Diabetes Metab Res Rev* **35**, e3103, doi:10.1002/dmrr.3103 (2019).
- 26 Hoetker, D. *et al.* Exercise alters and beta-alanine combined with exercise augments histidyl dipeptide levels and scavenges lipid peroxidation products in human skeletal muscle. *J Appl Physiol* (1985), doi:10.1152/japplphysiol.00007.2018 (2018).
- 27 Teufel, M. *et al.* Sequence identification and characterization of human carnosinase and a closely related non-specific dipeptidase. *J Biol Chem* **278**, 6521-6531, doi:10.1074/jbc.M209764200 (2003).
- 28 Aydin, A. F., Kusku-Kiraz, Z., Dogru-Abbasoglu, S. & Uysal, M. Effect of carnosine treatment on oxidative stress in serum, apoB-containing lipoproteins fraction and erythrocytes of aged rats. *Pharmacol Rep* **62**, 733-739, doi:10.1016/s1734-1140(10)70331-5 (2010).
- 29 Anderson, E. J. *et al.* A carnosine analog mitigates metabolic disorders of obesity by reducing carbonyl stress. *The Journal of clinical investigation* **128**, 5280-5293, doi:10.1172/JCI94307 (2018).
- 30 Riedl, E. *et al.* Carnosine prevents apoptosis of glomerular cells and podocyte loss in STZ diabetic rats. *Cell Physiol Biochem* **28**, 279-288, doi:10.1159/000331740 (2011).
- 31 Pfister, F. *et al.* Oral carnosine supplementation prevents vascular damage in experimental diabetic retinopathy. *Cell Physiol Biochem* **28**, 125-136, doi:10.1159/000331721 (2011).
- 32 Mong, M. C., Chao, C. Y. & Yin, M. C. Histidine and carnosine alleviated hepatic steatosis in mice consumed high saturated fat diet. *Eur J Pharmacol* **653**, 82-88, doi:10.1016/j.ejphar.2010.12.001 (2011).
- 33 Barca, A. *et al.* Responsiveness of Carnosine Homeostasis Genes in the Pancreas and Brain of Streptozotocin-Treated Mice Exposed to Dietary Carnosine. *Int J Mol Sci* **19**, doi:10.3390/ijms19061713 (2018).
- 34 Stegen, S. *et al.* Muscle histidine-containing dipeptides are elevated by glucose intolerance in both rodents and men. *PLoS One* **10**, e0121062, doi:10.1371/journal.pone.0121062 (2015).
- 35 Kamal, M. A., Jiang, H., Hu, Y., Keep, R. F. & Smith, D. E. Influence of genetic knockout of Pept2 on the in vivo disposition of endogenous and exogenous carnosine in wild-type and Pept2 null mice. *Am J Physiol Regul Integr Comp Physiol* **296**, R986-991, doi:10.1152/ajpregu.90744.2008 (2009).
- 36 Liu, W. *et al.* Molecular cloning of PEPT 2, a new member of the H<sup>+</sup>/peptide cotransporter family, from human kidney. *Biochim Biophys Acta* **1235**, 461-466, doi:10.1016/0005-2736(95)80036-f (1995).
- 37 Brown, B. E. *et al.* Supplementation with carnosine decreases plasma triglycerides and modulates atherosclerotic plaque composition in diabetic apo E(-/-) mice. *Atherosclerosis* **232**, 403-409, doi:10.1016/j.atherosclerosis.2013.11.068 (2014).
- 38 Lee, Y. T., Hsu, C. C., Lin, M. H., Liu, K. S. & Yin, M. C. Histidine and carnosine delay diabetic deterioration in mice and protect human low density lipoprotein against oxidation and glycation. *Eur J Pharmacol* **513**, 145-150, doi:10.1016/j.ejphar.2005.02.010 (2005).
- 39 Houjehani, S., Kheirouri, S., Faraji, E. & Jafarabadi, M. A. l-Carnosine supplementation attenuated fasting glucose, triglycerides, advanced glycation end products, and tumor necrosis factor-alpha levels in patients with type 2 diabetes: a double-blind placebo-controlled randomized clinical trial. *Nutr Res* **49**, 96-106, doi:10.1016/j.nutres.2017.11.003 (2018).



- 40 Everaert, I. *et al.* Development and validation of a sensitive LC-MS/MS assay for the quantification of anserine in human plasma and urine and its application to pharmacokinetic study. *Amino Acids* **51**, 103-114, doi:10.1007/s00726-018-2663-y (2019).
- 41 Peters, V. *et al.* Protective Actions of Anserine Under Diabetic Conditions. *Int J Mol Sci* **19**, doi:10.3390/ijms19092751 (2018).
- 42 Qiu, J. *et al.* Identification and characterisation of carnostatine (SAN9812), a potent and selective carnosinase (CN1) inhibitor with in vivo activity. *Amino Acids* **51**, 7-16, doi:10.1007/s00726-018-2601-z (2019).
- 43 Ghosh, S. *et al.* Moderate exercise attenuates caspase-3 activity, oxidative stress, and inhibits progression of diabetic renal disease in db/db mice. *Am J Physiol Renal Physiol* **296**, F700-708, doi:10.1152/ajprenal.90548.2008 (2009).
- 44 Sominen, H. K., Boivin, G. P. & Elased, K. M. Daily exercise training protects against albuminuria and angiotensin converting enzyme 2 shedding in db/db diabetic mice. *The Journal of endocrinology* **221**, 235-251, doi:10.1530/JOE-13-0532 (2014).
- 45 Boor, P. *et al.* Regular moderate exercise reduces advanced glycation and ameliorates early diabetic nephropathy in obese Zucker rats. *Metabolism* **58**, 1669-1677, doi:10.1016/j.metabol.2009.05.025 (2009).
- 46 Rodrigues, A. M. *et al.* P2X(7) receptor in the kidneys of diabetic rats submitted to aerobic training or to N-acetylcysteine supplementation [corrected]. *PLoS One* **9**, e97452, doi:10.1371/journal.pone.0097452 (2014).
- 47 Lappalainen, J. *et al.* Suppressed heat shock protein response in the kidney of exercise-trained diabetic rats. *Scand J Med Sci Sports* **28**, 1808-1817, doi:10.1111/sms.13079 (2018).
- 48 Larsen, S. *et al.* Biomarkers of mitochondrial content in skeletal muscle of healthy young human subjects. *J Physiol* **590**, 3349-3360, doi:10.1113/jphysiol.2012.230185 (2012).
- 49 Uddin, G. M., Youngson, N. A., Sinclair, D. A. & Morris, M. J. Head to Head Comparison of Short-Term Treatment with the NAD(+) Precursor Nicotinamide Mononucleotide (NMN) and 6 Weeks of Exercise in Obese Female Mice. *Front Pharmacol* **7**, 258, doi:10.3389/fphar.2016.00258 (2016).
- 50 Liu, H. W., Kao, H. H. & Wu, C. H. Exercise training upregulates SIRT1 to attenuate inflammation and metabolic dysfunction in kidney and liver of diabetic db/db mice. *Nutr Metab (Lond)* **16**, 22, doi:10.1186/s12986-019-0349-4 (2019).
- 51 Moien-Afshari, F. *et al.* Exercise restores coronary vascular function independent of myogenic tone or hyperglycemic status in db/db mice. *Am J Physiol Heart Circ Physiol* **295**, H1470-1480, doi:10.1152/ajpheart.00016.2008 (2008).
- 52 Solomon, T. P., Malin, S. K., Karstoft, K., Haus, J. M. & Kirwan, J. P. The influence of hyperglycemia on the therapeutic effect of exercise on glycemic control in patients with type 2 diabetes mellitus. *JAMA Intern Med* **173**, 1834-1836, doi:10.1001/jamainternmed.2013.7783 (2013).



## Chapter 4

### Leptin deficiency affects glucose homeostasis and results in adiposity in zebrafish

Junling He\*, Yi Ding\*, Natalia Nowik, Charel Jager, Muhamed N. H. Eeza, A.  
Alia, Hans J. Baelde, Herman P. Spaink.

\*These authors contributed equally to this work

*J Endocrinol. 2021 May;249(2):125-134.*



## Abstract

Leptin is a hormone which functions in the regulation of energy homeostasis via suppression of appetite. In zebrafish, there are two paralogous genes encoding leptin, called *lepa* and *lepb*. In a gene expression study, we found that the *lepb* gene, not the *lepa* gene, was significantly downregulated under the state of insulin-resistance in zebrafish larvae, suggesting that the *lepb* plays a role in glucose homeostasis. In the current study, we characterised *lepb*-deficient (*lepb*<sup>-/-</sup>) adult zebrafish generated via a CRISPR-CAS9 gene editing approach by investigating whether the disruption of the *lepb* gene would result in the development of type 2 diabetes mellitus (T2DM) and diabetic complications. We observed that *lepb*<sup>-/-</sup> adult zebrafish had an increase in body weight, length and visceral fat accumulation, compared to age-matched control zebrafish. In addition, *lepb*<sup>-/-</sup> zebrafish had significantly higher blood glucose levels compared to control zebrafish. These data collectively indicate that *lepb*<sup>-/-</sup> adult zebrafish display the features of T2DM. Furthermore, we showed that *lepb*<sup>-/-</sup> adult zebrafish had glomerular hypertrophy and thickening of the glomerular basement membrane, compared to control zebrafish, suggesting that *lepb*<sup>-/-</sup> adult zebrafish develop early signs of diabetic nephropathy. In conclusion, our results demonstrate that *lepb* regulates glucose homeostasis and adiposity in zebrafish, and suggest that *lepb*<sup>-/-</sup> mutant zebrafish are a promising model to investigate the role of leptin in the development of T2DM and are an attractive model to perform mechanistic and therapeutic research in T2DM and its complications.

## Introduction

Human leptin is a 16-kDa protein hormone which is predominantly secreted by adipocytes <sup>1</sup>. Leptin plays a role in diverse physiological processes including energy homeostasis <sup>2</sup>, immune regulation <sup>3,4</sup>, endocrine regulation <sup>5</sup>, and reproduction <sup>6,7</sup>. Congenital leptin deficiency causes extreme obesity in children <sup>8,9</sup>. Rodents lacking the gene encoding leptin are commonly characterised by hyperphagia, obesity, insulin resistance and impaired glucose tolerance. For instance, *leptin*-deficient mice (*ob/ob* mice) exhibit the features of obesity and type 2 diabetic mellitus (T2DM) <sup>10</sup>. Growing evidence suggests that leptin treatment has a beneficial effect on glucose metabolism <sup>11-14</sup> and insulin resistance <sup>15-18</sup>, indicating that leptin might be a crucial factor in the development of T2DM. However, the function of leptin in the pathogenesis of T2DM is still obscure.

Leptin and leptin receptor are highly conserved across mammalian species. The most widely used animal models in T2DM research are the congenial *leptin*- or *leptin* receptor-deficient rodent models, such as *ob/ob* and *db/db* mice. Besides, the basic structural features and intracellular signaling mechanisms of leptin and its receptor appear to be conserved throughout vertebrates <sup>19</sup>. Several studies have reported that administration of exogenous leptin in fish reduces food intake, indicating the conservation of the function of the leptin signaling system throughout vertebrates <sup>20-22</sup>. In recent decades, zebrafish have become a promising animal model with numerous advantages, including fast development and generation time, small size, easily accessible, and cost-effective. In zebrafish, there are two divergent leptin paralogues: *lepa* and *lepb*, and one leptin receptor gene (*lepr*) <sup>23</sup>. Michel et al. <sup>24</sup> demonstrated that *lepr*-deficient zebrafish larvae have increased numbers of  $\beta$ -cells and increased insulin mRNA expression, compared to control zebrafish larvae. They also found that the leptin receptor deficiency contributes to higher blood glucose levels in adult zebrafish. Their findings indicated that the regulation of glucose homeostasis by the leptin receptor is conserved across vertebrates. However, they observed no significant difference in the whole body adiposity phenotype between *lepr*-deficient zebrafish and control zebrafish at the adult stage. On the other hand, Chisada et al. <sup>25</sup> showed that the deletion of leptin receptor in medaka results in a modest increase in visceral fat accumulation compared to the wild type (WT) medaka fish. More recently, Audira et al. <sup>26</sup> found that *lepa*-deficient adult zebrafish display an obesity phenotype. Thus, there are some conflicting results in the literature regarding the relationship between disruption of leptin signaling and adiposity in zebrafish. In a previous study, our group found that the *lepb* gene, not the *lepa* gene, was significantly downregulated in zebrafish larvae under an insulin-resistance state, resulting from acute hyperinsulinemia, which suggests that *lepb*

plays a role in insulin homeostasis in zebrafish <sup>27</sup>. Since the roles of *lepa* and *lepr* in zebrafish have already been investigated by other groups, therefore, the focus in the current work is to study the function of the *lepb* gene in zebrafish at an adult stage to obtain more insights into the relationship between the leptin signaling pathway and T2DM.

This study aims to investigate whether *lepb* deficiency contributes to the development of T2DM in adult zebrafish. To address this question, we examined the body weight and length, blood glucose levels, and the body fat distribution in 1.5 years old *lepb*<sup>-/-</sup> adult zebrafish and compared them to age-matched WT controls. Furthermore, we examined the renal histopathologic changes of these zebrafish by performing hematoxylin and eosin (HE) or Periodic-acid Schiff (PAS) staining, and transmission electron microscopy (TEM) methods.

## Methods and Materials

### Animals

Zebrafish strains were handled in compliance with the local animal welfare regulations and maintained according to standard protocols (zfin.org). The use of adult zebrafish was approved by the local animal welfare committee (DEC) of the University of Leiden (license number: AVD1060020171767) and adhered to the international guidelines specified by the EU Animal Protection Directive 2010/63/EU.

The CRISPR-CAS9 gene editing approach was used to knock out the *lepb* in the ABTL zebrafish to generate the *lepb*-deficient zebrafish. The sgRNA CTACCCAATCCCGAGACCCC targeted the exon 2 in *lepb*. The *lepb* primer (for: 5'-AGGAACTGGCCGTCTCACAG-3'; rev: 5'-CGGGGAAGGCTGTTTCTTCTT-3') was used for *lepb*-deficient zebrafish genotyping. Sanger sequencing showed that a 7bp (*lepb*<sup>7-/-</sup>) or 8bp (*lepb*<sup>8-/-</sup>) stretch of nucleotides was missing in the *lepb* gene in two different mutant lines (Supplementary Fig. 1A). Both deletions resulted in a frameshift mutation of *lepb* (Supplementary Fig. 1B). The deletion of the *lepb* gene was in codon 110 in zebrafish, which is close to the non-sense mutation in codon 105 of the *leptin* gene of C57BL/6J *ob/ob* mice. In the C57BL/6J *ob/ob* mice, this mutation in the *leptin* gene leads to a truncated protein that cannot bind to the leptin receptor anymore <sup>1</sup>. Therefore, although we cannot be sure that our mutant has a complete null phenotype, it is very likely that our truncation in the *lepb* gene leads to a leptin b protein which cannot bind to the leptin receptor in the zebrafish.

The *lepb*<sup>+/+</sup> and *lepb*<sup>-/-</sup> zebrafish are obtained from an incross of *lepb* heterozygous fish (*lepb*<sup>+/-</sup>); (Supplementary Fig. 1C). *Lepb*<sup>+/+</sup>, *lepb*<sup>+/-</sup> and *lepb*<sup>-/-</sup> zebrafish were mixed and raised in the same tank before genotyping. After genotyping, *lepb*<sup>+/+</sup>, *lepb*<sup>+/-</sup> and *lepb*<sup>-/-</sup> fish were separated

and raised in different sizes of tanks depending on the number of fish per volume of water. The ABTL (control) fish of 1.5 years old were kept in the big-sized-tanks. We raised all zebrafish in the same circulating water system and maintained the normal mixed-sex environment. Adult zebrafish were fed twice per day. One meal is a mixture of GEMMA Micro 300 and GEMMA Diamond (Skretting; Nutreco company) whose amount is based on 5% of zebrafish body weight; another is the life Artemia (ZebCare). Both amounts are positively proportional to the number of fish per tank and given by highly skilled caretakers.

We included both *lepb*<sup>7-/7-</sup> and *lepb*<sup>8-/8-</sup> mutants in the current study since two independent mutants have more certainty to rule out off-target effects of CRISPR-CAS9 approach. The age-matched ABTL adult zebrafish of the same lineage as used for the CRISPR-CAS9 procedure were used as the controls. In an independent study, a wild type (*lepb*<sup>+/+</sup>) from an incross of heterozygotes *lepb*<sup>7+/-</sup> was compared with the ABTL control, showing no significant difference in blood glucose levels (Supplementary Fig. 2; female:  $t_{(3)}=-0.149$ ,  $p=0.891$ ; male:  $t_{(3)}=-2.820$ ,  $p=0.067$ ), further excluding off-target effects of the CRISPR-CAS9 procedure. For the current study, adult zebrafish (ABTL female fish, n=9; *lepb*<sup>-/-</sup> female fish, n=11; ABTL male fish, n=9; *lepb*<sup>-/-</sup> male fish, n=15) were sacrificed at the age of 1.5 years, since we observed that all *lepb*<sup>-/-</sup> mutants displayed an obese phenotype, compared to control zebrafish. Because there was no difference in body weight, body length, body mass index (BMI), and 2 hours postprandial blood glucose levels between *lepb*<sup>7-/7-</sup>, *lepb*<sup>8-/8-</sup> and *lepb*<sup>7-/8-</sup> mutants (Supplementary Fig. 3), we pooled *lepb*<sup>7-/7-</sup>, *lepb*<sup>8-/8-</sup> and *lepb*<sup>7-/8-</sup> mutants into one group which is named as *lepb*<sup>-/-</sup> for the subsequent analyses.

### Body weight and body length measurement

Two hours after feeding, fish were sacrificed by putting them into ice-cold aquarium water which was filled with some ice chips to maintain the temperature near 0°C for 3-6 s. After there was no response of the fish to external stimuli, the euthanized fish was placed on a paper tissue, drying the body as much as possible. Then, the fish size (from the tip of the mouth to the caudal peduncle) was measured with a calliper, and the fish were weighed with a precision analytical scale.

### Blood collection

A steel blade was used to cut the fish between anal fin and caudal fin just after euthanasia to collect zebrafish blood. The blood was collected into a 500µl Eppendorf tube with a 20 µl micro-pipet. Following the blood collection, the remaining body of the zebrafish was fixed in

4% paraformaldehyde (PFA). After 2 hours of coagulation at room temperature, the blood was spun down in a centrifuge at 13,000 g for 10 minutes. Subsequently, the blood serum and the blood cells were separated into different Eppendorf tubes and kept at -80°C for further analysis.

### **Blood glucose level measurement**

A PicoProbe™ Glucose Fluorometric Assay kit (Biovision, Milpitas, CA) was used to measure the glucose levels in the serum of zebrafish. The serum samples were diluted 50 times with milli-Q water. Nine µl of the diluted serum was added into a 96-well white plate, and then the total volume was adjusted to 50µl with 36µl glucose assay buffer and 5µl reaction mix which was composed of 0.5µl PicoProbe™, 1µl glucose substrate mix, 1µl glucose enzyme mix and 2.5µl glucose assay buffer. The 100mM glucose standard was diluted into a series of wells in 96 well plates to generate 0, 1.5, 3, 6, 9, 12, 15 micromolar per well for making the glucose standard curve. The volumes of different concentrations of glucose standards were also adjusted to 50µl with glucose assay buffer and reaction mix. The samples were incubated for 30 minutes at 37°C, protected from light. Fluorescence was measured at Excitation/Emission = 535/587 nm in a microtiter plate reader. The concentrations of glucose in the serum of zebrafish were calculated according to the glucose standard curve.

### **MRI measurement**

After one week fixation in 4% PFA at 4°C, the whole adult fish were washed twice with PBS and then transferred to MR silent liquid (Fomblin, perfluoropolyether) for MRI measurement. All MR imaging scans were performed at 300 MHz Bruker vertical wide-bore system, using a birdcage radiofrequency coil with an inner diameter of 10 mm. Data acquisition and processing were performed with Para Vision 5.1 (Bruker Biospin, Germany). Before each measurement, the magnetic field homogeneity was optimized by shimming. Each session of measurements began with a multi-slice orthogonal gradient-echo sequence for position determination and selection of the desired region for subsequent experiments.

For anatomical images, a rapid acquisition with relaxation enhancement (RARE) sequences was used. Basic measurement parameters used for the RARE sequence were: Echo time (TE)=8.5 ms with an effective echo time of 18.1 ms; Repetition time (TR)=3000 ms; Number of scans (ns)=12; Total scan time= 17 min. RARE factor=4. The field of view (FOV) was 1.2 cm with a matrix size of 256 x 256, the slice thickness was 0.2 mm, and the interslice distance was also 0.2 mm.



For selective fat imaging, a Chemical Shift Selective (CHESS) sequence was used. The CHESS consists of a single frequency-selective excitation pulse with a flip angle of  $\pi/2$  followed by a dephasing gradient (homogeneity spoiling gradient). The procedure leaves the spin system in a state where no net magnetization of the unwanted component is retained while the wanted component remains entirely unaffected in the form of z-magnetization. A narrow bandwidth of 90 degree Gaussian pulse was used for on resonance frequency selective excitation. Further basic parameters used are as follows: TE=13.3 ms; TR=800 ms; ns=16; Scan time 27 min.

For quantitative analysis of fat in CHESS images, the image slices were exported and analyzed in ImageJ software ([https:// imagej.nih.gov/ij/](https://imagej.nih.gov/ij/)). By using a plugin, the area of the fish was defined, and a certain threshold was adjusted to eliminate any contribution of noise. Subsequently, the hyperintense signal of fat was calculated. The data were exported to Origin Pro v. 8 software for further analysis.

### **Renal histopathology**

After 1 week fixation in 4% PFA at 4°C, the whole adult zebrafish were washed twice with PBS and then transferred to EDTA (100mM, pH=8) for the decalcification at room temperature for another 1 week, followed by embedding in paraffin. The zebrafish tissue was cut (4- $\mu$ m thickness) on a Leica microtome (Wetzlar) and then stained with HE or PAS using standard protocols.

Stained slides were digitalized using a Philips Ultra-Fast Scanner 1.6 RA (Philips Electronics, Amsterdam, the Netherlands). The surface areas ( $\mu\text{m}^2$ ) of Bowman's capsule, Bowman's space, and glomerular tuft were measured in the digitalized PAS-stained slides using ImageJ software. All available glomeruli (5~11 glomeruli per slide) in each zebrafish were included in the measurements.

### **Transmission electron microscopy (TEM)**

Zebrafish kidneys were harvested and fixed in EM fixation buffer (1.5% G.A/ 1% PF) for 24 hours. Subsequently, the renal tissue was fixed with 2.5% glutaraldehyde/1.2% acrolein in fixation buffer (0.1 mol/l cacodylate, 0.1 mol/l sucrose, pH 7.4) and 1% osmium tetroxide, and embedded in epon resin. Ultrathin sections were stained with uranyl acetate. The images were collected using a JEM-1200 EX transmission electron microscope (JEOL, Tokyo, Japan).

The thickness of the glomerular basement membrane (GBM) of zebrafish was analyzed with ImageJ software. One glomerulus per fish was analyzed. Photos of eight distinct areas (25.000X) of the glomerular capillaries from each glomerulus at randomly selected places were taken. The

mean thickness of the GBM in each photograph was determined by measuring the thickness of 15 nonoverlapping places of the GBM area. The mean of these 8 distinct areas was taken as the thickness for each glomerulus.

### **Statistical analyses**

Statistical analysis was performed using SPSS Statistics 25 (IBM, Armonk, NY). Differences between groups were analyzed using Student's *t*-test. Data are presented as the mean  $\pm$  SD. Differences with  $p < 0.05$  were considered as statistically significant.

## Results

### Deficiency of *lepb* has an effect on body weight, length and blood glucose levels in adult zebrafish

In this study, we first examined the basic parameters, including body weight, length and blood glucose levels, in control and *lepb*<sup>-/-</sup> adult zebrafish in both genders at the age of 1.5 years. The body weight of *lepb*<sup>-/-</sup> zebrafish in both genders was significantly increased compared to their respective controls (Fig. 1A; female:  $t_{(8,191)}=4.219$ ,  $p=0.003$ ; male:  $t_{(16)}=2.396$ ,  $p=0.029$ ). Accordingly, the body length of *lepb*<sup>-/-</sup> zebrafish was also significantly increased compared to the controls, in both genders (Fig. 1B; female:  $t_{(12)}=2.680$ ,  $p=0.020$ ; male:  $t_{(16)}=3.266$ ,  $p=0.005$ ). Two hours postprandial blood glucose levels (Fig. 1C; female:  $t_{(12)}=0.357$ ,  $p=0.727$ ; male:  $t_{(14)}=2.230$ ,  $p=0.043$ ) and fasting blood glucose levels (Supplementary Fig. 4; female:  $t_{(4)}=0.999$ ,  $p=0.374$ ; male:  $t_{(4)}=3.289$ ,  $p=0.030$ ) in *lepb*<sup>-/-</sup> male zebrafish group were significantly higher compared to control male zebrafish group, but we did not find that in the female group.

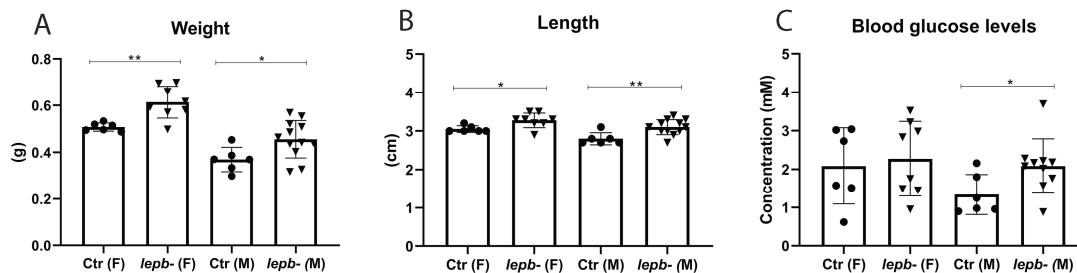


**Figure 1. Body weight, length and blood glucose levels in control and *lepb*-deficient adult zebrafish** (A) The body weight of control and *lepb*<sup>-/-</sup> female (\*\* $p < 0.01$ ) and male (\* $p < 0.05$ ) adult zebrafish. (B) The body length of control and *lepb*<sup>-/-</sup> female (\* $p < 0.05$ ) and male (\*\* $p < 0.01$ ) adult zebrafish. (C) Two hours postprandial blood glucose levels in control and *lepb*<sup>-/-</sup> female and male (\* $p < 0.05$ ) adult zebrafish. Ctr: control zebrafish; *lepb*<sup>-/-</sup>: *lepb*<sup>-/-</sup> zebrafish; F: female; M: male.

### *Lepb*-deficient adult zebrafish have more visceral fat accumulation

After observing the obese phenotype in *lepb*<sup>-/-</sup> zebrafish, we examined the body fat distribution in zebrafish with a non-invasive MRI approach. Successive slices were imaged from top to bottom in the coronal plane of control and *lepb*<sup>-/-</sup> zebrafish in both genders (Fig. 2). We observed a substantial increase in visceral fat accumulation in both *lepb*<sup>-/-</sup> female (Fig. 2B) and male (Fig. 2D) zebrafish compared to control female (Fig. 2A) and male (Fig. 2C) zebrafish. Furthermore, we performed the chemical shift selective (CHESS) imaging to acquire clear fat distribution images (Fig. 2A'-D'). A quantitative analysis of body fat from CHESS images clearly showed

a significant increase in fat accumulation in *lepb*<sup>-/-</sup> zebrafish in both genders compared to their respective controls (Fig. 2E; female:  $t_{(10)}=7.057$ ,  $p<0.001$ ; male:  $t_{(10)}=5.231$ ,  $p<0.001$ ).

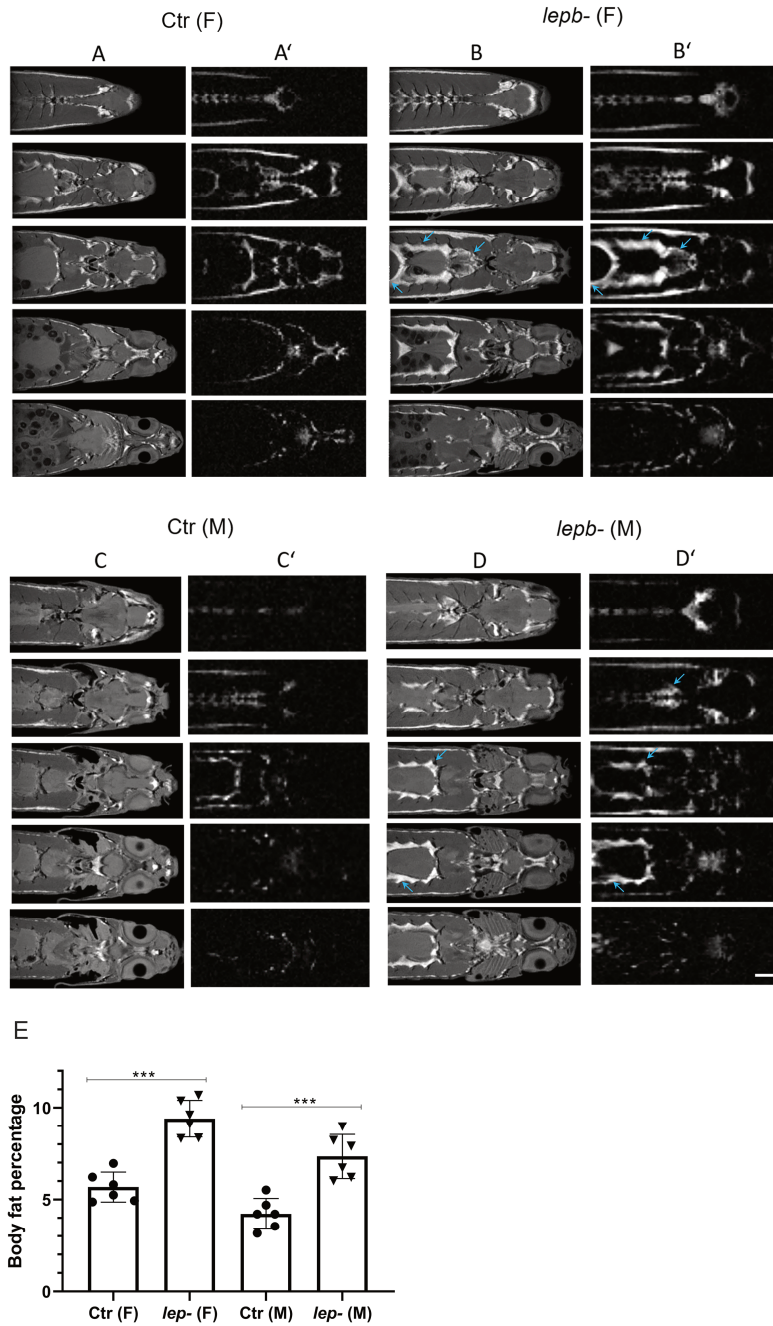


**Figure 2. Magnetic resonance anatomical imaging and selective fat imaging in control and *lepb*-deficient female and male adult zebrafish**

(A-D) Successive slices (top to bottom) in the coronal plane obtained using  $T_2$  weighted RARE pulse sequence. (A'-D') Successive images (top to bottom) of fat distribution in the coronal plane, acquired with Chemical Shift Selective (CHESS) pulse sequence. (A, A') Control female; (B, B') *lepb*<sup>-/-</sup> female;

(C, C') Control male; (D, D') *lepb*<sup>-/-</sup> male adult zebrafish. A substantial visceral fat accumulation was seen in *lepb*<sup>-/-</sup> adult zebrafish (arrow) as compared to control adult zebrafish (female and male). Scale bar: 2.5 mm. (E) Quantification of body fat in control and *lepb*<sup>-/-</sup> female (\*\*\*) and male (\*\*\*) adult zebrafish was measured from CHESS MR images. Ctr: control zebrafish; *lepb*<sup>-/-</sup>: *lepb*<sup>-/-</sup> zebrafish; F: female; M: male.

### ***Lepb*-deficient male adult zebrafish develop glomerular hypertrophy**

Subsequently, we investigated the histopathology of the zebrafish kidney, an organ with a high vulnerability under the diabetic condition. We found a substantial increase in the surface area of the glomeruli of *lepb*<sup>-/-</sup> male zebrafish (Fig. 3B), compared to control male zebrafish (Fig. 3A), on PAS-stained slides. A quantitative analysis of the surface area of the glomeruli showed significant enlargement of Bowman's capsule (Fig. 3C;  $t_{(13)}=3.725$ ,  $p=0.003$ ) and glomerular tuft (Fig. 3D;  $t_{(13)}=3.176$ ,  $p=0.007$ ) in *lepb*<sup>-/-</sup> male zebrafish compared to control male zebrafish, indicating that *lepb*<sup>-/-</sup> male zebrafish develop glomerular hypertrophy. The surface area of Bowman's space was also larger in *lepb*<sup>-/-</sup> male zebrafish compared to controls. However, this difference did not reach statistical significance (Fig. 3E;  $t_{(13)}=2.108$ ,  $p=0.055$ ).

Besides, we did not observe severe mesangial matrix expansion in the glomeruli of *lepb*<sup>-/-</sup> male zebrafish. Tubular injury and interstitial fibrosis, the final events of chronic tubular injury, contribute to the loss of kidney function. The tubular histology of *lepb*<sup>-/-</sup> male zebrafish was as normal as control male zebrafish on both PAS- (Fig. 3A and 3B) and HE- stained slides (Fig. 3F and 3G), and no signs of the tubular atrophy and interstitial fibrosis were observed.

### ***Lepb*-deficient male adult zebrafish show a thickening of the GBM**

Thickening of the GBM is an early sign of diabetic nephropathy (DN). We found a significant increase (2.6 times) in the thickness of GBM in *lepb*<sup>-/-</sup> male zebrafish (Fig. 4A-4D, and 4H;  $t_{(4)}=10.281$ ,  $p=0.001$ ) compared to controls via TEM approach.

Furthermore, we observed some fibers surrounding the GBM in the glomeruli of *lepb*<sup>-/-</sup> male zebrafish (Fig. 4G), suggesting there might have the extracellular matrix accumulation. However, we did not observe obvious podocyte foot process effacement and endothelial cell damage in the glomeruli of *lepb*<sup>-/-</sup> male zebrafish. Besides, the ultrastructure of the renal proximal tubules of *lepb*<sup>-/-</sup> male zebrafish was normal and indistinguishable when comparing to control male zebrafish (Fig. 4E and 4F), which is consistent with the findings from HE and PAS staining.

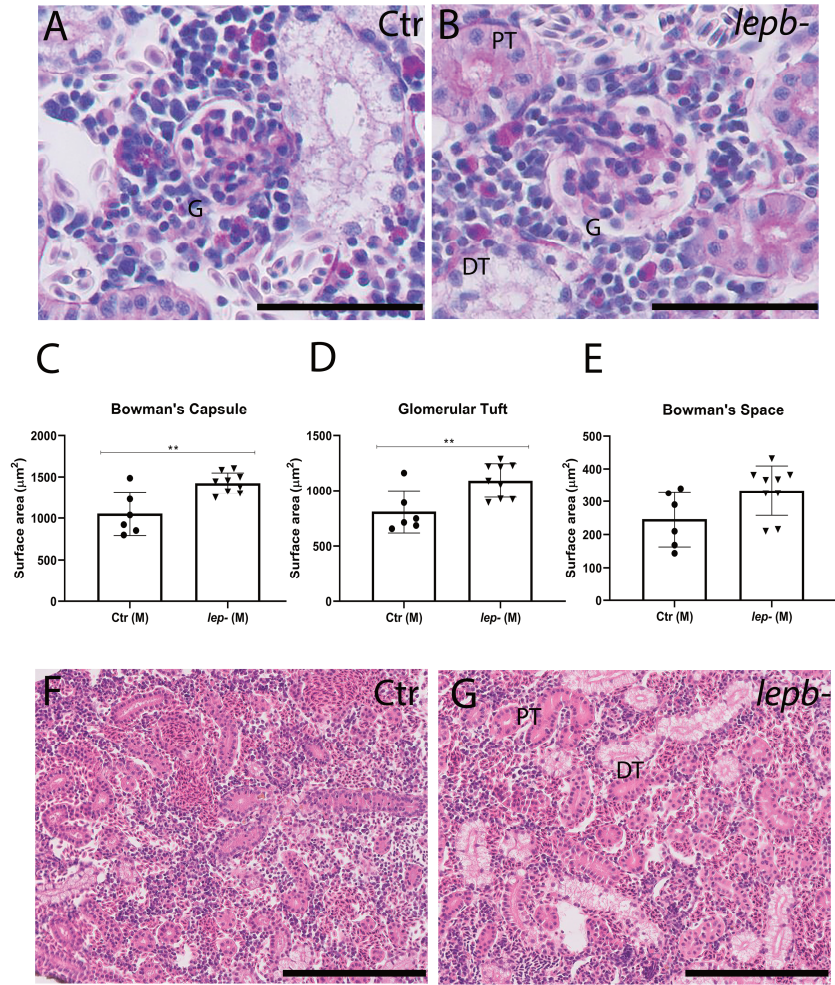


**Figure 3. *Lepb*-deficient male adult zebrafish develop glomerular hypertrophy**

(A-B) Representative images of the glomeruli of control (A) and *lep<sup>-/-</sup>* (B) male adult zebrafish; the scale bars represent 50 μm; PAS staining. (C) Summary of the surface areas of Bowman's capsule of control and *lep<sup>-/-</sup>* male adult zebrafish (\*\* $p < 0.01$ ). (D) Summary of the surface areas of Glomerular tuft of control and *lep<sup>-/-</sup>* male adult zebrafish (\*\* $p < 0.01$ ). (E) Summary of the surface areas of Bowman's space of control and *lep<sup>-/-</sup>* male adult zebrafish. (F-G) Representative images of the tubules of control (F) and *lep<sup>-/-</sup>* (G) male adult zebrafish; the scale bars represent 50 μm; HE staining. Ctr: control zebrafish; *lep<sup>-/-</sup>*: *lep<sup>-/-</sup>* zebrafish; M: male; G: glomeruli; PT: proximal tubule; DT: distal tubule.



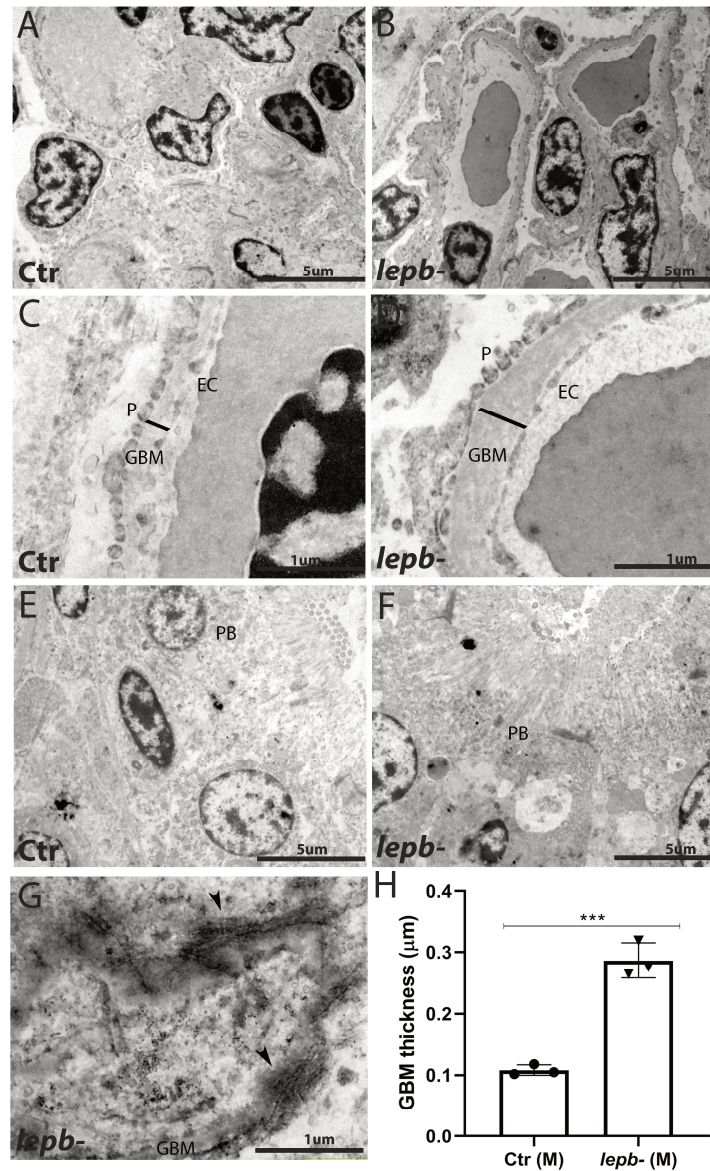


**Figure 4. Transmission electron microscopy pictures of glomeruli and tubules from control and *lepb*-deficient male adult zebrafish**

(A-B) Representative images of glomeruli from control (A) and *lepb*<sup>-/-</sup> (B) male adult zebrafish; magnification 5000X. (C-D) High magnification view of one segment of a glomerular capillary from control (C) and *lepb*<sup>-/-</sup> (D) male adult zebrafish (the thickness of GBM was marked by black lines); magnification 25,000X. (E-F) Representative images of the tubular brush border of the proximal tubule of control (E) and *lepb*<sup>-/-</sup> (F) male adult zebrafish; magnification 5000X. (G) High magnification of the fibrillar mesangial matrix in *lepb*<sup>-/-</sup> male adult zebrafish (black arrowheads); magnification 50,000X. (H) Summary of the thickness of GBM in the control and *lepb*<sup>-/-</sup> male adult zebrafish. The thickness of GBM in *lepb*<sup>-/-</sup> male zebrafish is 2.6 times thicker than that in control male zebrafish (\*\* $p < 0.01$ ). Ctr: control zebrafish; *lepb*<sup>-/-</sup>: *lepb*<sup>-/-</sup> zebrafish; M: male; GBM: glomerular basement membrane; P: podocytes; EC: endothelial cells; PB: proximal tubular brush border.

## Discussion

In the current study, we generated *lepb*-deficient zebrafish by using the CRISPR/CAS9 gene editing approach. We demonstrated that 1.5 years old *lepb*<sup>-/-</sup> adult zebrafish in both genders had an increase in body weight, length and visceral fat accumulation compared to their respective controls. Furthermore, we found that the blood glucose levels in *lepb*<sup>-/-</sup> male adult zebrafish were significantly higher than control male adult zebrafish. Lastly, we showed that *lepb*<sup>-/-</sup> male adult zebrafish developed early signs of DN.

There are conflicting reports whether the disruption of leptin signaling induces adiposity in zebrafish. Audira et al. reported that *lepa*-deficient adult zebrafish display an obese phenotype<sup>26</sup>. On the other hand, Michel et al.<sup>24</sup> did not detect an increased fat mass or higher body weight in *lepr*-deficient adult zebrafish. In the current study, we observed that all *lepb* mutants had an increased body weight and body length compared to controls at the adult stage. However, no difference in BMI between control and *lepb*<sup>-/-</sup> zebrafish, in both genders, was found (Supplementary Fig. 3C; female:  $t_{(12)}=1.120$ ,  $p=0.285$ ; male:  $t_{(16)}=0.070$ ,  $p=0.945$ ). It is well known that increased visceral fat accumulation is a typical feature of obesity. In addition, it has been suggested in the literature that body fat percentage and visceral fat level can predict type II diabetes<sup>28</sup> or insulin resistance<sup>29</sup> better than BMI. To more precisely compare the body fat distribution between control and *lepb*<sup>-/-</sup> zebrafish, the successive slices from top to bottom in the coronal plane were imaged via an MRI approach. We found a significantly increased visceral fat accumulation in the *lepb*<sup>-/-</sup> zebrafish compared to control zebrafish in both genders. The increase of body weight and visceral fat accumulation in *lepb*<sup>-/-</sup> zebrafish in both genders jointly suggested that *lepb* deficiency results in adiposity in zebrafish. How can we reconcile our findings with the study of Michel et al.<sup>24</sup> showing that *lepr*-deficient zebrafish did not develop obesity? The different findings between these two studies might be due to the different age of zebrafish investigated, or different feeding protocols. Alternatively, leptin signaling in zebrafish might also have functions that are independent of the leptin receptor. Besides, to exclude off-target effects in our study, we investigated three different mutants, including *lepb*<sup>7-/-</sup>, *lepb*<sup>8-/-</sup> and *lepb*<sup>7-/-8-/-</sup> mutants, in the *lepb*-deficient (*lepb*<sup>-/-</sup>) group. We found that all these three mutants of *lepb*<sup>-/-</sup> adult zebrafish had an increased body weight and body length, compared to the controls, which makes it unlikely that our results are caused by the off-target effects of the CRISPR-CAS9 procedure.

Recently, researchers have generated different diabetic models in zebrafish. For instance, Zhang et al. developed a zebrafish model for T2DM by overfeeding 4~6 months old fish with diet-induced obesity (DIO) food over 8 weeks, and they showed that these obese fish have



increased fasting blood glucose levels<sup>30</sup>. Olsen et al. induced a type 1 diabetes mellitus (T1DM) in 4~6 months old zebrafish by injecting streptozotocin (STZ) to ablate beta cells from the pancreas<sup>31</sup>. This STZ-induced T1DM zebrafish model represents several diabetic complications, such as retinal thinning (an early sign of retinopathy) and GBM thickening (an early sign of nephropathy). However, to further investigate diabetes in zebrafish, there is still a lack of a congenital diabetic zebrafish line which does not require time-consuming feeding schemes or invasive procedures which might cause side effects when induces the diabetic symptoms.

Diabetes is characterised by hyperglycemia which plays a crucial role in the development of diabetes complications. In the current study, we found that 2 hours postprandial blood glucose levels and fasting blood glucose levels of *lepb*<sup>-/-</sup> male zebrafish were significantly higher than the levels of control male zebrafish. However, we did not detect this difference in female zebrafish. A review from Wang et al. illustrated that diabetic manifestations in some of the rodent models do not develop in females or are not as apparent as in males<sup>32</sup>. Therefore, it is very interesting that we got similar results in the current study in a fish model. The increased body weight, length and visceral fat accumulation and higher blood glucose levels in *lepb*<sup>-/-</sup> male zebrafish collectively indicate that *lepb*-deficient male adult zebrafish display the features of T2DM. To further explore the glucose homeostasis in the *lepb*-deficient zebrafish model, it would be very interesting to investigate whether the whole-body glucose level has already increased in the *lepb*-deficient zebrafish at the larvae stage.

Growing literature provides evidence that leptin has a glucose-lowering effect. A previous study reported that the infusion of leptin into the brain could normalize the hyperglycemia in *ob/ob* mice<sup>33</sup>. Insulin has a robust role in the regulation of glucose homeostasis, and insulin resistance is a fundamental aspect of the etiology of T2DM. Several studies have demonstrated that leptin can improve insulin sensitivity<sup>18,34</sup>. An experimental study from Morton et al. suggested that reduced leptin in the mediobasal hypothalamus leads to severe insulin resistance and glucose intolerance in Koletsky rats, and phosphatidylinositol-3-OH kinase signaling is a vital mediator of this effect<sup>35</sup>. In addition, Yu et al. reported that leptin could reverse the hyperglycemia and ketosis by suppressing the action of glucagon on the liver and improving the utilization of glucose in the skeletal muscle in insulin-deficient diabetic rodents<sup>11</sup>. These studies indicated that leptin acts on glucose metabolism in both insulin-dependent and insulin-independent ways. Earlier work from our laboratory had demonstrated that *lepb* was significantly downregulated in zebrafish larvae under an insulin-resistance state<sup>27</sup>. Future studies should investigate whether the diabetic phenotype of *lepb* mutants is caused by disruption of the insulin signaling pathway.

The segmental anatomy of the nephron is conserved among the vertebrates<sup>36</sup>. Olsen et al. found that STZ-induced T1DM zebrafish have a thickening of the GBM (an early sign of DN)<sup>31</sup>. In the current study, we want to address whether *lepb*<sup>-/-</sup> adult zebrafish develop DN or not. We found the *lepb*<sup>-/-</sup> male group had higher blood glucose levels compared to the control male group, but not in the female group. Therefore, the kidney in male zebrafish was further investigated by performing histopathological examination. Glomerular hypertrophy, mesangial expansion, and thickening of the GBM are the particular characteristics of the histopathology of DN<sup>37</sup>. We found that *lepb*<sup>-/-</sup> male zebrafish develop glomerular hypertrophy and thickening of the GBM, compared to control male zebrafish. However, we did not observe severe mesangial expansion, podocyte damage, or tubular cell damage in the kidney tissue of *lepb*<sup>-/-</sup> male zebrafish. These findings collectively indicate that the renal injury in *lepb*<sup>-/-</sup> male zebrafish is relatively mild. In summary, we demonstrated that *lepb* regulates glucose homeostasis and adiposity in zebrafish, and deletion of the *lepb* gene results in the development of T2DM and the early stage of DN. These results suggest that *lepb*-deficient zebrafish can be used as a T2DM model, and further investigation would give us new insights into the mechanistic function of leptin in T2DM.

#### **Declaration of interest**

All authors declare no competing interests.

#### **Funding**

The work was supported by the Polish National Science Center (grant number 2016/21/N/NZ6/01162).

#### **Acknowledgements**

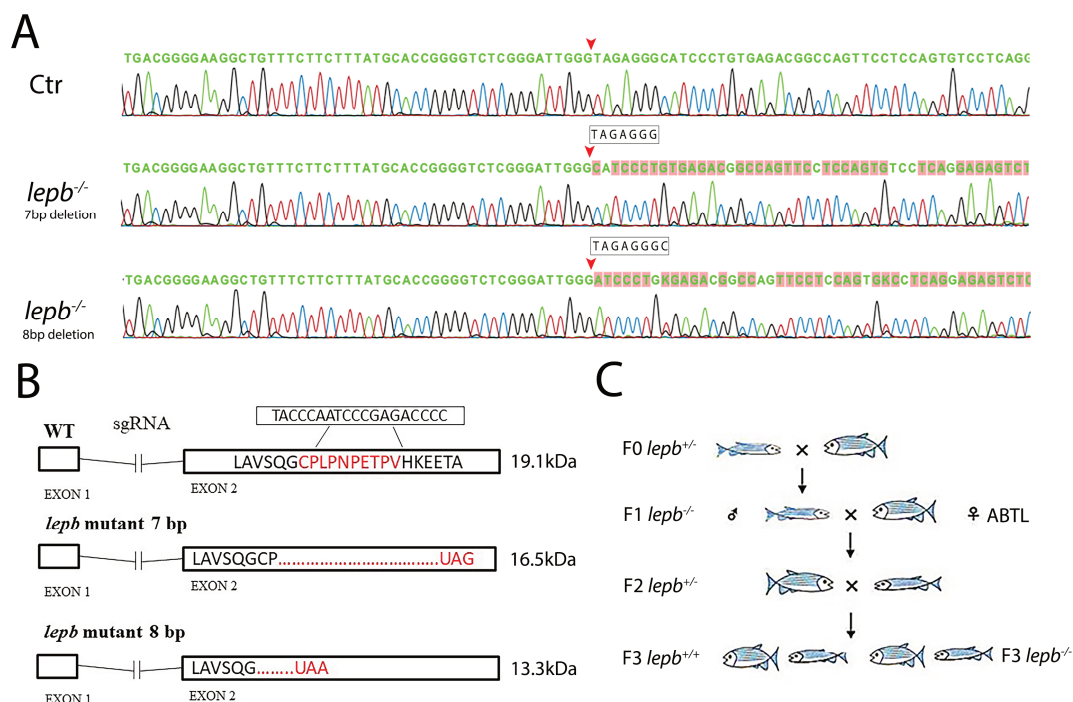
The first authors (J. He and Y. Ding) were supported by the China Scholarship Council (CSC). We would like to thank Peter Neeskens for the technical support of the transmission electron microscopy (TEM).

## References

- 1 Zhang, Y. *et al.* Positional cloning of the mouse obese gene and its human homologue. *Nature* **372**, 425-432, doi:10.1038/372425a0 (1994).
- 2 Ahima, R. S., Prabakaran, D. & Flier, J. S. Postnatal leptin surge and regulation of circadian rhythm of leptin by feeding. Implications for energy homeostasis and neuroendocrine function. *The Journal of clinical investigation* **101**, 1020-1027, doi:10.1172/JCI1176 (1998).
- 3 Lord, G. M. *et al.* Leptin modulates the T-cell immune response and reverses starvation-induced immunosuppression. *Nature* **394**, 897-901, doi:10.1038/29795 (1998).
- 4 Matarese, G., Moschos, S. & Mantzoros, C. S. Leptin in immunology. *J Immunol* **174**, 3137-3142, doi:10.4049/jimmunol.174.6.3137 (2005).
- 5 Meier, U. & Gressner, A. M. Endocrine regulation of energy metabolism: review of pathobiochemical and clinical chemical aspects of leptin, ghrelin, adiponectin, and resistin. *Clin Chem* **50**, 1511-1525, doi:10.1373/clinchem.2004.032482 (2004).
- 6 Caprio, M., Fabbri, E., Isidori, A. M., Aversa, A. & Fabbri, A. Leptin in reproduction. *Trends Endocrinol Metab* **12**, 65-72, doi:10.1016/s1043-2760(00)00352-0 (2001).
- 7 Licinio, J. *et al.* Phenotypic effects of leptin replacement on morbid obesity, diabetes mellitus, hypogonadism, and behavior in leptin-deficient adults. *Proc Natl Acad Sci U S A* **101**, 4531-4536, doi:10.1073/pnas.0308767101 (2004).
- 8 Farooqi, I. S. *et al.* Effects of recombinant leptin therapy in a child with congenital leptin deficiency. *N Engl J Med* **341**, 879-884, doi:10.1056/NEJM199909163411204 (1999).
- 9 Funcke, J. B. *et al.* Monogenic forms of childhood obesity due to mutations in the leptin gene. *Mol Cell Pediatr* **1**, 3, doi:10.1186/s40348-014-0003-1 (2014).
- 10 Drel, V. R. *et al.* The leptin-deficient (ob/ob) mouse: a new animal model of peripheral neuropathy of type 2 diabetes and obesity. *Diabetes* **55**, 3335-3343, doi:10.2337/db06-0885 (2006).
- 11 Yu, X., Park, B. H., Wang, M. Y., Wang, Z. V. & Unger, R. H. Making insulin-deficient type 1 diabetic rodents thrive without insulin. *Proc Natl Acad Sci U S A* **105**, 14070-14075, doi:10.1073/pnas.0806993105 (2008).
- 12 Fujikawa, T., Chuang, J. C., Sakata, I., Ramadori, G. & Coppari, R. Leptin therapy improves insulin-deficient type 1 diabetes by CNS-dependent mechanisms in mice. *Proc Natl Acad Sci U S A* **107**, 17391-17396, doi:10.1073/pnas.1008025107 (2010).
- 13 Hedbacker, K. *et al.* Antidiabetic effects of IGFBP2, a leptin-regulated gene. *Cell Metab* **11**, 11-22, doi:10.1016/j.cmet.2009.11.007 (2010).
- 14 German, J. P. *et al.* Leptin activates a novel CNS mechanism for insulin-independent normalization of severe diabetic hyperglycemia. *Endocrinology* **152**, 394-404, doi:10.1210/en.2010-0890 (2011).
- 15 Muzzin, P., Eisensmith, R. C., Copeland, K. C. & Woo, S. L. Correction of obesity and diabetes in genetically obese mice by leptin gene therapy. *Proc Natl Acad Sci U S A* **93**, 14804-14808, doi:10.1073/pnas.93.25.14804 (1996).
- 16 Pocaï, A. *et al.* Central leptin acutely reverses diet-induced hepatic insulin resistance. *Diabetes* **54**, 3182-3189, doi:10.2337/diabetes.54.11.3182 (2005).
- 17 Park, S., Hong, S. M., Sung, S. R. & Jung, H. K. Long-term effects of central leptin and resistin on body weight, insulin resistance, and beta-cell function and mass by the modulation of hypothalamic leptin and insulin signaling. *Endocrinology* **149**, 445-454, doi:10.1210/en.2007-0754 (2008).
- 18 German, J. *et al.* Hypothalamic leptin signaling regulates hepatic insulin sensitivity via a neurocircuit involving the vagus nerve. *Endocrinology* **150**, 4502-4511, doi:10.1210/en.2009-0445 (2009).
- 19 Denver, R. J., Bonett, R. M. & Boorse, G. C. Evolution of leptin structure and function. *Neuroendocrinology* **94**, 21-38, doi:10.1159/000328435 (2011).
- 20 Volkoff, H., Eykelbosh, A. J. & Peter, R. E. Role of leptin in the control of feeding of goldfish *Carassius auratus*: interactions with cholecystokinin, neuropeptide Y and orexin A, and modulation by fasting. *Brain Res* **972**, 90-109, doi:10.1016/s0006-8993(03)02507-1 (2003).

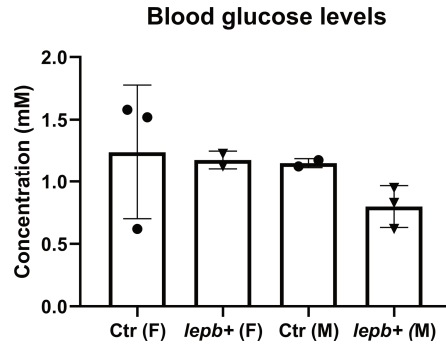
- 21 Murashita, K., Uji, S., Yamamoto, T., Ronnestad, I. & Kurokawa, T. Production of recombinant leptin and its effects on food intake in rainbow trout (*Oncorhynchus mykiss*). *Comp Biochem Physiol B Biochem Mol Biol* **150**, 377-384, doi:10.1016/j.cbpb.2008.04.007 (2008).
- 22 Aguilar, A. J., Conde-Sieira, M., Lopez-Patino, M. A., Miguez, J. M. & Soengas, J. L. In vitro leptin treatment of rainbow trout hypothalamus and hindbrain affects glucosensing and gene expression of neuropeptides involved in food intake regulation. *Peptides* **32**, 232-240, doi:10.1016/j.peptides.2010.11.007 (2011).
- 23 Gorissen, M., Bernier, N. J., Nabuurs, S. B., Flik, G. & Huising, M. O. Two divergent leptin paralogues in zebrafish (*Danio rerio*) that originate early in teleostean evolution. *The Journal of endocrinology* **201**, 329-339, doi:10.1677/JOE-09-0034 (2009).
- 24 Michel, M., Page-McCaw, P. S., Chen, W. & Cone, R. D. Leptin signaling regulates glucose homeostasis, but not adipostasis, in the zebrafish. *Proc Natl Acad Sci U S A* **113**, 3084-3089, doi:10.1073/pnas.1513212113 (2016).
- 25 Chisada, S. *et al.* Leptin receptor-deficient (knockout) medaka, *Oryzias latipes*, show chronical up-regulated levels of orexigenic neuropeptides, elevated food intake and stage specific effects on growth and fat allocation. *Gen Comp Endocrinol* **195**, 9-20 (2014).
- 26 Audira, G. *et al.* Zebrafish Mutants Carrying Leptin a (*lepa*) Gene Deficiency Display Obesity, Anxiety, Less Aggression and Fear, and Circadian Rhythm and Color Preference Dysregulation. *Int J Mol Sci* **19**, doi:10.3390/ijms19124038 (2018).
- 27 Marin-Juez, R., Jong-Raadsen, S., Yang, S. & Spaink, H. P. Hyperinsulinemia induces insulin resistance and immune suppression via Ptpn6/Shp1 in zebrafish. *The Journal of endocrinology* **222**, 229-241, doi:10.1530/JOE-14-0178 (2014).
- 28 Lebovitz, H. E. & Banerji, M. A. Point: visceral adiposity is causally related to insulin resistance. *Diabetes Care* **28**, 2322-2325, doi:10.2337/diacare.28.9.2322 (2005).
- 29 Kurniawan, L. B., Bahrin, U., Hatta, M. & Arif, M. Body Mass, Total Body Fat Percentage, and Visceral Fat Level Predict Insulin Resistance Better Than Waist Circumference and Body Mass Index in Healthy Young Male Adults in Indonesia. *J Clin Med* **7**, doi:10.3390/jcm7050096 (2018).
- 30 Zang, L., Shimada, Y. & Nishimura, N. Development of a Novel Zebrafish Model for Type 2 Diabetes Mellitus. *Sci Rep* **7**, 1461, doi:10.1038/s41598-017-01432-w (2017).
- 31 Olsen, A. S., Sarra, M. P., Jr. & Intine, R. V. Limb regeneration is impaired in an adult zebrafish model of diabetes mellitus. *Wound Repair Regen* **18**, 532-542, doi:10.1111/j.1524-475X.2010.00613.x (2010).
- 32 Wang, B., Chandrasekera, P. C. & Pippin, J. J. Leptin- and leptin receptor-deficient rodent models: relevance for human type 2 diabetes. *Curr Diabetes Rev* **10**, 131-145, doi:10.2174/1573399810666140508121012 (2014).
- 33 Kamohara, S., Burcelin, R., Halaas, J. L., Friedman, J. M. & Charron, M. J. Acute stimulation of glucose metabolism in mice by leptin treatment. *Nature* **389**, 374-377, doi:10.1038/38717 (1997).
- 34 Shimomura, I., Hammer, R. E., Ikemoto, S., Brown, M. S. & Goldstein, J. L. Leptin reverses insulin resistance and diabetes mellitus in mice with congenital lipodystrophy. *Nature* **401**, 73-76, doi:10.1038/43448 (1999).
- 35 Morton, G. J. *et al.* Leptin regulates insulin sensitivity via phosphatidylinositol-3-OH kinase signaling in mediobasal hypothalamic neurons. *Cell Metab* **2**, 411-420, doi:10.1016/j.cmet.2005.10.009 (2005).
- 36 McCampbell, K. K. & Wingert, R. A. New tides: using zebrafish to study renal regeneration. *Transl Res* **163**, 109-122, doi:10.1016/j.trsl.2013.10.003 (2014).
- 37 Tervaert, T. W. *et al.* Pathologic classification of diabetic nephropathy. *J Am Soc Nephrol* **21**, 556-563, doi:10.1681/ASN.2010010010 (2010).

## Supplementary data



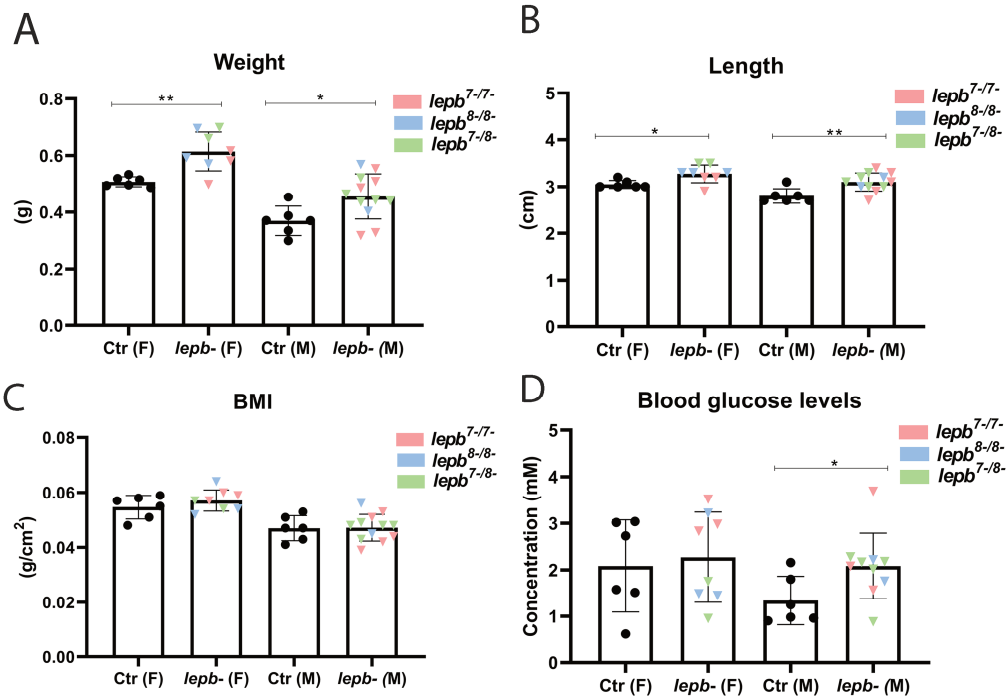
## Supplementary Figure 1. Lepb-deficient zebrafish line

(A) The wild type zebrafish (Ctrl) is showing a partial sequence of the *lepb* gene. Seven base pairs (TAGAGGG) were deleted in *lepb*<sup>7-/7-</sup> zebrafish and eight base pairs (TAGAGGGC) were deleted in *lepb*<sup>8-/8-</sup> zebrafish. The arrowheads show the start point of the deletion. (B) The wild type *lepb* gene translates into the predicted 19.1 kDa *lepb* protein in zebrafish. The seven base pairs deletion creates a premature stop codon UAG in exon 2, which results in a truncated 16.5 kDa protein. And the eight base pairs deletion causes a premature stop codon UAA in exon 2, which results in a truncated 13.3 kDa protein. (C) Homozygous F1 carriers were outcrossed once against the wild type zebrafish (ABTL) and the offspring (heterozygote *lepb*<sup>+/-</sup>) were subsequently incrossed, resulting in the used *lepb*<sup>+/+</sup> and *lepb*<sup>-/-</sup> siblings. Because of the limitations of the number of adult zebrafish during this study, we used adult WT-ABTL (Ctrl) and all *lepb*<sup>-/-</sup> (*lepb*<sup>7-/7-</sup>, *lepb*<sup>8-/8-</sup> and *lepb*<sup>7-/8-</sup>) for the experiments.



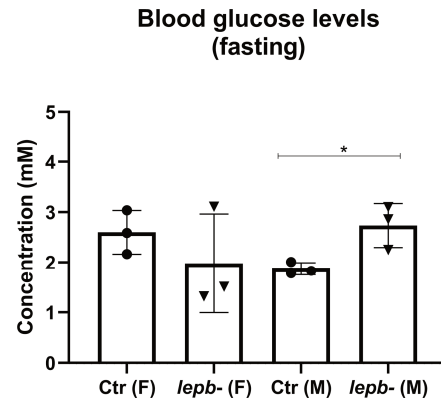
**Supplementary Figure 2. Blood glucose levels in *lepb<sup>+/+</sup>* adult zebrafish and age-matched ABTL control zebrafish**

Two hours postprandial blood glucose levels in ABTL control and *lepb<sup>+/+</sup>* zebrafish (female and male). Ctr: ABTL control zebrafish; *lepb<sup>+/+</sup>*: *lepb<sup>+/+</sup>* zebrafish; F: female; M: male.



**Supplementary Figure 3. Body weight, length, BMI and blood glucose levels in different *lepb<sup>-/-</sup>* mutants**

(A) The body weight of control and *lepb<sup>-/-</sup>* female (\*\* $p < 0.01$ ) and male (\* $p < 0.05$ ) adult zebrafish. (B) The body length of control and *lepb<sup>-/-</sup>* female (\* $p < 0.05$ ) and male (\*\* $p < 0.01$ ) adult zebrafish. (C) The BMI of control and *lepb<sup>-/-</sup>* female and male adult zebrafish. (D) Two hours postprandial blood glucose levels in control and *lepb<sup>-/-</sup>* female and male (\* $p < 0.05$ ) adult zebrafish. Different *lepb<sup>-/-</sup>* mutants were marked in different colors. *lepb<sup>7-7-</sup>* in red, *lepb<sup>8-8-</sup>* in blue and *lepb<sup>7-8-</sup>* in green. Ctr: control zebrafish; *lepb<sup>-/-</sup>*: *lepb<sup>-/-</sup>* zebrafish; F: female; M: male.



**Supplementary Figure 4. Fasting blood glucose levels in control and *lepb*-deficient adult zebrafish**

Fasting blood glucose levels in control and *lepb*<sup>-/-</sup> female and male (\**p*<0.05) adult zebrafish. Ctr: control zebrafish; *lepb*<sup>-/-</sup>: *lepb*<sup>-/-</sup> zebrafish; F: female; M: male.



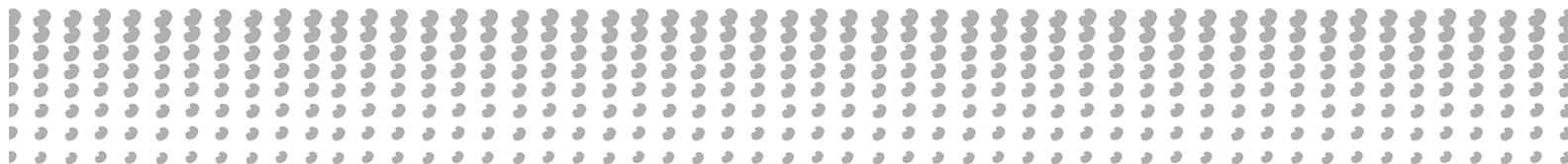


# Chapter 5

## *Ctns* mutant adult zebrafish develop nephropathic cystinosis

Junling He\*, Sante Princiero Berlingerio\*, Bert van den Heuvel, Hans J Baelde,  
Elena Levtchenko.

\*These authors contributed equally to this work



## Abstract

Cystinosis is a lysosomal storage disease caused by mutations of the *CTNS* gene encoding cystinosin. Defective cystinosin function results in the intralysosomal accumulation of cystine in all cells. Most patients with cystinosis have kidney disease presenting as generalized proximal tubular dysfunction (called renal Fanconi syndrome) followed by glomerular damage and progressing towards end-stage kidney failure. In our previous study, we generated a *ctns* mutant zebrafish that displayed glomerular and tubular dysfunction at the larval stage. In the current study, we further investigated the renal histopathology of *ctns* mutant zebrafish at the adult stage. We observed hyaline-like eosinophilic droplets and cytoplasmic vacuoles in the renal proximal tubular epithelial cells of *ctns* mutant adult zebrafish, in both genders, on HE- and PAS- stained slides, which were not present in controls. Additionally, we found that these cytoplasmic vacuoles have a rectangular or polymorphous shape on toluidine blue-stained slides and images captured by transmission electron microscopy. These findings indicate that cystine crystals, the hallmark of cystinosis, are present in the renal proximal tubular cells of *ctns* mutant adult zebrafish. Further, compared with controls, the *ctns* mutant adult zebrafish had glomerular hypertrophy and increased expression of cleaved caspase-3 in the renal proximal tubular cells. Collectively, our data indicate that the kidney pathology of *ctns* mutant adult zebrafish has features of human nephropathic cystinosis and might be a promising model for understanding the pathogenesis of nephropathic cystinosis.

## Introduction

Cystinosis is a rare and incurable lysosomal storage disease. Mutations in the *CTNS* gene encoding cystinosin cause the defective lysosomal cystine transport <sup>1,2</sup>, resulting in the intralysosomal accumulation of cystine in all cells and tissues. In most patients with cystinosis, the disease initially manifests in the kidney, being the most common cause of inherited renal Fanconi syndrome in humans <sup>3</sup>. Fanconi syndrome is a result of inadequate reabsorption of nutrients and minerals in the renal proximal tubule leading to losses of essential molecules and metabolism into the urine. The proximal tubular damage is followed by progressive glomerular dysfunction and, when left untreated, leads to end-stage kidney failure. The underlying mechanisms of nephropathic cystinosis are still incompletely understood, and current therapy with cystine depleting drug cysteamine is not curative <sup>3</sup>. Therefore, further understanding the pathogenesis of nephropathic cystinosis and finding new therapeutic options are urgently needed.

Although cystine accumulation is the crucial feature of cystinosis, numerous studies suggested the role of inflammation <sup>4</sup>, oxidative stress <sup>5,6</sup> and altered cell death mechanisms (autophagy <sup>7-9</sup> and apoptosis <sup>10,11</sup>) in the development of kidney phenotype. To better understand the molecular mechanisms of a particular disease, a suitable animal model is needed. The first *Ctns*<sup>-/-</sup> mouse model was generated in a mixed 129Sv x C57BL/6 strain <sup>12</sup>. In this *Ctns*<sup>-/-</sup> mouse model, cystine accumulation was found in kidney, liver, and muscle tissues. However, these mice failed to develop renal proximal tubulopathy or glomerular dysfunction. Afterwards, Nevo and colleagues generated *Ctns*<sup>-/-</sup> mice on a C57BL/6 and FVB/N background <sup>13</sup>. They showed that *Ctns*<sup>-/-</sup> mice with C57BL/6 background had an accumulation of cystine in all studied tissues. Additionally, these *Ctns*<sup>-/-</sup> mice had pronounced histological renal lesions in the proximal tubules and eventually developed chronic renal failure. In contrast, the *Ctns*<sup>-/-</sup> mice with FVB/N background did not develop renal dysfunction. This finding indicated that the genetic background influences the renal phenotype in mice. Recently, Shimizu *et al.* established a novel congenic *Ctns*<sup>ugl</sup> mutation in a rat strain with the F344 genetic background <sup>14</sup>. The F344-*Ctns* mutant rats developed remarkable renal lesions and showed the cystine crystals in the lysosomes of the kidney cortex.

The rodent models are commonly used to investigate human diseases with a lot of advantages. However, generating a new murine model are usually time-consuming and expensive. To date, zebrafish models become an attractive tool for investigating human diseases <sup>15</sup>. In a previous study, we generated a congenic zebrafish model (*ctns*<sup>-/-</sup>) with a homozygous nonsense mutation in the exon 8 of the *ctns* gene, resulting in a functional loss of cystinosin <sup>16</sup>. The *ctns* mutant

zebrafish larvae present with delayed development, cystine accumulation, and signs of pronephric glomerular and tubular dysfunction, which closely resemble the phenotype of human nephropathic cystinosis. Additionally, we found that eight-month-old adult zebrafish had 20-fold increased cystine levels in the kidney compared with controls. Until now, data of *ctns* mutant adult zebrafish are lacking. In the current study, we aim to characterize the *ctns* mutant adult zebrafish' renal features and compare them with the age-matched control adult zebrafish by performing histopathological examinations.

## **Methods and Materials**

### **Animals**

Zebrafish were handled in compliance with the local animal welfare regulations and maintained according to standard protocols (zfin.org). The details of generating the *ctns* mutant zebrafish were described in our previous study (11). For this study, we included *ctns* mutant zebrafish at 3 (female=3 and male=3), 6 (female=3 and male=3) and 18 (female=6 and male=6) months old and the age and sex-matched AB control zebrafish. This study was approved by the local animal welfare committee (DEC) of the University of Leuven (number of the project:142/2019).

### **HE & PAS staining**

After zebrafish were sacrificed, the whole zebrafish were immediately fixed in 4% buffered paraformaldehyde (4% PFA) at 4°C for 1 week. After being washed with PBS twice, the zebrafish were transferred to EDTA solution (100mM, pH=8) for the decalcification for another 1 week, followed by embedding into paraffin. Paraffin-embedded zebrafish tissue was cut (4- $\mu$ m thickness) on a Leica microtome (Wetzlar). Sections were stained with hematoxylin and eosin (HE) and Periodic-acid Schiff (PAS) according to the standard protocols.

### **Immunohistochemistry (cleaved caspase-3 staining)**

Sections with the fresh-cut zebrafish tissue were deparaffinized and rehydrated. For cleaved caspase-3 staining, sections were subjected to heat-induced antigen retrieval using 10mM citrate buffer (pH=6). After blocking with 5% Normal Goat Serum (NGS) in PBS, the sections were incubated with rabbit anti-cleaved caspase-3 (1:200, Cell Signaling Technology Europe, The Netherlands) followed by an anti-rabbit-Envision, HRP-labelled secondary antibody (Dako, Denmark). As a negative control, a normal rabbit serum was used instead of the primary antibody. Diaminobenzidine (DAB+; Dako, Denmark) was used as the chromogen. Subsequently, sections were counterstained with HE, dehydrated and mounted.

**Toluidine blue staining and Transmission electron microscopy (TEM)**

Zebrafish renal tissues were harvested and fixed in the EM fixation buffer (1.5% glutaraldehyde / 1% paraformaldehyde) for 24 hours. Subsequently, the renal tissues were post-fixed with 2.5% glutaraldehyde/1.2% acrolein in fixation buffer (0.1 mol/l cacodylate, 0.1 mol/l sucrose, pH 7.4) and 1% osmium tetroxide, and embedded into epon resin. Semi-thin sections (0.5- $\mu$ m thickness) were stained with toluidine blue. The ultrathin sections were stained with uranyl acetate. The images were collected using a JEM-1200 EX transmission electron microscopy (JEOL, Tokyo, Japan) with different magnifications.

**Digital image analysis**

Stained slides were digitized using a Philips Ultra-Fast Scanner 1.6 RA (Philips Electronics). To analyze glomerular hypertrophy in zebrafish, the surface area ( $\mu\text{m}^2$ ) of Bowman's capsule, Bowman's space, and glomerular tuft was measured on PAS-stained slides. All available glomeruli per section were included and measured using ImageJ software (<https://imagej.nih.gov/ij/>). The average of the measurements from each zebrafish was used for statistical analyses.

Two observers scored the cleaved caspase-3 expression in the tubules of each zebrafish. The semiquantitative score was conducted on the three random chosen tubular fields in each fish (20X magnification). The percentage of caspase-3 positive area relative to the total area of tubules was scored as 1 (negative staining), 2 (1-10% positive staining), 3 (10%-25% positive staining), 4 (>25% positive staining). The mean of the score from each zebrafish was used for statistical analyses.

**Statistical analyses**

Statistical analysis was performed using SPSS (IBM, New York). Data of two groups was analyzed using Student's *t*-test. Differences with  $P < 0.05$  were considered as statistically significant.

## Results

### ***Ctns* mutant zebrafish show renal proximal tubular damage**

First, we examined the histological characteristics of renal tubules in control and *ctns* mutant adult zebrafish of both genders at 3, 6 and 18 months of age. Proximal tubules showed eosinophilic cytoplasm (dark pink cytoplasm) and brush borders which were easy to identify on HE-stained slides (Fig.1A and 1E). Distal tubules had less eosinophilic cytoplasm (light pink cytoplasm) on HE-stained slides (Fig.1A and 1E). In all control zebrafish, no structural changes were found in both proximal and distal tubules (Fig.1A, 1C, and 1E). However, we observed the histological alterations including cloudy swelling, hyaline-like eosinophilic droplets and cytoplasmic vacuoles in the renal proximal tubules of *ctns* mutant female and male zebrafish at all three ages (Fig. 1B, 1D, and 1F). Furthermore, the cytoplasmic vacuoles were more frequently observed in the renal proximal tubules of 18 months old *ctns* mutant zebrafish, compared to *ctns* mutant zebrafish of younger ages (Fig.1B,1D, and 1F).

On PAS-stained slides, we did not find any histological alterations in the tubules of control zebrafish (Fig.1G). The hyaline droplets and cytoplasmic vacuoles were only observed in the renal proximal tubules of *ctns* mutant zebrafish (Fig. 1H) on PAS-stained slides, which is in line with the findings on HE-stained slides.

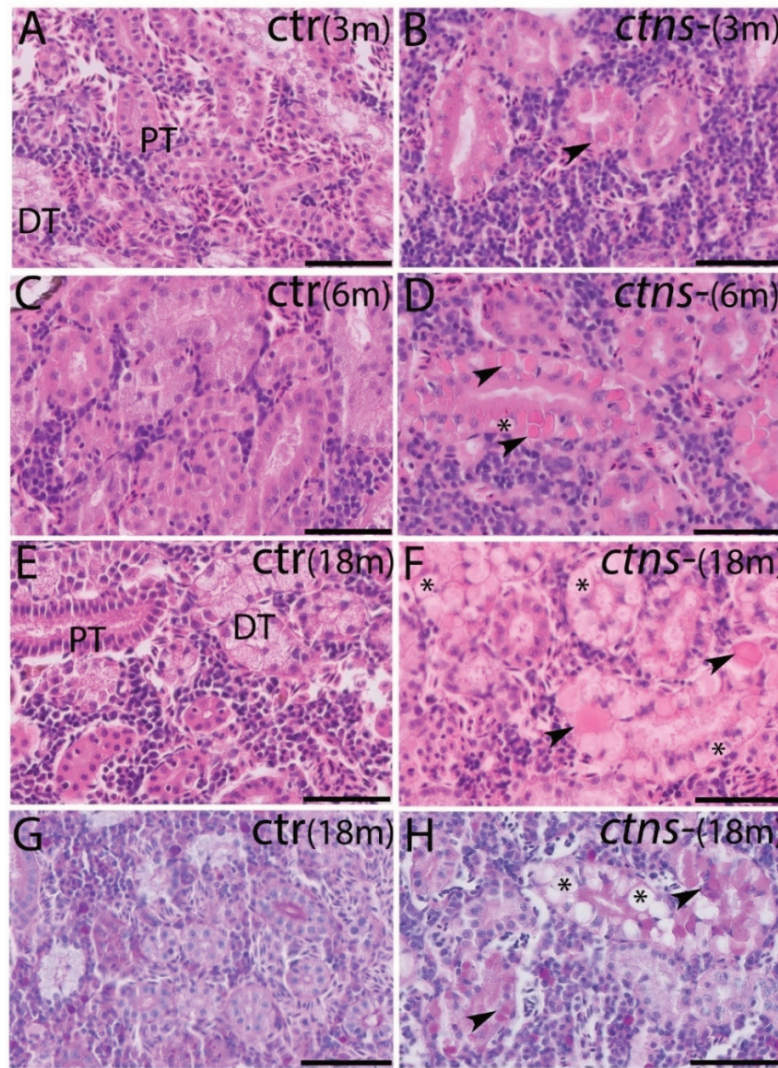


**Figure 1. Cloudy swelling, hyaline-like eosinophilic droplets and cytoplasmic vacuoles in the renal proximal tubules of *ctns* mutant zebrafish**

(A-B) Representative images of renal tubules of control (A) and *ctns* mutant (B) zebrafish at 3 months. Details of proximal tubules with hyaline-like eosinophilic droplets (black arrowhead). HE staining; the scale bars represent 50µm. (C-D) Representative images of renal tubules of control (C) and *ctns* mutant (D) zebrafish at 6 months. Details of proximal tubules with hyaline-like eosinophilic droplets (black arrowhead) and cytoplasmic vacuoles (\*). HE staining; the scale bars represent 50µm. (E-F) Representative images of renal tubules of control (E) and *ctns* mutant (F) zebrafish at 18 months. Details of proximal tubules with hyaline-like eosinophilic droplets (black arrowhead) and cytoplasmic vacuoles (\*). HE staining, the scale bars represent 50µm. (G-H) Representative images of the PAS staining of renal tubules of control (G) and *ctns* mutant (H) zebrafish at 18 months. Details of proximal tubules with hyaline-like droplets (black arrowhead) and cytoplasmic vacuoles (\*). The scale bars represent 50µm. PT: proximal tubule; DT: distal tubule. ctr: control zebrafish; *ctns* -: *ctns* mutant zebrafish; 3m: 3 months old; 6m: 6 months old; 18m: 18 months old.

### Male *ctns* mutant zebrafish show glomerular hypertrophy

Since the proximal tubular damage was most pronounced at the age of 18 months, glomerular histology was studied in detail at this age. The *ctns* mutant male zebrafish had significant enlargement of Bowman's capsule (Fig. 2B and 2C) and glomerular tuft (Fig. 2B and 2D), but not Bowman's space (Fig. 2B and 2E) when compared with control male zebrafish (Fig. 2A, 2C, 2D, and 2E). Moreover, the surface area of Bowman's capsule, glomerular tuft and Bowman's space was also larger in *ctns* mutant female zebrafish, compared with control female zebrafish (Fig. 2C-2E). However, this difference did not reach statistical significance. No proliferation of mesangial cells or glomerulosclerosis were observed in both control or *ctns* mutant zebrafish.

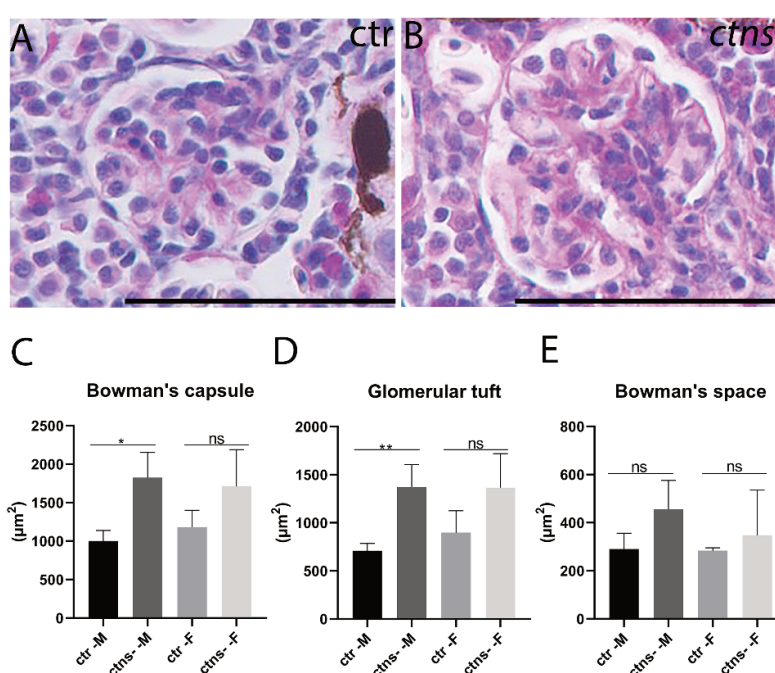


### Figure 2. Male *ctns* mutant zebrafish have glomerular hypertrophy

(A-B) Representative images of the PAS staining of the glomerulus of control (A) and *ctns* mutant (B) zebrafish. The scale bars represent 50  $\mu\text{m}$ . (C-E) Summary of the surface areas of the Bowman's capsule (C), the glomerular tuft (D), and Bowman's space (E) of control and *ctns* mutant zebrafish in both genders (\* $P < 0.05$ ; \*\* $P < 0.01$ ; ns: no significance). ctr: control zebrafish, *ctns* -: *ctns* mutant zebrafish, M: male zebrafish, F: female zebrafish.



**Cystine crystal accumulation in the renal proximal tubules of *ctns* mutant zebrafish**

It has been reported that clear spaces reflecting dissolved crystals can be detected on toluidine blue-stained slides <sup>17</sup>. On toluidine blue-stained slides, we observed numerous cytoplasmic vacuoles with rectangular or polymorphous shape in the renal proximal epithelial cells of *ctns* mutant zebrafish (Fig. 3B and 3C), not controls (Fig. 3A). The rectangular or polymorphous shape of the cytoplasmic vacuoles is suggestive of the cystine crystals. We also found the nuclear fragmentation in the proximal tubular epithelial cells of *ctns* mutant zebrafish, indicating that apoptosis occurs in the proximal tubular epithelial cells of *ctns* mutant zebrafish (Fig. 3D).

Next, we examined the renal ultrastructure of control and *ctns* mutant zebrafish. We found the apical microvilli were intact in control zebrafish (Fig. 3E). However, a partial loss of brush borders and numerous cytoplasmic vacuoles were observed in the renal proximal tubules of *ctns* mutant zebrafish (Fig. 3F). The cytoplasmic vacuoles with rectangular or polymorphous shapes were also seen on the TEM images (Fig. 3F), suggesting the cystine crystals accumulation. On the TEM images, we did not observe the thickening of the glomerular basement membrane, podocyte foot process effacement, or abnormal fenestrated endothelial cells in the glomeruli of both control and *ctns* mutant zebrafish (Fig. 3G and 3H).

**Apoptosis is involved in the pathogenesis of nephropathic cystinosis in zebrafish**

Finally, we performed the cleaved caspase-3 staining on the renal tissues of control and *ctns* mutant zebrafish. We found that the cleaved caspase-3 expression was significantly increased in the renal proximal tubular cells of *ctns* mutant female and male zebrafish (Fig. 4G), compared with the control female and male zebrafish, in which the cleaved caspase-3 expression was almost negative in the renal proximal tubular cells (Fig. 4A and 4C). The expression of cleaved caspase-3 was mainly present in cells showing the cytoplasmic vacuoles (Fig. 4B and 4D), indicating that apoptosis takes place in the injured proximal tubules in *ctns* mutant zebrafish. The cleaved caspase-3 staining in glomeruli in both control and *ctns* mutant zebrafish, in both genders, was negative (Fig. 4E and 4F).

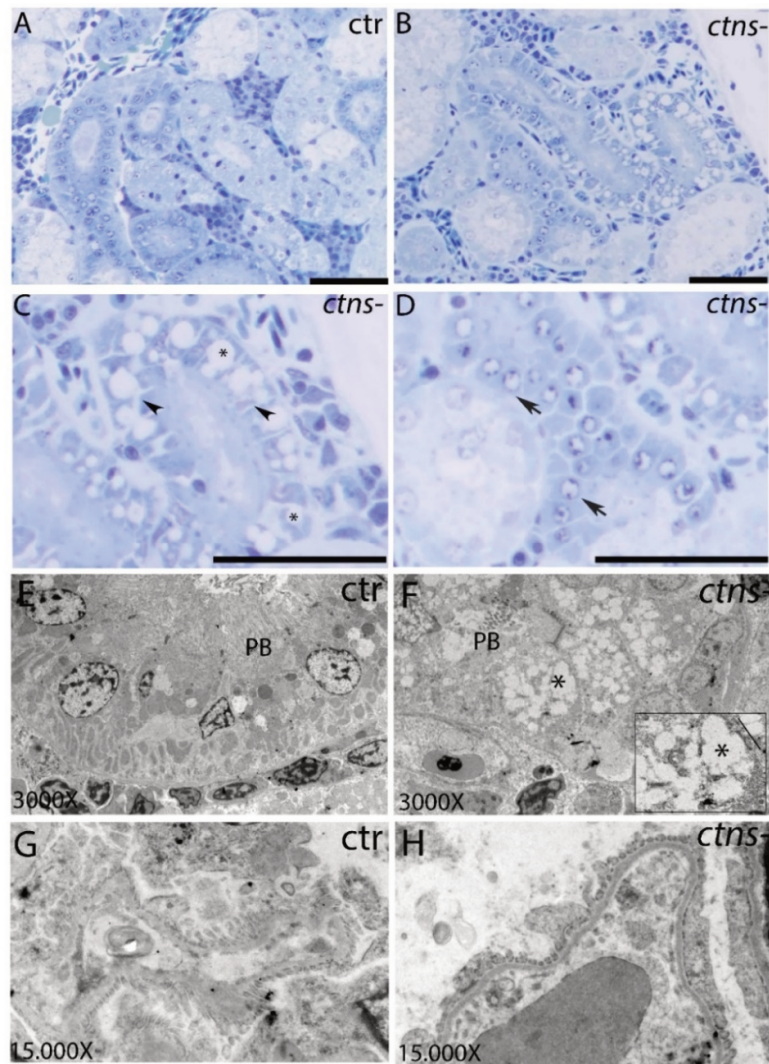


**Figure 3. Presence of cytoplasmic vacuoles in the renal proximal tubules of *ctns* mutant zebrafish at 18 months**

(A-B) Representative toluidine blue-stained images of renal proximal tubules in control (A) and *ctns* mutant (B) zebrafish. The scale bars represent 50 $\mu$ m. (C-D) Fig C and D show a higher magnification of Fig B. Details of renal proximal tubules with cytoplasmic vacuoles (C; \*) and the rectangular and polymorphous vacuolar spaces (C; black arrowhead), and nuclear fragmentation (D; black arrow). (E-F) Representative TEM images of the renal proximal tubule of control (E) *ctns* mutant zebrafish (F). Partial loss of brush borders (PB) and an abundance of the rectangular and polymorphous vacuoles (\*) were observed in the renal proximal tubule of *ctns* mutant zebrafish. The high-magnification view of the rectangle in the bottom right corner shows the polymorphous vacuoles and a large vacuole with straight membrane border segments (straight line); magnification 3000X. (G-H) Representative images of the glomerulus of control (G) and *ctns* mutant (H) zebrafish; magnification 15,000X. PB: proximal tubule brush border; ctr: control zebrafish, *ctns*-: *ctns* mutant zebrafish.

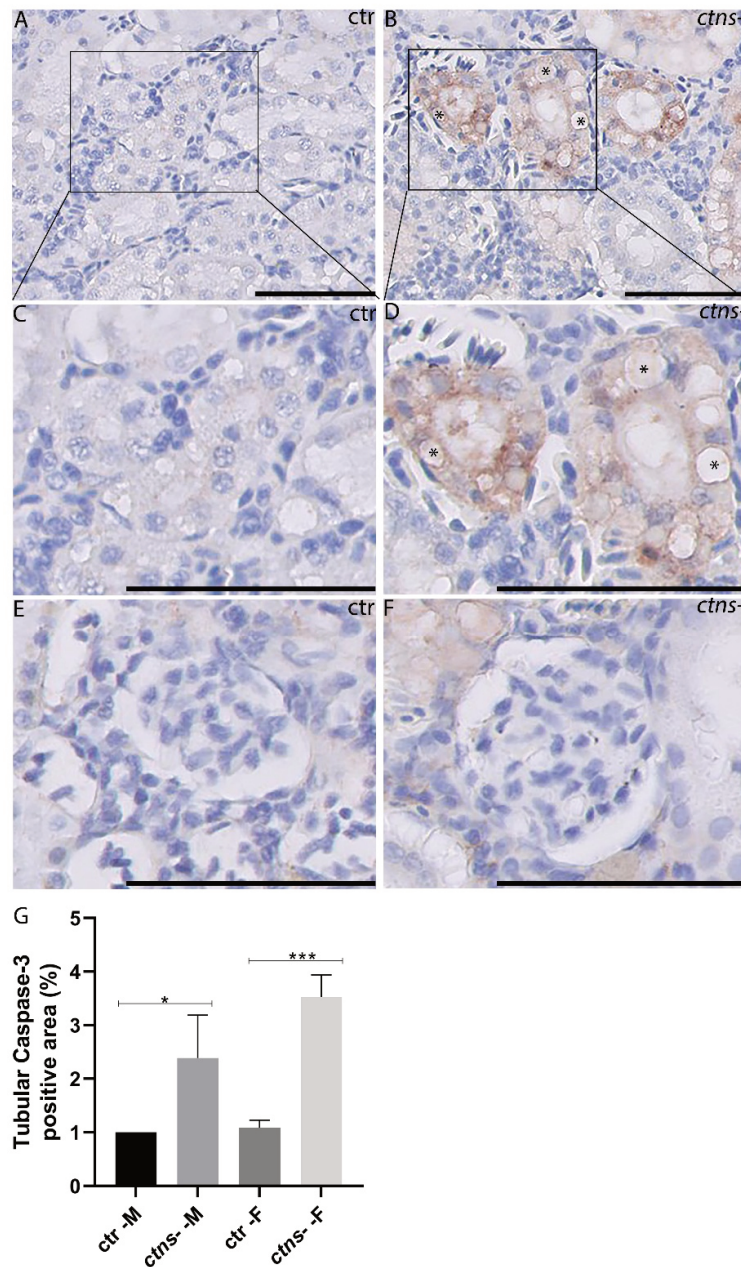


**Figure 4. Apoptosis takes place in proximal tubular cells with vacuoles in *ctns* mutant zebrafish at 18 months**

(A-B) Representative images of the cleaved caspase-3 immunostaining of tubules of control (A) and *ctns* mutant (B) zebrafish. The scale bars represent 50 $\mu$ m. (C-D) The bottom panels show a higher magnification of the boxed areas in the upper panels. Details of proximal tubular cells with cytoplasmic vacuoles (\*); the scale bars represent 50 $\mu$ m. (E-F) Representative images of the cleaved caspase-3 immunostaining of glomerulus of control (E) and *ctns* mutant (F) zebrafish. The scale bars represent 50 $\mu$ m. (G) The summary of the tubular caspase-3 staining positive area in control and *ctns* mutant zebrafish (both female and male). (\* $P$  < 0.05, \*\*\* $P$  < 0.001). ctr: control zebrafish, *ctns* -: *ctns* mutant zebrafish, M: male, F: female.

## Discussion

In the current study, the renal histopathology of *ctns* mutant zebrafish at the adult stage was investigated. We found numerous hyaline-like eosinophilic droplets, cytoplasmic vacuoles, and partial loss of brush borders in the proximal tubules of *ctns* mutant female and male zebrafish. We observed that the cytoplasmic vacuoles were in rectangular or polymorphous shape, indicating cystine crystals accumulation. We also found that *ctns* mutant male zebrafish developed glomerular hypertrophy. Lastly, we showed that cleaved-caspase 3 expression was significantly increased in the renal proximal tubular epithelial cells of *ctns* mutant female and male zebrafish, compared with controls, indicating that apoptosis is involved in the pathogenesis of nephropathic cystinosis in zebrafish.

Lysosomes are the sites of intracellular digestion that facilitate the degradation of foreign materials, and they are considered as the vital metabolic coordinators of cells<sup>18</sup>. Being a lysosomal storage disease, the key feature of cystinosis is the lysosomal cystine accumulation<sup>12,19</sup>. Previously, lysosomal swelling and hyaline-like eosinophilic droplets inside the lysosomes has been reported in cystine-loaded proximal tubules<sup>20,21</sup>. In the current study, the accumulation of hyaline-like eosinophilic droplets and cytoplasmic vacuoles in the proximal tubules was found in the *ctns* mutant zebrafish indicative for cystine accumulation and has been further confirmed by toluidine blue staining and electron microscopy.

In the human biopsies, cystine crystals are seen as clear spaces within interstitial macrophages and tubular epithelial cytoplasm<sup>17</sup>. Interestingly, in our previous study, cystine crystals were not detected in the *ctns* mutant zebrafish at the larval stage<sup>16</sup>. We suppose that tissue cystine crystallization is a cumulative process that needs time to develop. In the current study, we observed fewer cytoplasmic vacuoles in the renal proximal tubules at 3 months old *ctns* mutant zebrafish than at 18 months when the fish showed abundant cytoplasmic vacuoles having a rectangular or polymorphous shape in the renal proximal tubules. These findings are consistent with our previous study, which reported that 8 months old *ctns* mutant adult zebrafish had a 20-fold increase of cystine expression in the kidney than that of age-matched control zebrafish<sup>16</sup>. Aside from the cystine crystals accumulation in the lysosomes of the renal proximal tubules, multinucleated glomerular epithelial cells (particularly podocytes) and "swan neck" atrophy of tubular cells are the histopathological hallmarks of human renal disease in cystinosis<sup>17</sup>. However, in fish, we neither observe the multinucleated podocytes or the 'swan neck' deformity of the proximal tubules.

To assess the histological changes of the glomeruli of *ctns* mutant zebrafish, we measured the surface areas of Bowman's capsule, the glomerular tuft, and Bowman's space of *ctns* mutant

zebrafish on routine PAS-stained sections. We found that *ctns* mutant male zebrafish developed glomerular hypertrophy, which possibly related to hyperfiltration. However, no thickening of the glomerular basement membrane, podocytes foot process effacement, and abnormal fenestrated endothelial cells were found in the *ctns* mutant zebrafish of both genders. It has been well known that zebrafish has a unique ability to regenerate injured kidney<sup>22</sup>, which might explain only mild glomerular damage. Taken together, we conclude that the primary renal lesion in *ctns* mutant zebrafish is the severe proximal tubulopathy.

Consistently with the previous study<sup>16</sup>, we also observed a significantly increased cleaved caspase-3 expression and nuclear fragmentation in the proximal tubular epithelial cells of *ctns* mutant zebrafish. The expression of cleaved caspase-3 was mainly present in cells showing the cytoplasmic vacuoles, indicating that apoptosis takes place in the injured proximal tubules. It has been reported that lysosomal cystine release could activate protein kinase C $\delta$ , resulting in stimulation of apoptosis in cultured renal proximal tubular epithelial cells<sup>23</sup>. Sumayao et al. demonstrated that excessive lysosomal cystine accumulation reduced glutathione levels which elevated intracellular reactive oxygen species production, and then disrupted the mitochondrial integrity and augmented apoptosis in the renal proximal tubular epithelial cells<sup>6</sup>. Due to the shortage of the materials, we could not investigate the precise mechanisms leading to apoptosis in these zebrafish, which should be further elucidated.

Nephropathic cystinosis, if untreated, will gradually progress to chronic renal failure. Aminoethiol cysteamine is a standard therapy for cystinosis<sup>24</sup>. It can enter into the lysosomes and split the cystine molecule into cysteine and a cysteamine-cysteine mixed disulfide which can exit lysosomes bypassing the defective cystinosin. Cysteamine can prevent cystine accumulation and delays the disease's progression but cannot correct renal Fanconi syndrome<sup>24,25</sup>. As a lifelong treatment, cysteamine also has undesirable side effects. From this perspective, suitable animal models to test novel potential therapies are urgently needed. Our previous study demonstrated that *ctns* mutant larvae showed a significant decrease in cystine levels upon treatment with increasing concentrations of cysteamine<sup>16</sup>. In an experimental setting using zebrafish, drugs can be easily put into the water for testing the oral administration route. Hence, the *ctns* mutant zebrafish is a suitable and valuable animal model for exploring the pathogenesis and therapeutic strategies in cystinosis.

### Acknowledgements

The first author, J. He was supported by the China Scholarship Council (CSC). We would like to thank Peter Neeskens for the technical support of transmission electron microscopy (TEM).

## References

- 1 Town, M. *et al.* A novel gene encoding an integral membrane protein is mutated in nephropathic cystinosis. *Nat Genet* **18**, 319-324, doi:10.1038/ng0498-319 (1998).
- 2 Touchman, J. W. *et al.* The genomic region encompassing the nephropathic cystinosis gene (CTNS): complete sequencing of a 200-kb segment and discovery of a novel gene within the common cystinosis-causing deletion. *Genome Res* **10**, 165-173, doi:10.1101/gr.10.2.165 (2000).
- 3 Cherqui, S. & Courtoy, P. J. The renal Fanconi syndrome in cystinosis: pathogenic insights and therapeutic perspectives. *Nat Rev Nephrol* **13**, 115-131, doi:10.1038/nrneph.2016.182 (2017).
- 4 Prencipe, G. *et al.* Inflammasome activation by cystine crystals: implications for the pathogenesis of cystinosis. *J Am Soc Nephrol* **25**, 1163-1169, doi:10.1681/ASN.2013060653 (2014).
- 5 Galarreta, C. I. *et al.* The swan-neck lesion: proximal tubular adaptation to oxidative stress in nephropathic cystinosis. *Am J Physiol Renal Physiol* **308**, F1155-1166, doi:10.1152/ajprenal.00591.2014 (2015).
- 6 Sumayao, R., McEvoy, B., Newsholme, P. & McMorro, T. Lysosomal cystine accumulation promotes mitochondrial depolarization and induction of redox-sensitive genes in human kidney proximal tubular cells. *J Physiol* **594**, 3353-3370, doi:10.1113/JP271858 (2016).
- 7 Ivanova, E. A. *et al.* Altered mTOR signalling in nephropathic cystinosis. *J Inherit Metab Dis* **39**, 457-464, doi:10.1007/s10545-016-9919-z (2016).
- 8 Sansanwal, P. & Sarwal, M. M. Abnormal mitochondrial autophagy in nephropathic cystinosis. *Autophagy* **6**, 971-973, doi:10.4161/auto.6.7.13099 (2010).
- 9 Sansanwal, P. *et al.* Mitochondrial autophagy promotes cellular injury in nephropathic cystinosis. *J Am Soc Nephrol* **21**, 272-283, doi:10.1681/ASN.2009040383 (2010).
- 10 Taranta, A. *et al.* Cystinosin-LKG rescues cystine accumulation and decreases apoptosis rate in cystinotic proximal tubular epithelial cells. *Pediatr Res* **81**, 113-119, doi:10.1038/pr.2016.184 (2017).
- 11 Park, M., Helip-Wooley, A. & Thoene, J. Lysosomal cystine storage augments apoptosis in cultured human fibroblasts and renal tubular epithelial cells. *J Am Soc Nephrol* **13**, 2878-2887, doi:10.1097/01.asn.0000036867.49866.59 (2002).
- 12 Cherqui, S. *et al.* Intralysosomal cystine accumulation in mice lacking cystinosin, the protein defective in cystinosis. *Mol Cell Biol* **22**, 7622-7632, doi:10.1128/mcb.22.21.7622-7632.2002 (2002).
- 13 Nevo, N. *et al.* Renal phenotype of the cystinosis mouse model is dependent upon genetic background. *Nephrol Dial Transplant* **25**, 1059-1066, doi:10.1093/ndt/gfp553 (2010).
- 14 Shimizu, Y. *et al.* A deletion in the Ctns gene causes renal tubular dysfunction and cystine accumulation in LEA/Tohm rats. *Mamm Genome* **30**, 23-33, doi:10.1007/s00335-018-9790-3 (2019).
- 15 Dooley, K. & Zon, L. I. Zebrafish: a model system for the study of human disease. *Curr Opin Genet Dev* **10**, 252-256, doi:10.1016/s0959-437x(00)00074-5 (2000).
- 16 Elmonem, M. A. *et al.* Cystinosis (ctns) zebrafish mutant shows pronephric glomerular and tubular dysfunction. *Sci Rep* **7**, 42583, doi:10.1038/srep42583 (2017).
- 17 Lusco, M. A., Najafian, B., Alpers, C. E. & Fogo, A. B. AJKD Atlas of Renal Pathology: Cystinosis. *Am J Kidney Dis* **70**, e23-e24, doi:10.1053/j.ajkd.2017.10.002 (2017).
- 18 Saftig, P. & Klumperman, J. Lysosome biogenesis and lysosomal membrane proteins: trafficking meets function. *Nat Rev Mol Cell Biol* **10**, 623-635, doi:10.1038/nrm2745 (2009).
- 19 Raggi, C. *et al.* Dedifferentiation and aberrations of the endolysosomal compartment characterize the early stage of nephropathic cystinosis. *Hum Mol Genet* **23**, 2266-2278, doi:10.1093/hmg/ddt617 (2014).
- 20 Hard, G. C. Some aids to histological recognition of hyaline droplet nephropathy in ninety-day toxicity studies. *Toxicol Pathol* **36**, 1014-1017, doi:10.1177/0192623308327413 (2008).
- 21 Sakarcn, A., Timmons, C. & Baum, M. Intracellular distribution of cystine in cystine-loaded proximal tubules. *Pediatr Res* **35**, 447-450 (1994).

- 22 Kroeger, P. T., Jr. & Wingert, R. A. Using zebrafish to study podocyte genesis during kidney development and regeneration. *Genesis* **52**, 771-792, doi:10.1002/dvg.22798 (2014).
- 23 Park, M. A., Pejovic, V., Kerisit, K. G., Junius, S. & Thoene, J. G. Increased apoptosis in cystinotic fibroblasts and renal proximal tubule epithelial cells results from cysteinylolation of protein kinase Cdelta. *J Am Soc Nephrol* **17**, 3167-3175, doi:10.1681/ASN.2006050474 (2006).
- 24 Brodin-Sartorius, A. *et al.* Cysteamine therapy delays the progression of nephropathic cystinosis in late adolescents and adults. *Kidney Int* **81**, 179-189, doi:10.1038/ki.2011.277 (2012).
- 25 Gahl, W. A., Balog, J. Z. & Kleta, R. Nephropathic cystinosis in adults: natural history and effects of oral cysteamine therapy. *Ann Intern Med* **147**, 242-250, doi:10.7326/0003-4819-147-4-200708210-00006 (2007).





# Chapter 6

## Summary and General Discussion



In 2017, there were almost 700 million cases of chronic kidney disease worldwide <sup>1,2</sup>. Chronic kidney disease resulted in 1.2 million deaths in 2017, and it has been projected to rise to 2.2 million or might even up to 4.0 million by 2040 <sup>3</sup>. Diabetes is a major risk factor associated with chronic kidney disease, and it contributes to 30-50% of all chronic kidney diseases <sup>4</sup>. The global prevalence of diabetes is also rising <sup>5</sup>, with a concomitant increase in diabetic nephropathy. The global epidemiology of diabetic nephropathy will result in severe social and economic ramifications if treatments are not improved. Currently, glycemic control is still the primary therapy for patients diagnosed with diabetes. However, this treatment does not reduce the risk of the clinical renal outcome of diabetic nephropathy <sup>6</sup>. Therefore, to address this worldwide epidemic issue, it is crucial to understand the underlying mechanisms of the development of diabetic nephropathy and to find novel preventative and therapeutic strategies.

### ***Diabetic nephropathy***

Oxidative stress results from the overproduction of reactive oxygen species in excess of the cell's antioxidant response <sup>7</sup>. This stress can damage all cell components, including DNA, proteins, and lipids <sup>8,9</sup>. For adaptation to oxidative stress, cells contain a bunch of antioxidant defences to protect them against reactive oxygen species. The sustained oxidative stress-mediated injury can lead to cellular apoptosis. It has been hypothesized that all mechanisms of diabetic complications are activated by one upstream event: the overproduction of reactive oxygen species <sup>10</sup>. The kidney is a highly metabolic organ, and it is vulnerable to oxidative stress. Growing evidence supports that increased oxidative stress may contribute to the development of diabetic nephropathy <sup>11-13</sup>. Nowadays, intensive glucose control, anti-lipid, and anti-hypertensive agents are used as treatments for patients with diabetic nephropathy. Since oxidative stress contributes to the pathogenesis of diabetic nephropathy, the availability of an effective and target-specific antioxidant agent is highly desirable <sup>14</sup>.

### ***Clusterin (CLU) has protective properties in diabetic nephropathy***

A large body of evidence has shown that the *CLU* gene is an extremely sensitive biosensor to reactive oxygen species. It has a heat shock transcription factor-1 and an activator protein-1 element in its promoter sequence <sup>15</sup>. In **Chapter 2**, we demonstrated that, oxidative stress is the primary factor to induce *CLU* mRNA expression in podocytes under diabetic conditions. We also showed that recombinant clusterin protein could protect the podocytes against

oxidative stress-induced apoptotic cell death *in vitro*. This finding suggests that clusterin's antioxidant property might make clusterin a potential therapeutic agent to protect podocytes under oxidative stress. It has been reported that exogenous clusterin inhibits H<sub>2</sub>O<sub>2</sub>-induced reactive oxygen species generation and suppresses caspase-3 activity in the retinal pigment epithelium cells, and enhances the survival of cells mediated by the PI3K/Akt pathway <sup>16</sup>. Jun et al. demonstrated that the exogenous clusterin could protect cardiomyocytes against H<sub>2</sub>O<sub>2</sub>-induced oxidative injury via activating Akt/GSK-3 $\beta$  signaling pathway <sup>17</sup>. In accordance with these studies, we hypothesized that clusterin protects podocytes against oxidative stress-induced apoptosis by activating the Akt survival pathways. The detailed underlying molecular mechanisms of how clusterin protects podocytes against oxidative stress-induced apoptotic cell death need further elaboration. *In vivo* studies are required to confirm our hypothesis that clusterin may slow or even halt the progression of diabetic nephropathy.

Väkevä and colleagues reported that clusterin started to be deposited in affected regions of the heart soon after the onset of myocardial infarction. And clusterin binds to the components of the membrane attack complex and prevents the lysis of the cell <sup>18</sup>. In human kidney diseases, clusterin deposition was also found in association with glomerular membrane attack complex (MAC) formation in glomerulonephritis <sup>19</sup>. In a passive Heymann nephritis experimental model, clusterin deposits were detected along the glomerular capillary wall with an identical pattern to rat C5B-9. And clusterin's deposition was not observed in complement-depleted animals <sup>20</sup>. Rosenberg et al. demonstrated that ageing clusterin-deficient mice developed immune complex deposits in the mesangium, and moderate to severe mesangial lesions were found in these clusterin-deficient mice, while age-matched wild type controls have relatively few or no glomerular lesions <sup>21</sup>. A study by Bus et al. <sup>22</sup> and a review by Flyvbjerg et al. <sup>23</sup> suggest that complement activation contributes to the pathogenesis of diabetic nephropathy. Rastaldi et al. <sup>24</sup> demonstrated that recombinant clusterin protein can bind the podocytes via LDL receptor and suggested that binding of clusterin to the podocyte surface can prevent PKC activation by complement components. In **Chapter 2**, we showed that CLU expression was increased in micro-dissected glomeruli of patients with diabetic nephropathy compared to healthy subjects at both mRNA and protein levels. Therefore, we hypothesize that increased glomerular clusterin might also protect podocytes against complement activation in diabetic nephropathy. Therefore, an intriguing direction for future research is to investigate whether clusterin may offer protection by modulating complement activation in diabetic nephropathy.

### ***The role of carnosinase-1 (CNDP1) overexpression in the progression of diabetic nephropathy***

Carnosine is a natural antioxidant <sup>25</sup>, which has been suggested to protect against diabetic nephropathy in diverse rodent models <sup>26-29</sup>. It has been shown under diabetic conditions that carnosinase-1 (CNDP1, also called CN1) overexpression lowers carnosine concentrations. Compared to non-transgenic *db/db* mice, humanCN1 (hCN1) transgenic *db/db* mice with carnosinase-1 overexpression had lower carnosine serum concentrations, more severe impaired renal function, and significant renal hypertrophy <sup>30</sup>. In **Chapter 3**, our findings also support the evidence that hCN1 overexpression results in lower renal carnosine and anserine storage and aggravates the development of diabetic nephropathy in BTBR *ob/ob* mice <sup>31</sup>. We detected an increase of glomerular hypertrophy and more mesangial matrix expansion in hCN1 transgenic BTBR *ob/ob* mice compared to non-transgenic BTBR *ob/ob* mice. Furthermore, we showed that the decline in renal carnosine and anserine levels correlate with different markers of diabetic nephropathy. These findings jointly suggested that low renal carnosine and anserine concentrations can aggravate the pathogenesis of diabetic nephropathy. In future studies, a direct comparison between the effect of hCN1 overexpression and carnosine supplementation on both renal carnosine and anserine levels and diabetic nephropathy need to be considered. Meanwhile, high CNDP1 enzyme activity in human serum can degrade carnosine, which hampers the efficacy of carnosine treatment in humans. Therefore, novel treatments should be investigated to address the adverse effects of the CNDP1 enzyme on carnosine supplementation.

Exercise could increase resting muscle carnosine levels <sup>32</sup>. A higher carnosine content in the circulation was also found in animals after physically activity <sup>33,34</sup>. Researchers have shown that aerobic treadmill training has a beneficial effect on nephropathy in a high-fat <sup>35,36</sup> or streptozotocin-induced <sup>37</sup> diabetic rat model and in *db/db* mice <sup>38,39</sup>. One hypothesis is that the induced muscle contractile activity by the exercise training can release carnosine and/or anserine from muscular storage into the circulation. The increased circulating carnosine and/or anserine levels subsequently reduces the progression of diabetic nephropathy. In contrast to previous studies, in **Chapter 3**, we did not find any significant protective effect of 20 weeks of chronic exercise training on the progression of diabetic nephropathy in these BTBR *ob/ob* mice in both genders. However, in other studies <sup>35-39</sup>, animal models with milder renal damage were used in combination with 5 to 12 weeks of aerobic treadmill running as interventions. It has been shown in the literature that the BTBR *ob/ob* mice develop advanced diabetic nephropathy <sup>31</sup>. In **Chapter 3**, we kept all the BTBR *ob/ob* mice running for 20

weeks. We found that these BTBR *ob/ob* mice had very high glucose levels already, which possibly lead to severe ketoacidosis, lower exercise tolerance or dehydration during the chronic aerobic exercise training. Our data indicate that chronic aerobic exercise alone may not be sufficient to reverse the observed severe histological changes in BTBR *ob/ob* mice.

Another interesting finding in **Chapter 3** is that hCN1-overexpression BTBR *ob/ob* mice had higher fasting cholesterol and triglycerides at week 14. This finding indicated that hCN1 overexpression stimulates hyperlipidemia in diabetic mice and suggested an adverse effect of the carnosinase-1 enzyme on dyslipidemia. Studies have shown that long-term carnosine supplementation could improve dyslipidemia in different diabetes rodent models<sup>27,40,41</sup> and diabetic patients<sup>42</sup>. Barski et al. found that carnosine can inhibit low-density lipoprotein (LDL) oxidation by chelating copper<sup>43</sup>. As the underlying mechanism of carnosine's anti-hyperlipidemic effect remains unknown, future studies using lipidomic and proteomics approaches might help us to unravel the role of carnosine in lipid metabolism.

### ***Novel zebrafish models for chronic kidney diseases***

To understand the pathogenesis of human disease and provide systems for testing novel therapeutics and developing effective treatments, animal models are an indispensable part of biomedical research. Recently, zebrafish have become an attractive model to study developmental biology, genetics and human diseases<sup>44-46</sup>.

### ***The role of leptin in the development of diabetes and diabetic nephropathy***

Leptin is a hormone that functions in the regulation of energy homeostasis via suppression of appetite. Rodents lacking the *leptin* gene are commonly characterized by hyperphagia, obesity, insulin resistance and impaired glucose tolerance. For instance, leptin-deficient mice (*ob/ob* mice) exhibit the features of obesity and type 2 Diabetic Mellitus (T2DM)<sup>47</sup>. In **Chapter 4**, we found that *lepb*<sup>-/-</sup> adult zebrafish have an obese phenotype compared to the age-matched controls. We also demonstrated that, compared to control male adult zebrafish, *lepb*<sup>-/-</sup> male adult zebrafish have higher blood glucose, suggesting the leptin signaling regulates glucose homeostasis in zebrafish as well. A growing number of publications provide evidence that leptin has a glucose-lowering effect. Kamohara et al. showed that infusion of leptin into the brain could normalize the hyperglycemia in *ob/ob* mice<sup>48</sup>. It has been reported that leptin acts on glucose metabolism in both insulin-dependent and insulin-independent ways. Leptin can improve insulin sensitivity<sup>49,50</sup>. Reduced leptin in the mediobasal

hypothalamus leads to severe insulin resistance and glucose intolerance in Koletsky rats, and phosphatidylinositol-3-OH kinase signaling is a vital mediator of this effect in the hypothalamus <sup>51</sup>. Leptin can reverse hyperglycemia and ketosis by suppressing the action of glucagon on the liver and improving the utilization of glucose in the skeletal muscle in insulin-deficient diabetic rodents <sup>52</sup>. Our laboratory's earlier work demonstrated that *lepb* was significantly downregulated in zebrafish larvae in an insulin-resistant state <sup>53</sup>. Combining the previous study and the findings in **Chapter 4**, we propose that the diabetic phenotype of *lepb* mutants is caused by disruption of the insulin signaling pathway. We are currently performing transcriptomic analysis of *lepb*<sup>+/+</sup> and *lepb*<sup>-/-</sup> zebrafish larvae, which might give us new insights into the role of leptin in the insulin signaling pathway.

The initial aim of the study described in **Chapter 4** was to investigate whether *lepb*<sup>-/-</sup> adult zebrafish develop the features of diabetes and diabetic nephropathy. It is known that patients often develop diabetic nephropathy after a long period of diabetes (10~20 years) <sup>54</sup>, and leptin-deficient mice develop only mild renal histological changes <sup>55</sup>. The mean lifespan of domesticated zebrafish is 42 months <sup>56</sup>. We therefore decided to investigate zebrafish at the age of 1.5 years, which is relatively old for this species. Our data indicate that 1.5 years old *lepb*<sup>-/-</sup> male zebrafish develop early signs of diabetic nephropathy. We assume that it might be more challenging to observe the kidney phenotype in younger fish regarding our findings in **Chapter 4**. Nevertheless, it is still interesting to look at earlier time points to further investigate the progression of these early signs of diabetic nephropathy in future studies. To accelerate or aggravate kidney damage, conducting other interventions in *lepb*<sup>-/-</sup> zebrafish can be considered, for instance, by combining the leptin mutation with other gene mutations associated with the development of diabetic nephropathy or by overfeeding these zebrafish.

Anti-diabetic drugs which are effective for diabetic patients have been shown to ameliorate the hyperglycemia in overfed zebrafish, suggesting that the glucose homeostasis pathways are conserved between zebrafish and human <sup>57</sup>. In an experimental setting using zebrafish, potential anti-diabetic compounds to be tested can be easily put into the water for oral administration or be injected into embryos by using a robotic injection machine <sup>58</sup>. Screening efficient anti-diabetic drugs in zebrafish larvae have a high-throughput potential.

### ***Ctns* mutant adult zebrafish resembles the phenotype of human nephropathic cystinosis**

Cystinosis is a rare lysosomal storage disorder. Our group generated *ctns* mutant zebrafish, which showed retarded development, cystine accumulation, and the signs of pronephric glomerular and tubular dysfunction at the larval stage <sup>59</sup>. Lysosomes are the sites of

intracellular digestion. They facilitate the degradation of foreign materials, and they are considered the vital metabolic coordinators of cells <sup>60</sup>. Sakarcı et al. observed notable swelling of lysosomes with numerous cytoplasmic vesicles in the cystine-loaded proximal tubule cells <sup>61</sup>. The hyaline-like eosinophilic droplets in the proximal tubules are suggested to represent lysosome <sup>62</sup>. Being a lysosomal storage disease, the key feature of cystinosis is the lysosomal cystine accumulation <sup>63,64</sup>. In **Chapter 5**, we observed that the cytoplasmic vacuoles are more frequently localized in the renal proximal tubular cells at 18 months old *ctns* mutant adult zebrafish than at 3 months and 6 months. Moreover, abundant cytoplasmic vacuoles were found with rectangular or polymorphous shape in the renal proximal tubules, suggesting cystine crystals' accumulation. Until now, the underlying mechanisms of how cysteine accumulation leads to nephropathic cystinosis are still unknown. In **Chapter 5**, the upregulation of cleaved-caspase 3 expression and nuclear fragmentation were found in the proximal tubular epithelial cells of *ctns* mutant adult zebrafish. It has been reported that lysosomal cystine release can activate protein kinase C $\delta$ , resulting in a significant increase in apoptosis in cultured renal proximal tubular epithelial cells <sup>65</sup>. Sumayao et al. demonstrated that excessive lysosomal cystine accumulation reduced glutathione levels and enhanced intracellular reactive oxygen species production, which subsequently disrupted the mitochondrial integrity and augmented apoptosis in the renal proximal tubular epithelial cells <sup>66</sup>. The next step of research aims to unravel the precise mechanisms leading to apoptosis which could not be elucidated in **Chapter 5** due to materials limitation.

Nephropathic cystinosis, if untreated, will gradually progress to chronic renal failure. The administration of aminothiols cysteamine is the standard therapy for cystinosis <sup>67</sup>. Cysteamine also has undesirable side effects when it has to be taken lifelong. From this perspective, suitable animal models to test novel potential drugs could be useful. Our previous study demonstrated that *ctns* mutant zebrafish larvae showed a significant decrease in cystine levels upon treatment with increasing cysteamine concentrations <sup>59</sup>. It will be advantageous to use zebrafish larvae to screen potential drugs, followed by studying the curative effect in adult zebrafish in preclinical research.

As mentioned before, a defective cystinosis function results in the intralysosomal accumulation of cystine in all cells. Aside from the kidneys, also eyes, muscles, skin, and reproductive organs are affected in the course of cystinosis. Currently, we are investigating other organs in our zebrafish model to unravel this rare disease.

## Summary

It has been reported that diabetic nephropathy occurs in the familial clusters, suggesting a genetic predisposition in diabetic nephropathy <sup>68,69</sup>. The advantage of studies of genetic predisposition is that it is free of preconceived hypotheses. These studies have offered robust tools to analyze the pathogenesis of this disease which has also been shown to have complex traits. In the studies described in **Chapter 2** and **Chapter 3** of this thesis, we investigated the role of *CLU* and *CNDP1* in the development of diabetic nephropathy.

Several studies have shown that clusterin may have renal protective properties in various forms of kidney disease <sup>21,70-72</sup>. Microarray analysis revealed that *CLU* mRNA expression is increased in the glomeruli of patients with diabetic nephropathy compared to healthy subjects <sup>73</sup>. In the study described in **Chapter 2**, we investigated the role of glomerular clusterin in diabetic nephropathy. We first confirmed that clusterin expression was increased in glomeruli of patients with diabetic nephropathy both at the mRNA and protein levels in human biopsies. Furthermore, the immunohistochemical staining on both human and mice renal tissue revealed that glomerular clusterin is expressed in podocytes. In the *in vitro* experiments, we found that oxidative stress, not high glucose or angiotensin II, upregulates clusterin mRNA expression in podocytes, suggesting oxidative stress is an important factor that induces *CLU* mRNA expression under diabetic conditions. Lastly, we showed that recombinant clusterin protein enhances cell viability, reduces the elevated *Bax/Bcl2* mRNA ratio, and reduces the enhanced caspase 3/7 activity in podocytes under oxidative stress-induced damage *in vitro*. These findings indicate that clusterin can protect podocytes against oxidative stress-induced apoptotic cell death.

It has been shown that a polymorphism of the *CNDP1* gene strongly associates with the prevalence of diabetic nephropathy <sup>74,75</sup>. The *CNDP1* gene encodes for an enzyme that degrades carnosine, a dipeptide with multiple protective properties <sup>25,27,76</sup>. In humans, this enzyme is secreted by the liver into circulation. Carnosinase is present in human serum but not in that of rodents <sup>77,78</sup>. Compared to non-transgenic *db/db* mice, hCN1transgenic *db/db* mice had high CNDP1 serum levels resulting in low carnosine serum concentrations, a more severe impaired renal function, and significant renal hypertrophy <sup>30</sup>. Exercise increases circulating carnosine levels <sup>32</sup>. Besides, prolonged aerobic exercise prevents diabetic nephropathy in different rodent models <sup>79-82</sup>. In the study described in **Chapter 3**, we investigated the effect of two interventions, overexpressing the human carnosinase-1 enzyme and chronic aerobic exercise training, on the development of diabetic nephropathy in BTBR



*ob/ob* mice. Our study revealed that hCN1 overexpression further reduced the content of histidine-containing dipeptides (carnosine and anserine) in urine, kidney and gastrocnemius muscle, and significantly accelerated and aggravated diabetic nephropathy in BTBR *ob/ob* mice. Furthermore, we found that the amount of renal histidine-containing dipeptides was negatively correlated with mesangial matrix expansion and glomerular hypertrophy. We showed that hCN1-overexpression BTBR *ob/ob* mice had higher fasting cholesterol and triglycerides at week 14, indicating that hCN1 overexpression contributes to faster development of hyperlipidemia in diabetic mice. In contrast with previous studies<sup>79,80</sup>, we did not find a protective effect of chronic exercise training on the progression of diabetic nephropathy. Our data suggest that the amount of renal histidine-containing dipeptides correlates inversely with the severity of diabetic nephropathy.

In recent decades, zebrafish have become an attractive model for studying developmental biology, genetics and human diseases<sup>44-46</sup>. In the studies described in **Chapter 4** and **Chapter 5** of this thesis, we investigated whether two novel zebrafish models could resemble the pathologic features of human chronic kidney disease.

In humans, patients lacking leptin have evident obesity and glucose tolerance impairments, the hallmarks of type 2 diabetes<sup>83,84</sup>. The congenital leptin-deficient (*ob/ob* mutant) mice<sup>85,86</sup> or leptin receptor-deficient (*db/db* mutant) mice<sup>87</sup> are the most widely used animal models in type 2 diabetes mellitus (T2DM) research. It has been reported that the basic structural features and intracellular signaling mechanisms of leptin and its receptor are conserved throughout vertebrates<sup>88-91</sup>. In a previous study, our group found that the *lepb* gene, but not the paralogous *lepa* gene, is significantly downregulated in zebrafish larvae under an insulin-resistance state, resulting from acute hyperinsulinemia<sup>53</sup>. Moreover, this finding indicated that *lepb* plays a vital role in insulin homeostasis in zebrafish. In the study described in **Chapter 4**, we investigated whether *lepb* deficiency results in the development of T2DM in adult zebrafish. We found that *lepb*<sup>-/-</sup> adult zebrafish have an increment in body weight and length compared to the age-matched control adult zebrafish. In addition, the quantification of magnetic resonance anatomical imaging (MRI) data showed a significant increase of visceral fat accumulation in *lepb*<sup>-/-</sup> adult zebrafish, compared to control adult zebrafish, in both genders. The increased body weight and length and body fat composition jointly indicate that *lepb*<sup>-/-</sup> adult zebrafish have an obese phenotype. Furthermore, we found that 2 hours postprandial blood glucose levels and fasting blood glucose levels in *lepb*<sup>-/-</sup> male zebrafish group were significantly higher compared to control male zebrafish group. However, we did not find this difference in the female group. Lastly, we observed that *lepb*<sup>-/-</sup> male zebrafish

develop glomerular hypertrophy and thickening of the glomerular basement membrane, indicating that *lepb*<sup>-/-</sup> adult zebrafish have the early signs of diabetic nephropathy.

Cystinosis is a lysosomal storage disease caused by several mutations of the *CTNS* gene encoding cystinosin. Most patients with cystinosis have kidney disease (nephropathic cystinosis), which is the most common cause of inherited renal Fanconi syndrome in humans<sup>92</sup>. Nephropathic cystinosis will eventually develop chronic renal failure when left untreated. In our previous study, we generated a *ctns* mutant zebrafish that displayed glomerular and tubular dysfunction at the larval stage. We also found that cystine expression level in the kidney of eight months old *ctns* mutant adult zebrafish was 20-fold higher than that of age-matched control zebrafish<sup>59</sup>. In the study described in **Chapter 5**, we further investigated the renal histopathology of *ctns* mutant adult zebrafish. We observed cytoplasmic vacuoles and hyaline-like eosinophilic droplets in the renal proximal tubules in *ctns* mutant zebrafish in both genders. Additionally, we found that these vacuoles in the renal proximal tubular cells of *ctns* mutant adult zebrafish have a rectangular or polymorphous shape on toluidine blue-stained slides and the images captured by the transmission electron microscopy. These findings indicate that cystine crystals were present. We also showed that *ctns* mutant zebrafish had glomerular hypertrophy, which is possibly related to hyperfiltration. Lastly, we observed that *ctns* mutant adult zebrafish have increased levels of cleaved caspase-3 and increased nuclear fragmentation in the renal proximal tubular epithelial cells, compared to control zebrafish. This finding suggests that apoptosis is involved in the pathogenesis of cystinosis tubulopathy in zebrafish.

Summarized, in this thesis, two potential therapeutic targets for diabetic nephropathy were identified and investigated. First, we show that glomerular clusterin is upregulated in diabetic nephropathy and demonstrated that recombinant clusterin protein can protect the podocytes against oxidative stress *in vitro*. Second, we reveal that hCN1 overexpression accelerated and aggravated diabetic nephropathy in BTBR *ob/ob* mice. We also studied two novel zebrafish models to investigate chronic kidney disease. We showed that *lepb*<sup>-/-</sup> adult zebrafish have the early signs of human diabetic nephropathy, and we demonstrated that *ctns* mutant adult zebrafish have the kidney pathologic features of human nephropathic cystinosis.

## Future perspectives

The use of primary cells and cell lines (*in vitro* model systems) has advanced our understanding of the mechanisms of disease. However, it is impossible to interpret the intact organism's biology by only using *in vitro* cell cultures<sup>93</sup>. Comparative studies using murine models (*in vivo* model systems) can give a bigger picture. Rodents are pre-eminent in modelling human diseases because of the high similarity between mammalian genomes<sup>94</sup>. Rodents have many similarities with humans with respect to anatomy and physiology<sup>95</sup>. However, murine models are usually time-consuming and expensive. Therefore, zebrafish is becoming an attractive animal model due to many advantages<sup>96</sup>. They have high fecundity and rapid development. The externally fertilized eggs make them well amenable to rapid genetic manipulation techniques. The optical transparency of the larvae makes screening with different fluorescent labels straightforward. Their small size makes zebrafish embryos highly suitable for large scale and cost-effective screening strategies. Nowadays, most of the existing studies related to zebrafish have been conducted with larvae. On the other hand, adult zebrafish are more appropriate to investigate chronic kidney disease because it takes a long time to develop. Besides the advantages mentioned before, there are also some drawbacks in the zebrafish model to study chronic kidney disease. Due to the small size of zebrafish, it is not easy to obtain sufficient blood to perform various physiological and biochemical measurements on one sample. Furthermore, it is sometimes difficult to obtain suitable antibodies to perform immunohistochemistry and western blot techniques.

It is a well-known fact that proteinuria is an important indicator to evaluate the glomerular filtration barrier function. However, this cannot be directly measured in zebrafish. Two approaches have been established to address this issue. One way is to establish reabsorption of high-molecular-weight FITC-dextran by proximal tubules as an expression of the increased permeability of the glomerular filtration barrier in zebrafish<sup>97,98</sup>. Naturally, the intact glomerular filtration barrier prevents larger sized molecules from leaking out. For instance, 40kDa dextran passes freely through the intact glomerular filtration barrier, but 70KDa dextran cannot. However, the 70kDa dextran can leak out of the glomerular filtration barrier and be resorbed into the renal proximal tubules when the glomerular filtration barrier is damaged. Zhou et al. generated a transgenic zebrafish line expressing green fluorescent protein (GFP)-tagged vitamin D-binding protein (VDBP) as a tracer for proteinuria<sup>99</sup>. The VDBP has a similar size as albumin. Therefore, when the glomerular filtration barrier is damaged, GFP resorption droplets can be observed in the renal proximal tubules by

histological imaging or by measuring VDBP in the swimming water. Outcrossing the gene mutant zebrafish with VDBP-GFP transgenic zebrafish or injecting the high-molecular-weight FITC-dextran can be very useful to evaluate the function of the glomerular filtration barrier of mutant zebrafish.

As mentioned before, the possibility of screening on a large scale is a significant advantage of the zebrafish larval model. Because of the short generation time, data obtained in the larval model can be efficiently translated to the adult level and *vice versa*. In this thesis, we focused on investigating the histopathology of zebrafish. Next, making use of the technological advances in the zebrafish models will generate extensive “omics” data, including transcriptomic, metabolomic, and proteomic data, to further obtain additional insights to understand the mechanisms of chronic kidney disease. For instance, spatial transcriptomics, a promising novel technique, allows us to measure genome-wide gene expression and display its spatially resolved expression on the tissue section level. Spatial transcriptomics will remarkably increase the depth and breadth of histopathological research. In the future, we can use the mentioned techniques to analyze the function of a large number of genes or proteins with our generated zebrafish model to get a comprehensive view of mechanisms underlying chronic kidney disease.

Another advantage of zebrafish is that they have the ability to regenerate kidney tissue<sup>100</sup>, which cannot be found in mammals. In the future, it will be interesting to conduct comparative studies among patients, zebrafish, and mice to grab novel insights into renal regeneration and repair in chronic kidney disease. Although zebrafish are a valuable animal model for exploring the pathogenesis and therapy strategies for chronic kidney disease, they cannot fully replace cells culture techniques and murine models in fundamental research. Zebrafish models, embryos in particular, can fill the gap between the cell cultures and the highly organized murine models, especially in the light of drug screening or investigation of the gene functions. We believe that integrating the discoveries based on studies in cell cultures, zebrafish, and rodent models will deliver new biological insights that can drive the development of innovative treatments for chronic kidney diseases.

## References

- 1 Collaboration, G. B. D. C. K. D. Global, regional, and national burden of chronic kidney disease, 1990-2017: a systematic analysis for the Global Burden of Disease Study 2017. *Lancet* **395**, 709-733, doi:10.1016/S0140-6736(20)30045-3 (2020).
- 2 Disease, G. B. D., Injury, I. & Prevalence, C. Global, regional, and national incidence, prevalence, and years lived with disability for 354 diseases and injuries for 195 countries and territories, 1990-2017: a systematic analysis for the Global Burden of Disease Study 2017. *Lancet* **392**, 1789-1858, doi:10.1016/S0140-6736(18)32279-7 (2018).
- 3 Foreman, K. J. *et al.* Forecasting life expectancy, years of life lost, and all-cause and cause-specific mortality for 250 causes of death: reference and alternative scenarios for 2016-40 for 195 countries and territories. *Lancet* **392**, 2052-2090, doi:10.1016/S0140-6736(18)31694-5 (2018).
- 4 Jha, V., Wang, A. Y. & Wang, H. The impact of CKD identification in large countries: the burden of illness. *Nephrol Dial Transplant* **27 Suppl 3**, iii32-38, doi:10.1093/ndt/gfs113 (2012).
- 5 Saeedi, P. *et al.* Global and regional diabetes prevalence estimates for 2019 and projections for 2030 and 2045: Results from the International Diabetes Federation Diabetes Atlas, 9(th) edition. *Diabetes Res Clin Pract* **157**, 107843, doi:10.1016/j.diabres.2019.107843 (2019).
- 6 Coca, S. G., Ismail-Beigi, F., Haq, N., Krumholz, H. M. & Parikh, C. R. Role of intensive glucose control in development of renal end points in type 2 diabetes mellitus: systematic review and meta-analysis intensive glucose control in type 2 diabetes. *Arch Intern Med* **172**, 761-769, doi:10.1001/archinternmed.2011.2230 (2012).
- 7 Martindale, J. L. & Holbrook, N. J. Cellular response to oxidative stress: signaling for suicide and survival. *J Cell Physiol* **192**, 1-15, doi:10.1002/jcp.10119 (2002).
- 8 Cross, C. E. *et al.* Oxygen radicals and human disease. *Ann Intern Med* **107**, 526-545, doi:10.7326/0003-4819-107-4-526 (1987).
- 9 Droge, W. Free radicals in the physiological control of cell function. *Physiol Rev* **82**, 47-95, doi:10.1152/physrev.00018.2001 (2002).
- 10 Giacco, F. & Brownlee, M. Oxidative stress and diabetic complications. *Circ Res* **107**, 1058-1070, doi:10.1161/CIRCRESAHA.110.223545 (2010).
- 11 Suzuki, S. *et al.* Oxidative damage to mitochondrial DNA and its relationship to diabetic complications. *Diabetes Res Clin Pract* **45**, 161-168, doi:10.1016/s0168-8227(99)00046-7 (1999).
- 12 Mehrotra, S., Ling, K. L., Bekele, Y., Gerbino, E. & Earle, K. A. Lipid hydroperoxide and markers of renal disease susceptibility in African-Caribbean and Caucasian patients with Type 2 diabetes mellitus. *Diabet Med* **18**, 109-115, doi:10.1046/j.1464-5491.2001.00416.x (2001).
- 13 Calabrese, V. *et al.* Oxidative stress and cellular stress response in diabetic nephropathy. *Cell Stress Chaperones* **12**, 299-306, doi:10.1379/csc-270.1 (2007).
- 14 Singh, D. K., Winocour, P. & Farrington, K. Oxidative stress in early diabetic nephropathy: fueling the fire. *Nat Rev Endocrinol* **7**, 176-184, doi:10.1038/nrendo.2010.212 (2011).
- 15 Trougakos, I. P. & Gonos, E. S. Regulation of clusterin/apolipoprotein J, a functional homologue to the small heat shock proteins, by oxidative stress in ageing and age-related diseases. *Free Radic Res* **40**, 1324-1334, doi:10.1080/10715760600902310 (2006).
- 16 Kim, J. H. *et al.* Protective effect of clusterin from oxidative stress-induced apoptosis in human retinal pigment epithelial cells. *Invest Ophthalmol Vis Sci* **51**, 561-566, doi:10.1167/iovs.09-3774 (2010).
- 17 Jun, H. O. *et al.* Clusterin protects H9c2 cardiomyocytes from oxidative stress-induced apoptosis via Akt/GSK-3beta signaling pathway. *Exp Mol Med* **43**, 53-61, doi:10.3858/emmm.2011.43.1.006 (2011).
- 18 Vakeva, A., Laurila, P. & Meri, S. Co-deposition of clusterin with the complement membrane attack complex in myocardial infarction. *Immunology* **80**, 177-182 (1993).
- 19 Murphy, B. F., Kirszbaum, L., Walker, I. D. & d'Apice, A. J. SP-40,40, a newly identified normal human serum protein found in the SC5b-9 complex of complement and in the immune

- deposits in glomerulonephritis. *The Journal of clinical investigation* **81**, 1858-1864, doi:10.1172/JCI113531 (1988).
- 20 Eddy, A. A. & Fritz, I. B. Localization of clusterin in the epimembranous deposits of passive Heymann nephritis. *Kidney Int* **39**, 247-252, doi:10.1038/ki.1991.29 (1991).
- 21 Rosenberg, M. E. *et al.* Apolipoprotein J/clusterin prevents a progressive glomerulopathy of aging. *Mol Cell Biol* **22**, 1893-1902 (2002).
- 22 Bus, P. *et al.* Complement Activation in Patients With Diabetic Nephropathy. *Kidney Int Rep* **3**, 302-313, doi:10.1016/j.ekir.2017.10.005 (2018).
- 23 Flyvbjerg, A. The role of the complement system in diabetic nephropathy. *Nat Rev Nephrol* **13**, 311-318, doi:10.1038/nrneph.2017.31 (2017).
- 24 Rastaldi, M. P. *et al.* Glomerular clusterin is associated with PKC-alpha/beta regulation and good outcome of membranous glomerulonephritis in humans. *Kidney Int* **70**, 477-485, doi:10.1038/sj.ki.5001563 (2006).
- 25 Boldyrev, A. A., Stvolinsky, S. L., Fedorova, T. N. & Suslina, Z. A. Carnosine as a natural antioxidant and geroprotector: from molecular mechanisms to clinical trials. *Rejuvenation Res* **13**, 156-158, doi:10.1089/rej.2009.0923 (2010).
- 26 Albrecht, T. *et al.* Carnosine Attenuates the Development of both Type 2 Diabetes and Diabetic Nephropathy in BTBR ob/ob Mice. *Sci Rep* **7**, 44492, doi:10.1038/srep44492 (2017).
- 27 Aldini, G. *et al.* The carbonyl scavenger carnosine ameliorates dyslipidaemia and renal function in Zucker obese rats. *J Cell Mol Med* **15**, 1339-1354, doi:10.1111/j.1582-4934.2010.01101.x (2011).
- 28 Peters, V. *et al.* Carnosine treatment in combination with ACE inhibition in diabetic rats. *Regul Pept* **194-195**, 36-40, doi:10.1016/j.regpep.2014.09.005 (2014).
- 29 Peters, V. *et al.* Carnosine treatment largely prevents alterations of renal carnosine metabolism in diabetic mice. *Amino Acids* **42**, 2411-2416, doi:10.1007/s00726-011-1046-4 (2012).
- 30 Sauerhofer, S. *et al.* L-carnosine, a substrate of carnosinase-1, influences glucose metabolism. *Diabetes* **56**, 2425-2432, doi:10.2337/db07-0177 (2007).
- 31 Hudkins, K. L. *et al.* BTBR Ob/Ob mutant mice model progressive diabetic nephropathy. *J Am Soc Nephrol* **21**, 1533-1542, doi:10.1681/ASN.2009121290 (2010).
- 32 Culbertson, J. Y., Kreider, R. B., Greenwood, M. & Cooke, M. Effects of beta-alanine on muscle carnosine and exercise performance: a review of the current literature. *Nutrients* **2**, 75-98, doi:10.3390/nu2010075 (2010).
- 33 Dunnett, M., Harris, R. C., Dunnett, C. E. & Harris, P. A. Plasma carnosine concentration: diurnal variation and effects of age, exercise and muscle damage. *Equine Vet J Suppl*, 283-287, doi:10.1111/j.2042-3306.2002.tb05434.x (2002).
- 34 Nagai, K. *et al.* Possible role of L-carnosine in the regulation of blood glucose through controlling autonomic nerves. *Exp Biol Med (Maywood)* **228**, 1138-1145, doi:10.1177/153537020322801007 (2003).
- 35 Boor, P. *et al.* Regular moderate exercise reduces advanced glycation and ameliorates early diabetic nephropathy in obese Zucker rats. *Metabolism* **58**, 1669-1677, doi:10.1016/j.metabol.2009.05.025 (2009).
- 36 Rodrigues, A. M. *et al.* P2X(7) receptor in the kidneys of diabetic rats submitted to aerobic training or to N-acetylcysteine supplementation [corrected]. *PLoS One* **9**, e97452, doi:10.1371/journal.pone.0097452 (2014).
- 37 Lappalainen, J. *et al.* Suppressed heat shock protein response in the kidney of exercise-trained diabetic rats. *Scand J Med Sci Sports* **28**, 1808-1817, doi:10.1111/sms.13079 (2018).
- 38 Sominen, H. K., Boivin, G. P. & Elased, K. M. Daily exercise training protects against albuminuria and angiotensin converting enzyme 2 shedding in db/db diabetic mice. *The Journal of endocrinology* **221**, 235-251, doi:10.1530/JOE-13-0532 (2014).
- 39 Ghosh, S. *et al.* Moderate exercise attenuates caspase-3 activity, oxidative stress, and inhibits progression of diabetic renal disease in db/db mice. *Am J Physiol Renal Physiol* **296**, F700-708, doi:10.1152/ajprenal.90548.2008 (2009).
- 40 Brown, B. E. *et al.* Supplementation with carnosine decreases plasma triglycerides and modulates atherosclerotic plaque composition in diabetic apo E(-/-) mice. *Atherosclerosis* **232**, 403-409, doi:10.1016/j.atherosclerosis.2013.11.068 (2014).

- 41 Lee, Y. T., Hsu, C. C., Lin, M. H., Liu, K. S. & Yin, M. C. Histidine and carnosine delay diabetic deterioration in mice and protect human low density lipoprotein against oxidation and glycation. *Eur J Pharmacol* **513**, 145-150, doi:10.1016/j.ejphar.2005.02.010 (2005).
- 42 Houjehgani, S., Kheirouri, S., Faraji, E. & Jafarabadi, M. A. l-Carnosine supplementation attenuated fasting glucose, triglycerides, advanced glycation end products, and tumor necrosis factor-alpha levels in patients with type 2 diabetes: a double-blind placebo-controlled randomized clinical trial. *Nutr Res* **49**, 96-106, doi:10.1016/j.nutres.2017.11.003 (2018).
- 43 Barski, O. A. *et al.* Dietary carnosine prevents early atherosclerotic lesion formation in apolipoprotein E-null mice. *Arterioscler Thromb Vasc Biol* **33**, 1162-1170, doi:10.1161/ATVBAHA.112.300572 (2013).
- 44 Dooley, K. & Zon, L. I. Zebrafish: a model system for the study of human disease. *Curr Opin Genet Dev* **10**, 252-256, doi:10.1016/s0959-437x(00)00074-5 (2000).
- 45 Gibert, Y., Trengove, M. C. & Ward, A. C. Zebrafish as a genetic model in pre-clinical drug testing and screening. *Curr Med Chem* **20**, 2458-2466, doi:10.2174/0929867311320190005 (2013).
- 46 Lieschke, G. J. & Currie, P. D. Animal models of human disease: zebrafish swim into view. *Nat Rev Genet* **8**, 353-367, doi:10.1038/nrg2091 (2007).
- 47 Drel, V. R. *et al.* The leptin-deficient (ob/ob) mouse: a new animal model of peripheral neuropathy of type 2 diabetes and obesity. *Diabetes* **55**, 3335-3343, doi:10.2337/db06-0885 (2006).
- 48 Kamohara, S., Burcelin, R., Halaas, J. L., Friedman, J. M. & Charron, M. J. Acute stimulation of glucose metabolism in mice by leptin treatment. *Nature* **389**, 374-377, doi:10.1038/38717 (1997).
- 49 Shimomura, I., Hammer, R. E., Ikemoto, S., Brown, M. S. & Goldstein, J. L. Leptin reverses insulin resistance and diabetes mellitus in mice with congenital lipodystrophy. *Nature* **401**, 73-76, doi:10.1038/43448 (1999).
- 50 German, J. *et al.* Hypothalamic leptin signaling regulates hepatic insulin sensitivity via a neurocircuit involving the vagus nerve. *Endocrinology* **150**, 4502-4511, doi:10.1210/en.2009-0445 (2009).
- 51 Morton, G. J. *et al.* Leptin regulates insulin sensitivity via phosphatidylinositol-3-OH kinase signaling in mediobasal hypothalamic neurons. *Cell Metab* **2**, 411-420, doi:10.1016/j.cmet.2005.10.009 (2005).
- 52 Yu, X., Park, B. H., Wang, M. Y., Wang, Z. V. & Unger, R. H. Making insulin-deficient type 1 diabetic rodents thrive without insulin. *Proc Natl Acad Sci U S A* **105**, 14070-14075, doi:10.1073/pnas.0806993105 (2008).
- 53 Marin-Juez, R., Jong-Raadsen, S., Yang, S. & Spaink, H. P. Hyperinsulinemia induces insulin resistance and immune suppression via Ptpn6/Shp1 in zebrafish. *The Journal of endocrinology* **222**, 229-241, doi:10.1530/JOE-14-0178 (2014).
- 54 Molitch, M. E. *et al.* Nephropathy in diabetes. *Diabetes Care* **27 Suppl 1**, S79-83, doi:10.2337/diacare.27.2007.s79 (2004).
- 55 Wang, B., Chandrasekera, P. C. & Pippin, J. J. Leptin- and leptin receptor-deficient rodent models: relevance for human type 2 diabetes. *Curr Diabetes Rev* **10**, 131-145, doi:10.2174/1573399810666140508121012 (2014).
- 56 Gerhard, G. S. *et al.* Life spans and senescent phenotypes in two strains of Zebrafish (*Danio rerio*). *Exp Gerontol* **37**, 1055-1068, doi:10.1016/s0531-5565(02)00088-8 (2002).
- 57 Zang, L., Shimada, Y. & Nishimura, N. Development of a Novel Zebrafish Model for Type 2 Diabetes Mellitus. *Sci Rep* **7**, 1461, doi:10.1038/s41598-017-01432-w (2017).
- 58 Spaink, H. P. *et al.* Robotic injection of zebrafish embryos for high-throughput screening in disease models. *Methods* **62**, 246-254, doi:10.1016/j.ymeth.2013.06.002 (2013).
- 59 Elmonem, M. A. *et al.* Cystinosis (ctns) zebrafish mutant shows pronephric glomerular and tubular dysfunction. *Sci Rep* **7**, 42583, doi:10.1038/srep42583 (2017).
- 60 Saftig, P. & Klumperman, J. Lysosome biogenesis and lysosomal membrane proteins: trafficking meets function. *Nat Rev Mol Cell Biol* **10**, 623-635, doi:10.1038/nrm2745 (2009).
- 61 Sakarcan, A., Timmons, C. & Baum, M. Intracellular distribution of cystine in cystine-loaded proximal tubules. *Pediatr Res* **35**, 447-450 (1994).

- 62 Hard, G. C. Some aids to histological recognition of hyaline droplet nephropathy in ninety-day toxicity studies. *Toxicol Pathol* **36**, 1014-1017, doi:10.1177/0192623308327413 (2008).
- 63 Raggi, C. *et al.* Dedifferentiation and aberrations of the endolysosomal compartment characterize the early stage of nephropathic cystinosis. *Hum Mol Genet* **23**, 2266-2278, doi:10.1093/hmg/ddt617 (2014).
- 64 Cherqui, S. *et al.* Intralysosomal cystine accumulation in mice lacking cystinosin, the protein defective in cystinosis. *Mol Cell Biol* **22**, 7622-7632, doi:10.1128/mcb.22.21.7622-7632.2002 (2002).
- 65 Park, M. A., Pejovic, V., Kerisit, K. G., Junius, S. & Thoene, J. G. Increased apoptosis in cystinotic fibroblasts and renal proximal tubule epithelial cells results from cysteinylolation of protein kinase Cdelta. *J Am Soc Nephrol* **17**, 3167-3175, doi:10.1681/ASN.2006050474 (2006).
- 66 Sumayao, R., McEvoy, B., Newsholme, P. & McMorrow, T. Lysosomal cystine accumulation promotes mitochondrial depolarization and induction of redox-sensitive genes in human kidney proximal tubular cells. *J Physiol* **594**, 3353-3370, doi:10.1113/JP271858 (2016).
- 67 Brodin-Sartorius, A. *et al.* Cysteamine therapy delays the progression of nephropathic cystinosis in late adolescents and adults. *Kidney Int* **81**, 179-189, doi:10.1038/ki.2011.277 (2012).
- 68 Seaquist, E. R., Goetz, F. C., Rich, S. & Barbosa, J. Familial clustering of diabetic kidney disease. Evidence for genetic susceptibility to diabetic nephropathy. *N Engl J Med* **320**, 1161-1165, doi:10.1056/NEJM198905043201801 (1989).
- 69 Pettitt, D. J., Saad, M. F., Bennett, P. H., Nelson, R. G. & Knowler, W. C. Familial predisposition to renal disease in two generations of Pima Indians with type 2 (non-insulin-dependent) diabetes mellitus. *Diabetologia* **33**, 438-443, doi:10.1007/BF00404096 (1990).
- 70 Zhou, W. *et al.* Loss of clusterin expression worsens renal ischemia-reperfusion injury. *Am J Physiol Renal Physiol* **298**, F568-578, doi:10.1152/ajprenal.00399.2009 (2010).
- 71 Guo, J. *et al.* Relationship of clusterin with renal inflammation and fibrosis after the recovery phase of ischemia-reperfusion injury. *BMC Nephrol* **17**, 133, doi:10.1186/s12882-016-0348-x (2016).
- 72 Jung, G. S. *et al.* Clusterin attenuates the development of renal fibrosis. *J Am Soc Nephrol* **23**, 73-85, doi:10.1681/ASN.2011010048 (2012).
- 73 Baelde, H. J. *et al.* Gene expression profiling in glomeruli from human kidneys with diabetic nephropathy. *Am J Kidney Dis* **43**, 636-650 (2004).
- 74 Janssen, B. *et al.* Carnosine as a protective factor in diabetic nephropathy: association with a leucine repeat of the carnosinase gene CNDP1. *Diabetes* **54**, 2320-2327, doi:10.2337/diabetes.54.8.2320 (2005).
- 75 Ahluwalia, T. S., Lindholm, E. & Groop, L. C. Common variants in CNDP1 and CNDP2, and risk of nephropathy in type 2 diabetes. *Diabetologia* **54**, 2295-2302, doi:10.1007/s00125-011-2178-5 (2011).
- 76 Hipkiss, A. R. Glycation, ageing and carnosine: are carnivorous diets beneficial? *Mech Ageing Dev* **126**, 1034-1039, doi:10.1016/j.mad.2005.05.002 (2005).
- 77 Teufel, M. *et al.* Sequence identification and characterization of human carnosinase and a closely related non-specific dipeptidase. *J Biol Chem* **278**, 6521-6531, doi:10.1074/jbc.M209764200 (2003).
- 78 Margolis, F. L. & Grillo, M. Inherited differences in mouse kidney carnosinase activity. *Biochem Genet* **22**, 441-451, doi:10.1007/BF00484515 (1984).
- 79 Rodrigues, A. M. *et al.* Effects of training and nitric oxide on diabetic nephropathy progression in type I diabetic rats. *Exp Biol Med (Maywood)* **236**, 1180-1187, doi:10.1258/ebm.2011.011005 (2011).
- 80 Tufescu, A. *et al.* Combination of exercise and losartan enhances renoprotective and peripheral effects in spontaneously type 2 diabetes mellitus rats with nephropathy. *J Hypertens* **26**, 312-321, doi:10.1097/HJH.0b013e3282f2450b (2008).
- 81 Ward, K. M., Mahan, J. D. & Sherman, W. M. Aerobic training and diabetic nephropathy in the obese Zucker rat. *Ann Clin Lab Sci* **24**, 266-277 (1994).



- 82 Martinez, R. *et al.* Aerobic interval exercise improves renal functionality and affects mineral metabolism in obese Zucker rats. *Am J Physiol Renal Physiol* **316**, F90-F100, doi:10.1152/ajprenal.00356.2018 (2019).
- 83 Farooqi, I. S. *et al.* Effects of recombinant leptin therapy in a child with congenital leptin deficiency. *N Engl J Med* **341**, 879-884, doi:10.1056/NEJM199909163411204 (1999).
- 84 Funcke, J. B. *et al.* Monogenic forms of childhood obesity due to mutations in the leptin gene. *Mol Cell Pediatr* **1**, 3, doi:10.1186/s40348-014-0003-1 (2014).
- 85 Coleman, D. L. Obese and diabetes: two mutant genes causing diabetes-obesity syndromes in mice. *Diabetologia* **14**, 141-148, doi:10.1007/BF00429772 (1978).
- 86 Pellemounter, M. A. *et al.* Effects of the obese gene product on body weight regulation in ob/ob mice. *Science* **269**, 540-543, doi:10.1126/science.7624776 (1995).
- 87 Chen, H. *et al.* Evidence that the diabetes gene encodes the leptin receptor: identification of a mutation in the leptin receptor gene in db/db mice. *Cell* **84**, 491-495, doi:10.1016/s0092-8674(00)81294-5 (1996).
- 88 Volkoff, H., Eykelbosh, A. J. & Peter, R. E. Role of leptin in the control of feeding of goldfish *Carassius auratus*: interactions with cholecystokinin, neuropeptide Y and orexin A, and modulation by fasting. *Brain Res* **972**, 90-109, doi:10.1016/s0006-8993(03)02507-1 (2003).
- 89 Murashita, K., Uji, S., Yamamoto, T., Ronnestad, I. & Kurokawa, T. Production of recombinant leptin and its effects on food intake in rainbow trout (*Oncorhynchus mykiss*). *Comp Biochem Physiol B Biochem Mol Biol* **150**, 377-384, doi:10.1016/j.cbpb.2008.04.007 (2008).
- 90 Aguilar, A. J., Conde-Sieira, M., Lopez-Patino, M. A., Miguez, J. M. & Soengas, J. L. In vitro leptin treatment of rainbow trout hypothalamus and hindbrain affects glucosensing and gene expression of neuropeptides involved in food intake regulation. *Peptides* **32**, 232-240, doi:10.1016/j.peptides.2010.11.007 (2011).
- 91 Denver, R. J., Bonett, R. M. & Boorse, G. C. Evolution of leptin structure and function. *Neuroendocrinology* **94**, 21-38, doi:10.1159/000328435 (2011).
- 92 Cherqui, S. & Courtoy, P. J. The renal Fanconi syndrome in cystinosis: pathogenic insights and therapeutic perspectives. *Nat Rev Nephrol* **13**, 115-131, doi:10.1038/nrneph.2016.182 (2017).
- 93 Kaur, G. & Dufour, J. M. Cell lines: Valuable tools or useless artifacts. *Spermatogenesis* **2**, 1-5, doi:10.4161/spmg.19885 (2012).
- 94 Mouse Genome Sequencing, C. *et al.* Initial sequencing and comparative analysis of the mouse genome. *Nature* **420**, 520-562, doi:10.1038/nature01262 (2002).
- 95 Perlman, R. L. Mouse models of human disease: An evolutionary perspective. *Evol Med Public Health* **2016**, 170-176, doi:10.1093/emph/eow014 (2016).
- 96 Ali, S., Champagne, D. L., Spaink, H. P. & Richardson, M. K. Zebrafish embryos and larvae: a new generation of disease models and drug screens. *Birth Defects Res C Embryo Today* **93**, 115-133, doi:10.1002/bdrc.20206 (2011).
- 97 Kramer-Zucker, A. G., Wiessner, S., Jensen, A. M. & Drummond, I. A. Organization of the pronephric filtration apparatus in zebrafish requires Nephhrin, Podocin and the FERM domain protein Mosaic eyes. *Dev Biol* **285**, 316-329, doi:10.1016/j.ydbio.2005.06.038 (2005).
- 98 Hentschel, D. M. *et al.* Rapid screening of glomerular slit diaphragm integrity in larval zebrafish. *Am J Physiol Renal Physiol* **293**, F1746-1750, doi:10.1152/ajprenal.00009.2007 (2007).
- 99 Zhou, W. & Hildebrandt, F. Inducible podocyte injury and proteinuria in transgenic zebrafish. *J Am Soc Nephrol* **23**, 1039-1047, doi:10.1681/ASN.2011080776 (2012).
- 100 Bates, T., Naumann, U., Hoppe, B. & Englert, C. Kidney regeneration in fish. *Int J Dev Biol* **62**, 419-429, doi:10.1387/ijdb.170335ce (2018).



# Chapter 7

## Nederlandse samenvatting



## Nederlandse samenvatting

Chronische nierziekte is een algemene term voor nierziekten die leiden tot een geleidelijk verlies van de nierfunctie gedurende een langere periode. Als de nier eenmaal is beschadigd, kan dit na verloop van tijd erger worden. De progressie van chronische nierziekte omvat zowel glomerulaire als tubulaire beschadigingen en de ontwikkeling van interstitiële fibrose, wat gepaard gaat met de achteruitgang van de nierfunctie. Inzicht in de onderliggende mechanismen van de ontwikkeling van chronische nieraandoeningen opent mogelijkheden voor de ontwikkeling van preventieve en therapeutische strategieën.

Diabetes Mellitus is een stofwisselingsziekte die wordt gekenmerkt door langdurige hyperglykemie. Type 1 diabetes mellitus (T1DM) en type 2 diabetes mellitus (T2DM) zijn de meest voorkomende soorten diabetes. Diabetische nefropathie is een belangrijke complicatie van diabetes en de belangrijkste oorzaak van eindstadium nierfalen. Een genetische aanleg, ook wel genetische gevoeligheid genoemd, vormt een verhoogde kans op het ontwikkelen van een bepaalde ziekte op basis van de genetische achtergrond onder invloed van omgevingsfactoren. Ondanks de toenemende prevalentie van diabetes ontwikkelt slechts een minderheid van de mensen met diabetes diabetische nefropathie (30% ~ 50%), wat suggereert dat genetische determinanten de ontwikkeling en progressie van diabetische nefropathie kunnen beïnvloeden. Daarom is het van cruciaal belang om de rol van de genetische factoren bij diabetische nefropathie te begrijpen, aangezien het een nieuwe kijk zou kunnen geven op een vroege diagnose of mogelijke therapeutische strategieën.

Een verhoogde expressie van clusterin, een glycoproteïne, komt voor in de glomeruli van patiënten met verschillende vormen van nierziekte. In de studie beschreven in **hoofdstuk 2**, onderzochten we de rol van glomerulair clusterin in de ontwikkeling van diabetische nefropathie. We hebben eerst bevestigd dat clusterin-expressie verhoogd was in glomeruli van patiënten met diabetische nefropathie, zowel op het mRNA als op het eiwitniveau in nierbiopten. Immunohistochemische kleuringen op zowel humane als muizenieren lieten zien dat clusterin tot expressie wordt gebracht in glomerulaire podocyten. In de *in vitro* experimenten ontdekten we dat oxidatieve stress, maar niet hoog glucose of angiotensine II, de expressie van clusterin in podocyten opreguleert, wat suggereert dat oxidatieve stress een belangrijke factor is die clusterin expressie induceert onder diabetische omstandigheden. Ten slotte hebben we aangetoond dat clusterin de levensvatbaarheid van de cellen verbetert onder oxidatieve stress-geïnduceerde schade, de verhoogde Bax / Bcl2-mRNA-ratio verlaagt en de verhoogde caspase

3/7-activiteit in podocyten *in vitro* vermindert. Deze bevindingen geven aan dat clusterine podocyten kan beschermen tegen oxidatieve stress-geïnduceerde apoptotische celdood.

Carnosinase is een enzym dat carnosine hydrolyseert. Eerdere studies hebben een verband aangetoond tussen de genetische varianten van het CNBP1 (CN1)-gen en de gevoeligheid voor het ontwikkelen van diabetische nefropathie. In de studie beschreven in **hoofdstuk 3**, hebben we aangetoond dat expressie van hCN1 in muizen het gehalte aan histidinebevattende dipeptiden (carnosine en anserine) in urine, nieren en gastrocnemius verminderde, en leidde tot significant versnelde diabetische nefropathie bij BTBR *ob/ob*-muizen. Verder vonden we dat de hoeveelheid histidine-bevattende dipeptiden in de nier negatief gecorreleerd was met mesangiale matrix expansie en glomerulaire hypertrofie. We toonden aan dat BTBR *ob/ob*-muizen met hCN1-expressie een verhoogd nuchter cholesterol en triglyceriden hadden in week 14, wat aangeeft dat expressie van hCN1 bijdraagt aan een snellere ontwikkeling van hyperlipidemie bij diabetische muizen. In tegenstelling tot eerdere studies vonden we geen beschermend effect van chronische inspanningstraining op de progressie van diabetische nefropathie. Onze gegevens suggereren dat de hoeveelheid histidine-bevattende dipeptiden in de nier omgekeerd evenredig is met de ernst van diabetische nefropathie.

Leptine is een hormoon dat een rol speelt bij de regulatie van energiehuishouding via onderdrukking van de eetlust. In de studie beschreven in **hoofdstuk 4**, ontdekten we dat volwassen *lepb<sup>-/-</sup>* (leptine b knockout) zebravissen een toename in lichaamsgewicht en lengte hebben in vergelijking met de controlegroep volwassen zebravissen van dezelfde leeftijd. Bovendien toonde de kwantificering van MRI-gegevens (Magnetic Resonance Anatomical Imaging) een significante toename van de accumulatie van visceraal vet bij *lepb<sup>-/-</sup>* volwassen zebravissen, in vergelijking met volwassen zebravissen in de controlegroep, in zowel vrouwelijke als mannelijke zebravissen. Het toegenomen lichaamsgewicht, lengte van de vissen en hoeveelheid visceraal vet geven aan dat *lepb<sup>-/-</sup>* volwassen zebravissen een obees fenotype hebben. Verder vonden we dat zowel nuchtere als 2 uur postprandiale bloedsuikerspiegels in de *lepb<sup>-/-</sup>* mannelijke zebravissen significant hoger waren in vergelijking met de controlegroep mannelijke zebravissen. Dit verschil vonden we echter niet bij vrouwelijke zebravissen. Ten slotte hebben we waargenomen dat *lepb<sup>-/-</sup>* mannelijke zebravissen glomerulaire hypertrofie en verdikking van het glomerulaire basaalmembraan ontwikkelen, wat aangeeft dat *lepb<sup>-/-</sup>* volwassen zebravissen vroege tekenen van diabetische nefropathie hebben.

Cystinose is een zeldzame en ongeneeslijke lysosomale stapelingsziekte. Mutaties in het *CTNS*-gen dat codeert voor cystinosine, veroorzaken een defect lysosomaal cystinetransport. Cystinose heeft een autosomaal recessief overervingspatroon. Nefropathische cystinose is het

belangrijkste klinische kenmerk van cystinose, bekend als renaal Fanconi-syndroom. De onvoldoende reabsorptie in de proximale niertubulus leidt tot het uitscheiden van abnormale hoeveelheden glucose, urinezuur, aminozuur, bicarbonaat en fosfaat in de urine. De proximale tubulaire schade kan verder evolueren tot progressieve glomerulaire schade en eindstadium nierfalen, waardoor uiteindelijk niervervangende therapie nodig is. Tot nu is behandeling van nefropathische cystinose zonder ernstige bijwerkingen nog niet mogelijk. Daarom zou het genereren van goede diermodellen de mogelijkheid kunnen bieden om de onderliggende mechanismen van deze chronische nierziekte beter te begrijpen en nieuwe behandelingen te testen. In de studie beschreven in **hoofdstuk 5**, hebben we de nieren van volwassen *ctns*-deficiënte zebravissen onderzocht. We vonden cytoplasmatische vacuolen en hyaline-achtige eosinofiele druppeltjes in de proximale tubuli in zowel vrouwelijke als mannelijke zebravissen. Bovendien ontdekten we dat deze vacuolen in de renale proximale tubulaire cellen van *ctns*-deficiënte volwassen zebravissen een rechthoekige of polymorfe vorm hebben in toluïdineblauw gekleurde weefsels. Dit beeld werd bevestigd met transmissie-elektronenmicroscopie. Deze bevindingen suggereren dat cystine kristallen aanwezig waren. Ook hebben we aangetoond dat *ctns*-deficiënte zebravissen glomerulaire hypertrofie hadden, wat mogelijk verband houdt met hyperfiltratie. Ten slotte hebben we waargenomen dat *ctns*-deficiënte volwassen zebravissen verhoogde niveaus van geactiveerd caspase-3 en verhoogde nucleaire fragmentatie in de renale proximale tubulaire epitheelcellen hebben, vergeleken met controle zebravissen. Dit geeft aan dat apoptose betrokken is bij de pathogenese van cystinose tubulopathie bij zebravissen.

Voor de toekomst zou het interessant zijn om vergelijkende studies uit te voeren onder patiënten, zebravissen en muizen om nieuwe inzichten te verkrijgen in regeneratie en herstel van de nier bij chronische nieraandoeningen. Hoewel zebravissen een waardevol diermodel zijn voor het onderzoeken van de pathogenese en therapieën voor chronische nieraandoeningen, kunnen ze muismodellen in fundamenteel onderzoek niet volledig vervangen. Zebravismodellen, in het bijzonder embryo's, kunnen de kloof opvullen tussen de celkweek en de sterk georganiseerde muizenmodellen, vooral in het licht van drugscreening of onderzoek naar de functies van genen. Wij denken dat het integreren van de ontdekkingen op basis van studies in celkweek, zebravissen en knaagdiermodellen nieuwe biologische inzichten kan opleveren die de ontwikkeling van innovatieve behandelingen voor chronische nierziekten kunnen stimuleren.

# Appendices

Curriculum Vitae

List of Publications

Acknowledgements



## **Curriculum Vitae**

Junling He was born in Wanzhou, Chongqing, China, on the 10<sup>th</sup> of March 1988. In 2006, she attended medical school at Chongqing Medical University, China, to study Clinical Medicine. She earned her bachelor's degree in 2011. In the same year, she got 3-year National Scholarship for a postgraduate medical student and started her master program in Clinical Medicine at Chongqing Medical University, China. From 2011-2014, she completed the internal medicine clinical rotations at the First Affiliated Hospital of Chongqing Medical University, China. In 2012, she obtained the qualification for practicing physician in China. During her master studies, she participated in several scientific research projects on kidney diseases under the supervision of Prof. Xiaogang Du. She obtained her master's degree in 2014. In 2015, she was awarded 4-year financial support from China Scholarship Council for a PhD study at Leiden University, the Netherlands. In 2015, she became a PhD candidate at the Department of Animal Sciences, Institute of Biology Leiden, Leiden University and the Department of Pathology of the Leiden University Medical Center, the Netherlands. She started the work of studies on the pathogenesis of chronic kidney disease under the supervision of Prof. J.A. Bruijn, Prof. H.P. Spaink, and Dr J.J. Baelde. She presented her research at the American Society of Nephrology (ASN) kidney week (San Diego, 2017) and the Dutch Nephrology Days (Veldhoven, 2018). The results of the research were published in peer-reviewed international scientific journals and are presented in this thesis. Currently, she is working on a project about the applications of artificial intelligence in renal pathology under the supervision of Dr J. Kers at the Department of Pathology, Leiden University Medical Center, the Netherlands.



## List of Publications

**Junling He\***, Yi Ding\*, Natalia Nowik, Charel Jager, Muhamed N H Eeza, A Alia, Hans J Baelde, Herman P Spaink. *Leptin deficiency affects glucose homeostasis and results in adiposity in zebrafish*. \* These authors contributed equally to this work.

J Endocrinol. 2021 May;249(2):125-134.

**Junling He**, Kyra L Dijkstra, Kim Bakker, Pascal Bus, Jan A Bruijn, Marion Scharpfenecker, Hans J Baelde. *Glomerular clusterin expression is increased in diabetic nephropathy and protects against oxidative stress-induced apoptosis in podocytes*.

Sci Rep. 2020 Sep 10;10(1):14888.

Inge Everaert\*, **Junling He\***, Maxime Hanssens\*, Jan Stautemas, Kim Bakker, Thomas Albrecht, Shiqi Zhang, Thibaux Van der Stede, Kenneth Vanhove, David Hoetker, Michael Howsam, Frédéric J Tessier, Benito Yard, Shahid P Baba, Hans J Baelde, Wim Derave. *Carnosinase-1 overexpression, but not aerobic exercise training, affects the development of advanced diabetic nephropathy in BTBR ob/ob mice*. \* These authors contributed equally to this work.

Am J Physiol Renal Physiol. 2020 Apr 1;318(4):F1030-F1040.

Yi Ding, Mariëlle C Haks, Gabriel Forn-Cuní, **Junling He**, Natalia Nowik, Amy C. Harms, Thomas Hankemeier, Muhamed N. H. Eeza, Jörg Matysik, A. Alia, Herman P. Spaink. *Metabolomic and transcriptomic profiling of adult mice and larval zebrafish leptin mutants reveal a common pattern of changes in metabolites and signaling pathways*.

Cell Biosci. 2021 Jul 7;11(1):126.

Xu-Shun Jiang\*, Xing-Yang Xiang\*, Xue-Mei Chen, **Jun-Ling He**, Ting Liu, Hua Gan, Xiao-Gang Du. *Inhibition of soluble epoxide hydrolase attenuates renal tubular mitochondrial dysfunction and ER stress by restoring autophagic flux in diabetic nephropathy*. \* These authors contributed equally to this work.

Cell Death Dis. 2020 May 21;11(5):385.

Xu-Shun Jiang, Xue-Mei Chen, Wei Hua, **Jun-Ling He**, Ting Liu, Xun-Jia Li, Jiang-Min

Wan, Hua Gan, Xiao-Gang Du. *PINK1/Parkin Mediated Mitophagy Ameliorates Palmitic Acid-Induced Apoptosis Through Reducing Mitochondrial ROS Production in Podocytes*.  
Biochem Biophys Res Commun. 2020 May 14;525(4):954-961.

## Acknowledgements

Many thanks to everyone who kindly helped me throughout my entire PhD period. Here, I would like to thank some of them in particular who contributed to my scientific development.

*Dear Prof. Bruijn*, thank you for your guidance and support. You are a great motivator.

*Dear Prof. Spaink*, thank you for your mentorship. I admire your rigorous attitude in solving scientific problems.

*Dear Dr. Baelde*, thank you for imparting all your knowledge and experience without reservation. Gratitude, optimism, and compassion in you have a great influence on me.

*Dear Prof. Du*, thank you for giving me a good start and bringing me into the kidney field.

*Dear Dr. Wolterbeek* and *Dr. Bajema*, thank you for sharing your knowledge, skills and experience during the group meetings. Your mastery of professional knowledge inspired me.

*Dear Prof. Es*, thank you for your valuable time for sharing your knowledge and insights. I appreciate the discussions with you.

*Dear co-authors*, thank you for all your wonderful collaborations, which enabled our work to be published. *Pascal*, thanks for teaching me all the routine laboratory techniques when I started my PhD. *Marion*, thanks for your suggestions, comments, and support for my projects. I learned a lot from you when you revised my manuscript. *Inge*, *Yi*, and *Sante*, I was happy to work with you all. I enjoyed the moment that we put our minds together to solve scientific issues. Thank you for helping me to improve our work. *XuShun*, it was a pleasure working with you on some projects. *Kim* and *Charel*, guiding you through the project was a pleasant experience. I got a different vision and perspective on how to solve problems when I supervised you. *Kyra*, *Malu*, and *Kimberley*, thanks for your help in the lab.

*Colleagues at the Department of Pathology and IBL*, thank you for your advice, support, and kindness during this challenging time. It was a real privilege to work with you guys. Thank you all for adding so many sweet memories to my life.

*Dear friends in the Netherlands and China*, thank you for cheering me up when I am down and sharing my joy when I make progress.

*Dear Nina and Cleo*, my best paranymphs, thank you for your company over all these years.

Dear family members, *papas and mamas*, thank you for your unconditional love and support. *Zhan*, thank you for always being by my side.